

UNIVERSIDADE ESTADUAL DE MARINGÁ
CENTRO DE CIÊNCIAS DA SAÚDE
DEPARTAMENTO DE ANÁLISES CLÍNICAS E BIOMEDICINA
PROGRAMA DE PÓS-GRADUAÇÃO EM BIOCÊNCIAS E
FISIOPATOLOGIA

GABRIELLE MARCONI ZAGO FERREIRA DAMKE

Atividade antitumoral *in vitro* da hipericina encapsulada com o plurônico[®]
P123 em modelo de neoplasia cervical

Maringá
2020

GABRIELLE MARCONI ZAGO FERREIRA DAMKE

Atividade antitumoral *in vitro* da hipericina encapsulada com o plurônico®
P123 em modelo de neoplasia cervical

Tese apresentada ao Programa de Pós-Graduação em Biociências e Fisiopatologia do Departamento de Análises Clínicas e Biomedicina, Centro de Ciências da Saúde da Universidade Estadual de Maringá, como requisito parcial para obtenção do título de Doutora em Biociências e Fisiopatologia.
Área de concentração: Biociências e fisiopatologia aplicadas a farmácia.

Orientadora: Prof^ª. Dra. Marcia Edilaine Lopes Consolaro
Coorientadora: Prof^ª. Dra. Raquel Pantarotto Souza Padovan

Maringá
2020

Dados Internacionais de Catalogação-na-Publicação (CIP)
(Biblioteca Central - UEM, Maringá - PR, Brasil)

D161a	<p>Damke, Gabrielle Marconi Zago Ferreira</p> <p>Atividade antitumoral <i>in vitro</i> da hipericina encapsulada com o plurônico® P123 em modelo de neoplasia cervical / Gabrielle Marconi Zago Ferreira Damke. -- Maringá, PR, 2020.</p> <p>63 f.: il. color., figs., tabs.</p> <p>Orientadora: Profa. Dra. Marcia Edilaine Lopes Consolaro. Coorientadora: Profa. Dra. Raquel Pantarotto Souza Padovan. Tese (Doutorado) - Universidade Estadual de Maringá, Centro de Ciências da Saúde, Departamento de Análises Clínicas e Biomedicina, Programa de Pós-Graduação em Biociências e Fisiopatologia (PBF), 2020.</p> <p>1. Terapia fotodinâmica. 2. Câncer cervical. 3. Hipericina. 4. Plurônico® P123. I. Consolaro, Marcia Edilaine Lopes, orient. II. Padovan, Raquel Pantarotto Souza, coorient. III. Universidade Estadual de Maringá. Centro de Ciências da Saúde. Departamento de Análises Clínicas e Biomedicina. Programa de Pós-Graduação em Biociências e Fisiopatologia (PBF). IV. Título.</p> <p>CDD 23.ed. 615.831</p>
-------	---


FOLHA DE APROVAÇÃO

GABRIELLE MARCONI ZAGO FERREIRA DAMKE

Atividade antitumoral *in vitro* da hipericina encapsulada com o plurônico[®]
P123 em modelo de neoplasia cervical

Tese apresentada ao Programa de Pós-Graduação em Biociências e Fisiopatologia do Departamento de Análises Clínicas e Biomedicina, Centro de Ciências da Saúde da Universidade Estadual de Maringá, como requisito parcial para obtenção do título de Doutora em Biociências e Fisiopatologia pela Comissão Julgadora composta pelos membros:

COMISSÃO JULGADORA



Prof^ª. Dra Marcia Edilaine Lopes Consolaro
Universidade Estadual de Maringá (Presidente)

Prof^ª. Dra Vânia Ramos Sela da Silva
Universidade Estadual de Maringá

Prof. Dr. Renato Sonchini Gonçalves
Universidade Estadual de Maringá

Prof. Dr. Marcos Luciano Bruschi
Universidade Estadual de Maringá

Prof^ª. Dra. Silvy Stuchi Maria Engler
Universidade de São Paulo

Aprovada em: 18 de dezembro de 2020

Local de Defesa: de forma remota pela Universidade Estadual de Maringá

DEDICATÓRIA

Aos meus pais, minha irmã e meu marido, por estarem sempre ao meu lado, por acreditarem em mim, pelo amor infinito e pela confiança que sempre me dedicaram.

AGRADECIMENTOS

Agradeço a Deus, pelo dom da vida, pela sabedoria e cuidado que sempre conferiu a mim.

A professora **Dra. Marcia Edilaine Lopes Consolaro**, pela confiança, pela oportunidade de trabalhar em seu laboratório, contribuindo enormemente para minha formação acadêmica e pessoal. Deixo aqui o meu carinho e a minha eterna gratidão a essa pessoa admirável e profissional exemplar.

Ao meu marido **Edilson**, pelo apoio, por me encorajar a encarar esse desafio, pela confiança e pela valorização sempre entusiasta do meu trabalho. Agradeço ainda pela paciência, carinho e amor que sempre me tratou.

Aos meus **pais**, por mostrarem os aspectos da vida que mais importam, ensinar os valores mais importantes, sendo um deles a educação. Subo mais um degrau na minha formação, graças ao incentivo e apoio de vocês.

A minha **irmã**, por se fazer sempre presente em minha vida, pelo apoio, incentivo e amor.

A professora **Dra. Raquel Pantarotto Souza Padovan**, pela coorientação e amizade.

Aos pesquisadores do Núcleo de Pesquisa em Sistemas Fotodinâmicos, professor **Dr. Noboru Hioka**, professor **Dr. Wilker Caetano**, professor **Dr. Renato Sonchini Gonçalves** e **Dr. Gabriel Batista César**, não só pelos formulados sempre preparados com muita agilidade, mas também por toda apoio e suporte dispensados.

A professora **Dra. Bianca Altrão Ratti** e a professora **Dra. Patrícia de Souza Bonfim de Mendonça** por sempre serem prestativas e me auxiliarem quando precisei.

As professoras e demais alunos do Laboratório de Citologia Clínica e ISTs, em especial Livya, Maria Vitória e Natália, companheiras do laboratório de cultura de células.

Sentir gratidão é revelar a bondade que vive no nosso coração, é espalhar o melhor de nós, e ter sabedoria para entender que na vida há sempre um motivo para sorrir.

EPÍGAFE

“Para ser grande, sê inteiro: nada
Teu exagera ou exclui.
Sê todo em cada coisa. Põe quanto és
No mínimo que fazes.
Assim em cada lago a lua toda
Brilha, porque alta vive.” (Ricardo Reis)

Atividade antitumoral *in vitro* da hipericina encapsulada com o plurônico[®] P123 em modelo de neoplasia cervical

RESUMO

A terapia fotodinâmica (TFD) é uma modalidade terapêutica relativamente nova aplicada em diversas doenças proliferativas ou com crescimento celular anormal, como os tumores teciduais. Ela é baseada na utilização de um composto fotossensibilizador (FS) que sob a ação de luz de determinado comprimento de onda na presença de oxigênio molecular (O_2) pode gerar oxigênio singlete (1O_2) e espécies reativas de oxigênio (EROs), responsáveis pelos danos celulares. Essa técnica vem sendo utilizada para o tratamento de diversas patologias inclusive o câncer, visto que as opções de tratamento para obter efeitos citotóxicos em células neoplásicas e evitar, portanto, o avanço da doença, ainda são limitadas e apresentam elevadas taxas de insucesso. Nesta perspectiva, diversos trabalhos já demonstraram a atividade da TFD em estudos *in vitro*, *in vivo* e em humanos, inclusive alguns FS já são utilizados na prática clínica. No contexto da busca de novos tratamentos para o câncer, diversos estudos evidenciaram uma atividade multifacetada da hipericina (HIP) como FS na TFD, utilizando concentrações na ordem de micro a nanomolar sobre diversas linhagens celulares tumorais. Com relação ao câncer cervical, a busca para novos tratamentos se faz importante, visto que ele é um importante problema de saúde pública, sendo o quarto tipo mais comum de câncer em mulheres no mundo e o terceiro tumor mais frequente na população feminina brasileira, quando excluídos os casos de câncer de pele não melanoma. A infecção pelo *Papillomavirus* humano (HPV) está relacionada com o desenvolvimento deste câncer em 99,7% dos casos, bem como das lesões pré-neoplásicas cervicais. As opções de tratamento para obter efeitos citotóxicos a fim de evitar o avanço do câncer cervical ainda são limitadas e apresentam elevadas taxas de insucesso terapêutico, auxiliando no mau prognóstico da doença. Para explorar novos possíveis candidatos terapêuticos para o câncer cervical, no presente estudo foram avaliados os efeitos da HIP encapsulada plurônico[®] P123 (HIP/P123) na TFD em um painel abrangente de linhagens celulares derivadas de câncer cervical humano, incluindo HeLa (HPV 18-positivo), SiHa (HPV 16-positivo), CaSki (HPV 16 e 18-positivo) e C33A (HPV-negativo), em comparação com linhagem de células epiteliais humanas não tumorigênicas (HaCaT). Foram investigados os efeitos da TFD com

HIP/P123 quanto à: citotoxicidade celular e fototoxicidade; internalização e localização subcelular; via de morte celular e estresse oxidativo; migração e invasão. Nossos resultados mostraram que as micelas de HIP/P123 tiveram efeitos fototóxicos eficazes e seletivos, dependentes do tempo e da dose, nas células de câncer cervical, mas não em HaCaT. Além disso, as micelas de HIP/P123 acumularam-se no retículo endoplasmático, mitocôndrias e lisossomos, resultando na morte celular principalmente por necrose. A HIP/P123 induziu ao estresse oxidativo celular principalmente por meio do mecanismo da TFD do tipo II e inibiu a migração e invasão das células tumorais principalmente por meio da inibição da metaloproteinase de membrana do tipo 2 (MMP-2). Em conjunto, os resultados demonstraram que o tratamento com a TFD utilizando a HIP/P123 como FS teve efeito antitumoral seletivo em células de câncer cervical imortalizadas por HPV 16, HPV 18, HPV 16 e 18 juntos e sem HPV, indicando seu potencial como um candidato promissor para o tratamento do câncer cervical. Ainda, indicaram um papel potencialmente útil das micelas HYP/P123 como uma plataforma para a entrega de HIP para tratar de forma mais específica e eficaz o câncer cervical por meio de TFD, reforçando a necessidade da continuidade dos estudos especialmente dos testes pré-clínicos *in vivo*.

Palavras-chave: Terapia fotodinâmica. Câncer cervical. Hipericina. Plurônico® P123.

In vitro antitumor activity of hypericin encapsulated with pluronic[®] P123 in a model of cervical neoplasia

ABSTRACT

Photodynamic therapy (PDT) is a relatively new therapy applied in several proliferative diseases, such as tissue tumors. PDT uses a photosensitizing compound (FS) that under the action of light of a certain wavelength in the presence of molecular oxygen (O₂) can generate singlet oxygen (¹O₂) and reactive oxygen species (ROS), responsible for cell damage. This technique has been applied for the treatment of several pathologies, including cancer, since the treatment options to obtain cytotoxic effects on neoplastic cells and, therefore, to prevent the disease from advancing, are still limited and have high rates of failure. In this perspective, several studies presented the activity of TFD *in vitro*, *in vivo* and in humans, using the order of micro to nanomolar concentrations against several tumor cell lines. Regarding to cervical cancer, the search for new treatments is important, since it is an important public health problem, being the fourth most common type of cancer in women worldwide and the third most frequent tumor in the Brazilian female population, when cases of non-melanoma skin cancer were excluded. Infection with human papillomavirus (HPV) is associated to the development of this cancer in 99.7% of cases, as well as pre-neoplastic cervical lesions. The treatment options to obtain cytotoxic effects in order to prevent the progression of cervical cancer are still limited and present high rates of therapeutic failure. To explore new potential therapeutic candidates for cervical cancer, in the present study we investigated the antitumoral effects of HYP encapsulated on Pluronic[®] P123 (HYP/P123) PDT in a comprehensive panel of human cervical cancer-derived cell lines, including HeLa (HPV 18-positive), SiHa (HPV 16-positive), CaSki (HPV 16 and 18-positive) and C33A (HPV-negative), compared to a nontumorigenic human epithelial cell line (HaCaT). The effects of PDT with HYP/P123 were investigated regarding: cell cytotoxicity and phototoxicity, cellular uptake and subcellular distribution; cell death pathway and cellular oxidative stress; and migration and invasion. Our results showed that the HYP/P123 micelles presented effective and selective phototoxic effects, in a dose-time-dependent manner on cervical cancer cells, but not in HaCaT. In addition, the HYP/P123 micelles accumulated in the endoplasmic reticulum, mitochondria and lysosomes, resulting in cell death mainly by necrosis. HYP/P123 induced oxidative

stress mainly through the type II PDT mechanism and inhibited the migration and invasion of tumor cells mainly through the inhibition of matrix metalloproteinase-2 (MMP-2). Together, the results showed that the treatment with PDT using HYP/P123 as FS presented a selective antitumor effect on cervical cancer cells immortalized by HPV 16, HPV 18, HPV 16 and 18 together and without HPV, indicating its potential as a promising candidate for the treatment of cervical cancer. In addition, they indicated a potentially useful role of HYP/P123 micelles as a platform for HYP delivery to more specifically and effectively treat cervical cancers through PDT, reinforcing the need for continuing studies, especially for in vivo preclinical evaluations.

Keywords: Photodynamic therapy. Cervical cancer. Hypericin. Pluronic[®] P123.

Tese elaborada e formatada conforme as normas: Vancouver.

O artigo desta tese foi elaborado e formatado conforme as normas da publicação científica: *Life Sciences*.

Disponível em:

<https://www.elsevier.com/journals/lifesciences/0024-3205/guide-for-authors>

SUMÁRIO

CAPÍTULO I	10
1 - INTRODUÇÃO	10
1.1 - Terapia fotodinâmica: princípios e aplicações	10
1.2 – O tratamento do câncer e a terapia fotodinâmica	12
1.2.1 - Fotossensibilizadores	13
1.2.1.1- Hipericina, um fotossensibilizador promissor para uso na terapia fotodinâmica	14
1.2.2 – Fontes de luz	16
1.2.3 – Mecanismos de ação da terapia fotodinâmica	16
1.2.3.1 – Tipos de morte celular	19
1.2.3.2 – Danos na vascularização do tumor	20
1.2.3.3 – Ativação da resposta imune	21
2 – CÂNCER CERVICAL	22
2.1 – Epidemiologia mundial e no Brasil	22
2.2 – Lesões precursoras do câncer cervical e sua relação com o <i>Papillomavirus</i> humano	23
2.3 – Tratamentos de lesões precursoras e do câncer cervical invasivo	25
2.4 – A terapia fotodinâmica no tratamento de lesões cervicais	27
3 - JUSTIFICATIVA	29
4 - OBJETIVOS	30
4.1 - Objetivo geral	30
4.2 - Objetivos específicos	30
5 - Referências bibliográficas	32
6 - CAPÍTULO II	41
6.1 - Artigo	42
7 - CAPÍTULO III	62
7.1 - Conclusões	62
7.2 - Perspectivas futuras	63

CAPÍTULO I

1 - INTRODUÇÃO

1.1 - Terapia fotodinâmica: princípios e aplicações

A terapia fotodinâmica (TFD) pode ser definida como uma alternativa e promissora categoria de tratamento que emprega a combinação de luz, oxigênio e um composto fotossensibilizador (FS) para o tratamento de uma variedade de patologias de caráter oncológico (1), cardiovascular (2), dermatológico (3), oftálmico (4) e infecções bacterianas, virais, fúngicas e parasitárias como a leishmaniose (5). Na TFD, após a aplicação do FS por via tópica ou sistêmica, realiza-se a iluminação do tecido alvo com luz em comprimento de onda específico, que, na presença de oxigênio, leva à geração de espécies citotóxicas e, conseqüentemente, à morte celular e destruição de tecidos alvo (6).

Os primeiros relatos na literatura (Figura 1) de um "efeito fotodinâmico" foram fornecidos por Raab e Von Tappeiner (7, 8). Eles demonstraram que certos corantes como a acridina, um derivado do antraceno, na presença de luz eram capazes de gerar algum tipo de efeito fototóxico nos microrganismos, de forma que a exposição à luz solar rapidamente resultava em morte celular. Em 1948, Figge e colaboradores (9) resumiram uma série de estudos mostrando que as porfirinas, classificadas como FS de primeira geração, quando fornecidas exogenamente se acumulavam seletivamente em tumores murinos. Este estudo foi posteriormente estendido para incluir pacientes com câncer, baseando-se na utilização da injeção de uma preparação bruta de hematoporfirina que conduzia à fluorescência seletiva do tumor (10). O campo da TFD clínica avançou quando um grupo de médicos da Clínica Mayo nos Estados Unidos relatou que a fluorescência do tumor em pacientes foi aumentada quando um derivado da hematoporfirina foi empregado (11, 12). Após esses estudos, a abreviatura 'HPD' foi usada para se referir a este derivado da hematoporfirina não caracterizado. Estudos posteriores revelaram que consistia em uma mistura de monômeros, dímeros e oligômeros da porfirina (13).

Uma preparação semi-purificada da HPD conhecida como Photofrin[®] foi o primeiro FS a obter aprovação regulatória para tratamento de vários tipos de câncer em muitos países do mundo, incluindo os Estados Unidos (15). Nas últimas décadas, a TFD vem se mostrando eficaz no tratamento dos cânceres de bexiga (16), pulmão (17), esôfago (18), e cabeça e pescoço (19). Além disso, vem sendo considerada como o tratamento ideal para muitos casos de câncer de pele do tipo não-melanoma (20). Outras indicações para a TFD são: tratamento

da degeneração macular da retina (síndrome oftálmica) (21), psoríase (22), artrite reumatoide (23), leishmaniose (24), acne severa (25) e periodontite (26).

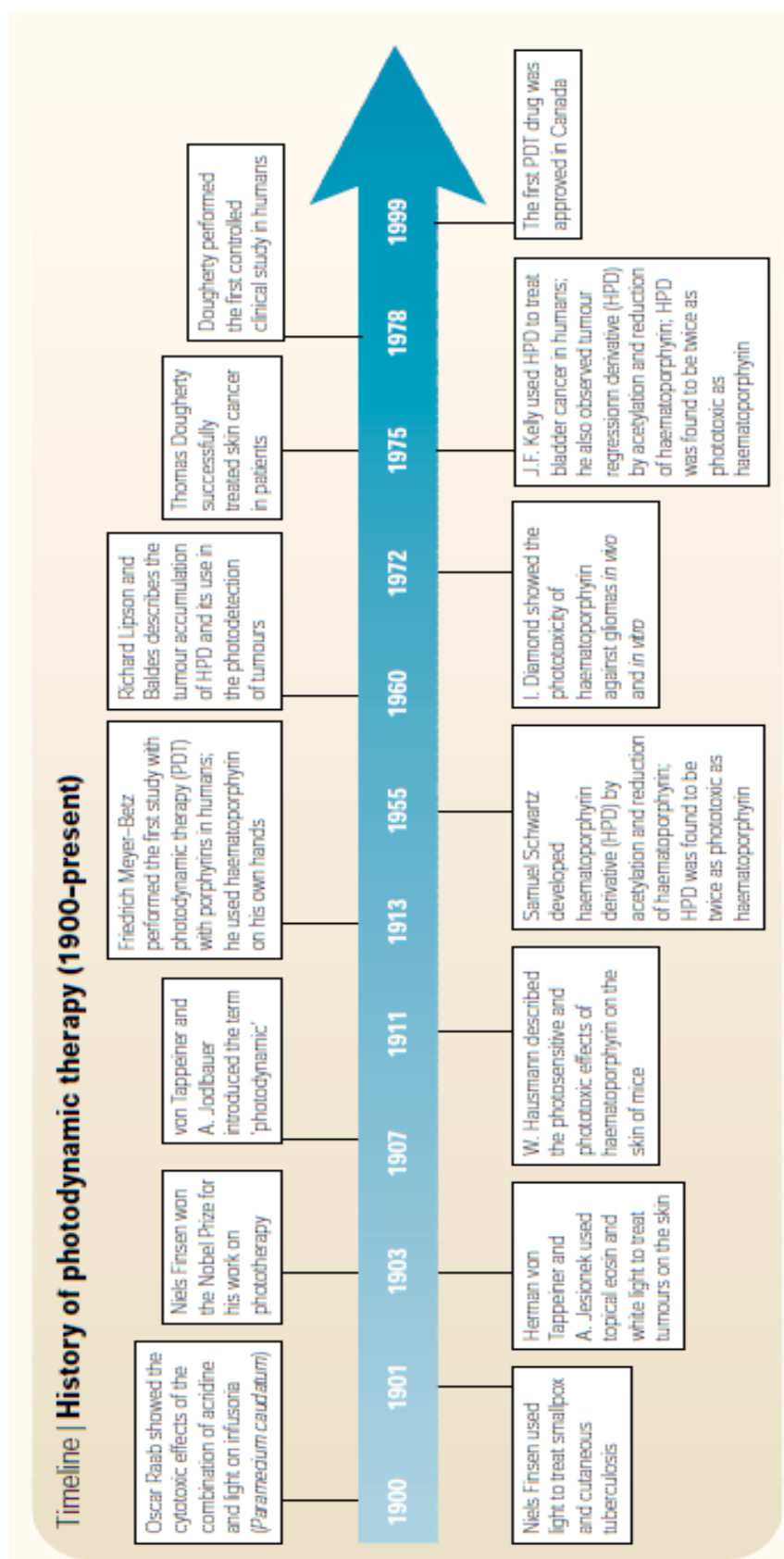


Figura 1 – Linha do tempo resumindo a evolução da TFD (14).

Diante do atual cenário pandêmico, especulações sobre a utilização da TFD no combate ao novo coronavírus também foram relatadas na literatura. Bagnato e colaboradores (27, 28) sugeriram uma possível utilização da TFD no tratamento da doença causada pelo SARS CoV-2 (COVID-19). Eles argumentam que a TFD pode ser uma ferramenta contra a COVID-19 e possíveis futuros surtos, mesmo considerando que o TFD não é uma "ferramenta de matança viral", ou seja, capaz de combater o vírus de forma sistêmica, mas ela pode ser aplicada como uma eficiente terapia para diminuir a carga microbiana (viral e bacteriana) no trato respiratório.

1.2 – O tratamento do câncer e a terapia fotodinâmica

Apesar do progresso na pesquisa básica que propiciou uma melhor compreensão da biologia tumoral e levou ao desenho de novas gerações de medicamentos direcionados às células tumorais, grandes ensaios clínicos recentes para o tratamento do câncer, com algumas exceções notáveis, foram capazes de detectar pequenas melhorias nos resultados do tratamento (29, 30). Além disso, o número de novos medicamentos aprovados clinicamente é baixo (31). O surgimento de técnicas sofisticadas de genômica, proteômica e bioinformática possibilitaram uma visão da complexa interação de numerosos genes celulares e elementos genéticos reguladores que são responsáveis pela manifestação de fenótipos cancerígenos. Com o uso de tecnologias genômicas modernas, a enorme complexidade do câncer está começando a ser desvendada (32).

O tratamento do câncer pode envolver uma ou mais técnicas como radioterapia, cirurgia e terapia sistêmica. A radioterapia, com sua natureza minimamente invasiva, pode tratar o câncer mesmo quando o tumor está misturado com tecido normal, permitindo também flexibilidade no ajuste de regimes de dosagem de acordo com as necessidades da doença (33, 34). A cirurgia é utilizada no tratamento do estágio inicial doença. Os pacientes de baixo risco são frequentemente tratados apenas com cirurgia, mas em muitos casos, uma combinação de tratamentos é necessária. Na doença metastática, a terapia sistêmica é a principal modalidade terapêutica, pois a disseminação do quimioterápico pela corrente sanguínea facilita o acesso aos locais de disseminação das células tumorais. As terapias sistêmicas incluem terapia hormonal, terapia direcionada, terapia imunológica e quimioterapia (35).

As drogas citotóxicas utilizadas na quimioterapia danificam as células em proliferação, porém a não seletividade destes agentes citotóxicos é uma grande desvantagem, e sua capacidade em causar danos em células normais significa que a cura com a

quimioterapia nem sempre é alcançada. Várias estratégias têm sido adotadas para aumentar o efeito antitumoral da quimioterapia, isso inclui a combinação de drogas com diferentes mecanismos de ação, utilização de sistemas de entrega de medicamentos diretamente ao tumor e superação dos mecanismos de resistência celular (36).

A resistência à quimioterapia é uma das principais razões para falha do tratamento, e em qualquer tipo de tumor geralmente há uma combinação de diferentes mecanismos que contribuem para essa resistência. Embora existam estratégias em desenvolvimento para tentar reverter à resistência às drogas quimioterápicas disponíveis, atualmente a única escolha para os médicos é mudar para um medicamento ou combinação citotóxica diferente da já utilizada. A ausência de uma alternativa válida normalmente anuncia a cessação da terapia medicamentosa ativa e uma mudança para o controle sintomático da doença (35).

Neste sentido, a TFD tem o potencial de atender a muitas necessidades médicas ainda não alcançadas. Embora ainda emergente, já é uma modalidade terapêutica de sucesso e clinicamente aprovada, utilizada para o tratamento de doenças neoplásicas e não neoplásicas (37). Esta técnica é constituída de 3 componentes essenciais: FS, luz e oxigênio (14, 38). Juntos eles iniciam uma reação fotoquímica que culmina na geração de espécies reativas de oxigênio (EROs), incluindo o oxigênio singlete ($^1\text{O}_2$), o qual pode levar à morte celular por apoptose ou necrose (37).

Os efeitos antitumorais da TFD derivam de 3 mecanismos inter-relacionados: efeitos citotóxicos diretos sobre células tumorais, danos à vasculatura tumoral e indução de uma reação inflamatória robusta que pode levar ao desenvolvimento de imunidade sistêmica. A contribuição relativa desses mecanismos depende em grande parte do tipo e da dose do FS usado, do tempo entre a administração do FS e a exposição à luz, da dose total de luz e sua taxa de fluência, da concentração de oxigênio no tumor e talvez de outras variáveis ainda pouco conhecidas. Portanto, a determinação das condições ideais para o uso da TFD requerem uma coordenação de esforços interdisciplinares (37).

1.2.1 - Fotossensibilizadores

Entre as características ideais de um FS estão a capacidade de localização específica em tecido neoplásico, o intervalo pequeno entre a administração da droga e a seletividade por alvos tumorais, a meia-vida curta, ter uma farmacocinética que favoreça a eliminação rápida nos tecidos saudáveis, a ativação por comprimentos de onda que compreenda a janela terapêutica e a capacidade de produzir grandes quantidades de EROs (39). Um FS com característica

físico-química adequada para emprego na TFD deve ainda ser capaz de penetrar na célula tumoral e se acumular em organelas estratégicas como mitocôndria, retículo endoplasmático, lisossomos e complexo de Golgi. A geração de EROs, por parte de um FS fotoativado nessas organelas (principalmente na mitocôndria), pode induzir a morte de células tumorais por apoptose (40).

Outro pré-requisito importante é que o FS possua um longo tempo de vida no estado excitado, dando tempo para que ocorra a transferência de energia e/ou elétrons do FS para a geração do oxigênio em sua forma citotóxica, o $^1\text{O}_2$. Assim, a geração de EROs será suficiente para que o tratamento seja efetivo. No entanto, alguns eventos podem prejudicar essa produção de EROs, dentre eles destacam-se a formação de agregados e a fotodegradação do FS (41, 42). A formação de agregados entre as moléculas do próprio FS pode prejudicar o processo de geração de EROs, uma vez que ocorrerem decaimentos não radiativos por conversão interna, dificultando a transferência de energia do FS para o oxigênio tripleto ($^3\text{O}_2$). Tais agregados tendem a formar-se à medida que aumenta a concentração do FS ou quando o mesmo, de caráter hidrofóbico, está presente num meio aquoso (43).

Em relação à sua solubilidade, os FS lipofílicos são captados pela célula por penetrarem diretamente pela membrana plasmática, e essa captação aumenta em proporção direta com a lipofilia. Já os FS hidrossolúveis são captados por pinocitose (44). Até o momento, não são bem esclarecidos os mecanismos pelos quais ocorre retenção seletiva dos FS nos tecidos malignos. Algumas hipóteses incluem a permeabilidade alterada da membrana celular, o aumento do número e da permeabilidade dos vasos sanguíneos, bem como a drenagem linfática diminuída. Além disso, o pH baixo no fluido intersticial nos tumores facilita a biodistribuição seletiva dos FS (45).

1.2.1.1 – Hipericina, um fotossensibilizador promissor para uso na terapia fotodinâmica

A hipericina (4,5,7,4',5',7'-hexahidroxil-2,2'-dimetilnaftodiantrona) (Figura 2) é um composto natural, biossintetizado por algumas espécies do gênero *Hypericum*, podendo também ser sintetizada quimicamente a partir de uma antraquinona precursora, a emodina antrona (46, 47). A hipericina (HIP) foi primeiramente isolada da espécie *Hypericum perforatum L.*, comumente conhecida como Erva de São João, que apresenta uma ampla aplicação farmacológica, sendo utilizada como antidepressivo, antimicrobiano, anticancerígeno, anti-inflamatório, cicatrizante e etc (48).

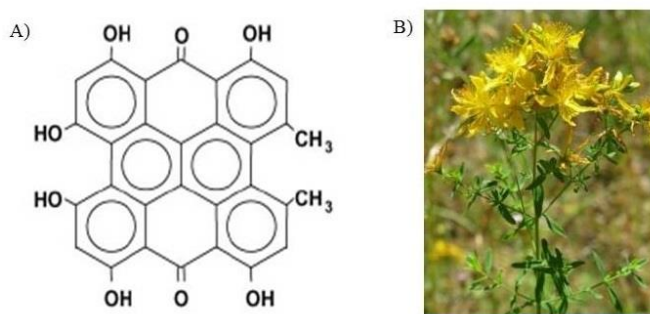


Figura 2 - A) Estrutura química da Hipericina. B) Ilustração da planta Erva de São João (46).

Com relação as suas características/propriedades fotofísicas, ela exibe uma brilhante fluorescência vermelha, em sua forma monomérica pode gerar altas taxas de $^1\text{O}_2$ e radicais livres quando fotoativado com luz de comprimento de onda específico, com baixa toxicidade na ausência de luz, acumulando-se preferencialmente em tecidos neoplásicos (46, 49-51). Os radicais livres e o $^1\text{O}_2$ gerados são responsáveis por induzir a morte por necrose, apoptose, morte associada à autofagia e até mesmo morte celular imunogênica. O mecanismo do tipo II é o responsável pela ativação da morte celular imunogênica, sendo a combinação da TFD com HIP uma estratégia promissora para a imunoterapia, pois provoca a translocação e secreção de padrões moleculares associados a danos (DAMPs) pelas células tumorais, que são capazes de ativar o sistema imune pela ligação a receptores específicos, aumentando a resposta imune antitumoral (52, 53). O efeito inibitório da HIP frente a enzimas relacionadas à regulação da sobrevivência e proliferação celular também colaboram para seu efeito antitumoral eficaz (54). Os mecanismos do tipo I e II da TFD serão discutidos mais a frente no tópico 1.2.3.

Contudo, como a maioria dos FS, a HIP apresenta alta hidrofobicidade e forma agregados em meio aquoso e fluidos corporais (55, 56). As interações hidrofóbicas podem afetar suas propriedades fotofísicas (reduzindo a geração de $^1\text{O}_2$), alterar suas características químicas (baixa solubilidade) e suas propriedades biológicas (mecanismo de ação prejudicado). Portanto, é essencial usar sistemas de entrega (*drug delivery systems*) para superar estes problemas (57, 58).

Uma tecnologia que tem sido bastante explorada nos últimos anos, baseada na nanomedicina, que utiliza sistemas carreadores para compostos hidrofóbicos como a HIP, residem na utilização de nanopartículas formadas por polímeros e sua aplicação tem sido frequentemente estudada como sistemas de entrega para TFD (59, 60).

O copolímero nomeado Plurônico[®] P123 tem sido muito utilizado na produção dessas

nanopartículas carreadoras de fármacos. Ele é composto quimicamente pela combinação de óxido de polietileno (PEO-região hidrofílica) e óxido de polipropileno (região PPO-hidrofóbica) formando um sistema tribloco de PEO e PPO com configuração $(EO)_{21}(PO)_{67}(EO)_{21}$ (59, 61, 62). O procedimento de micelização destes monômeros anfifílicos em meio aquoso consiste na montagem do grupo PPO para criar o núcleo hidrofóbico das micelas, responsável por incorporar as drogas hidrofóbicas. Além disso, os grupos PEO são responsáveis pela estabilização das micelas em meio aquoso, evitando sua adsorção e agregação (63, 64). Nas concentrações utilizadas, esses polímeros não são tóxicos, sendo então biocompatíveis, estáveis em fluidos biológicos, não são capazes de serem reconhecidos por macrófagos e não se ligam a proteínas, tendo uma baixa concentração micelar crítica (CMC) e farmacocinética favorável (64-67).

Recentemente foram publicados estudos importantes sobre as características dos plurônicos com diferentes FS, incluindo a HIP. Esses estudos mostraram a alta eficiência das micelas de Pluronic[®] P123 carregadas com HIP para uso em TFD frente a bactérias intestinais e células de carcinoma do cólon (68), células de câncer de mama (69) e frente a células planctônicas e prevenindo a formação de biofilmes formados por diferentes espécies do gênero *Candida* (70).

1.2.2 - Fontes de luz

As fontes de luz disponíveis para TFD pertencem a três grandes grupos: as lâmpadas de amplo espectro, as lâmpadas de diodo e os lasers. As fontes de luz descritas em estudos clínicos em TFD incluem as lâmpadas halógenas projetoras de diapositivos, as lâmpadas de diodo (LED) e, mais recentemente, a luz intensa pulsada (71). A luz deve ser levada para a região alvo do tratamento e para isso uma variedade de procedimentos foi desenvolvida (44). Fontes de luz podem ser introduzidas de forma confiável em praticamente todos os sítios da anatomia humana. Cabos de fibra óptica ou LED podem acessar o leito do tumor por introdução direta durante cirurgia ou endoscopia (72).

1.2.3 - Mecanismos de ação da terapia fotodinâmica

A TFD tem sido cada vez mais utilizada no tratamento de cânceres e seu mecanismo de ação ocorre graças a uma sequência de eventos físicos, químicos e biológicos (42). De forma simplificada, um agente FS é introduzido no tecido alvo e então ativado pela luz. Quando na presença de oxigênio, este FS ativo gera uma reação fotodinâmica (Figura 3) e

isso ocorre em uma interação complexa de tempo e espaço que resulta na destruição do tumor e preservação do tecido normal (72).

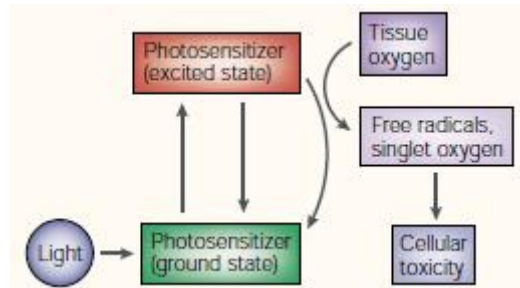


Figura 3 – Mecanismo de ação da TFD (14).

Um dos fatores que determina o resultado da TFD é como o FS interage com as células dentro do tecido alvo ou tumor. A principal característica dessa interação é a localização subcelular do FS, uma vez que os FS podem se localizar dentro de muitas organelas celulares diferentes como as mitocôndrias, lisossomos, retículo endoplasmático, aparelho de Golgi e membranas plasmáticas (73).

A captação do FS pelas células cancerosas é crucial para que a TFD seja eficaz, uma vez que EROs tem meia-vida curta e só podem atuar próximos ao local de geração. O tipo de fotodano que ocorre em células carregadas com um FS e iluminadas depende da localização subcelular precisa do FS. Assim, compreender a localização do FS é um princípio importante a considerar ao escolher o FS mais eficaz para cada aplicação (73).

O tratamento com TFD para cânceres consiste em duas etapas. Na primeira, o FS acumula-se preferencialmente nas células tumorais após sua administração local ou sistêmica. Na segunda, o tumor fotossensibilizado é exposto à luz de comprimento de onda específico que coincide com o espectro de absorção do FS. Esse agente ativado transfere energia ao oxigênio molecular, gerando EROs (74). A subsequente oxidação dos lipídios, aminoácidos e proteínas induz a necrose e/ou apoptose. Além disso, as EROs indiretamente estimulam a transcrição e liberação de mediadores da inflamação (44). A oxidação dos constituintes celulares pelas EROs danifica as membranas plasmáticas e as organelas celulares, com subsequente alteração de permeabilidade e função de transporte entre os meios intra e extracelular (38). Os alvos da TFD incluem as células tumorais, a microvasculatura do tecido e os sistemas inflamatório e imune do hospedeiro (Figura 4). A combinação de todos esses componentes é necessária para o controle do tumor a longo prazo (75).

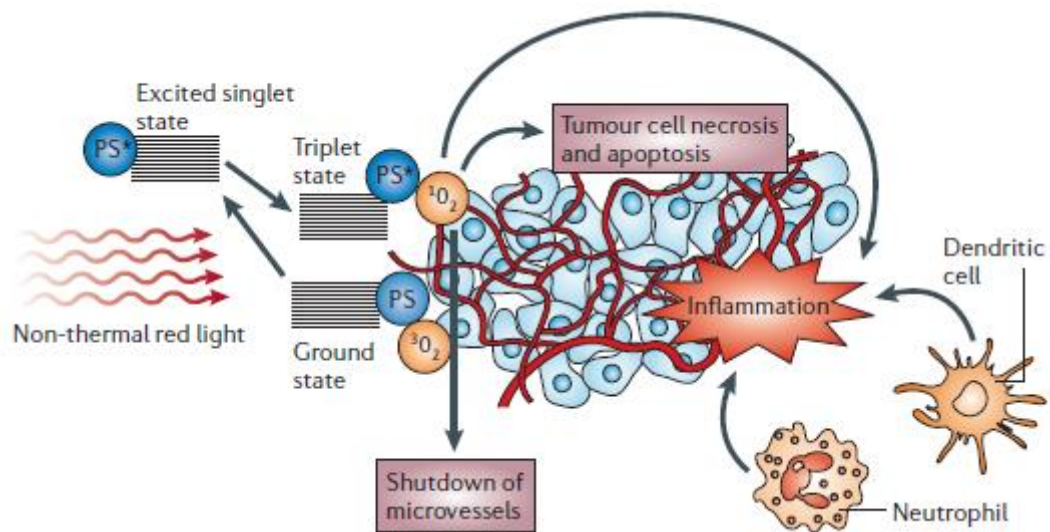


Figura 4 – Mecanismos de ação da TFD nos tumores (76).

As reações fotobiológicas restringem-se ao local de acúmulo do FS que são expostas à luz visível (14, 77). A seletividade da TFD é produzida pelo direcionamento preferencial do FS para o tecido alvo e pela habilidade de se ativar o FS por iluminação sítio específica. Dessa forma, a TFD permite a destruição seletiva dos tumores enquanto mantém intacto o tecido adjacente normal (78). O processo fotodinâmico inicia-se quando o FS, no estado fundamental, absorve um fóton de luz e sofre decaimentos sequenciais que resultam em reações de transferência de energia intramolecular, originando o estado tripleto excitado, capaz de reagir com o oxigênio molecular tecidual (tripleto), ocorrendo transferência de energia intermolecular. O oxigênio molecular absorve energia e origina o oxigênio singleto ($^1\text{O}_2$) que é citotóxico (77, 79). As reações de fotoxidação via $^1\text{O}_2$ são as responsáveis pela eliminação das células cancerosas (80).

Os mecanismos de produção de EROs durante o processo fotodinâmico podem ser do tipo I e/ou tipo II (Figura 5). O radical superóxido ($\text{O}_2^{\cdot-}$) é gerado no mecanismo tipo I, isto é, pela transferência de elétrons do FS, excitado pela luz, para o estado fundamental do oxigênio ($^3\text{O}_2$) (81). Já o $^1\text{O}_2$ é gerado no mecanismo tipo II, ou seja, pela transferência de energia do FS excitado para o $^3\text{O}_2$. O $\text{O}_2^{\cdot-}$ pode favorecer o aparecimento de outras espécies, como o radical hidroxila (HO^{\cdot}) e o peroxinitrito (ONOO^-). Tais espécies reativas são muito mais agressivas para o tecido tumoral do que o $\text{O}_2^{\cdot-}$. O surgimento dessas espécies, bem como do $^1\text{O}_2$, pode induzir a morte das células cancerígenas, principalmente por apoptose (82-85).

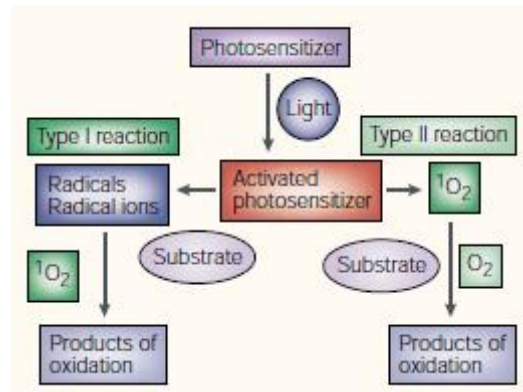


Figura 5 – Mecanismos do tipo I e II na TFD (14).

1.2.3.1 - Tipos de morte celular

Embora a TFD possa mediar muitos eventos de sinalização celular, seu objetivo principal é matar as células (Figura 6). Uma pesquisa recente elucidou muitos caminhos pelos quais as células de mamíferos podem morrer, e algumas das maneiras que a TFD pode iniciar esses processos. A concentração, propriedades físico-químicas e localização subcelular do FS, a concentração de oxigênio (86-88), o apropriado comprimento de onda, a intensidade da luz, e o tipo de célula podem influenciar no modo e extensão da morte celular (89).

Kerr e colaboradores (90) foram os primeiros a fornecer evidências de que as células podem sofrer pelo menos dois tipos distintos de morte celular: o primeiro tipo é conhecido como necrose, uma forma violenta e rápida de degeneração afetando extensas populações de células, caracterizadas por inchaço do citoplasma, destruição de organelas e ruptura da membrana plasmática, levando a liberação de conteúdo intracelular e inflamação. A necrose tem sido referida como morte acidental da célula, causada por dano físico ou químico e geralmente é considerada um processo não programado. Células necrosadas se caracterizam por um núcleo picnótico, edema citoplasmático e progressiva desintegração das membranas citoplasmáticas, sendo que todos esses processos levam à fragmentação celular e liberação de material para o compartimento extracelular.

Outra via de morte celular é denominada apoptose. Ela é considerada como um “suicídio celular” a fim de eliminar células indesejáveis ou desnecessárias ao organismo, mediante a ativação de um programa bioquímico de desmontagem dos componentes celulares, internamente controlado, que requer energia e não envolve inflamação (91). A morte celular programada não é sinônimo de apoptose, embora a maior parte dos processos de morte celular programada (MCP) em animais ocorra por apoptose (92), pois a MCP está relacionada com uma morte celular de caráter evolutivo, de células que estão em constante renovação para a

manutenção da homeostase dos organismos (93). No entanto, a apoptose pode ser induzida, por exemplo, por drogas anticâncer. Nesses casos, o programa de morte celular é iniciado, mas sem o tratamento das células, elas não morreriam; ou seja, não estamos lidando com um processo de MCP (93). Nessa via, quando as células entram em processo apoptótico, elas apresentam retração do citoplasma celular, também são identificadas bolhas na membrana plasmática e podem ser observadas geralmente rodeadas por células vizinhas de aparência saudável. Suas organelas e a membrana plasmática retêm sua integridade por um longo período. *In vitro*, as células apoptóticas são fragmentadas em várias vesículas esféricas envoltas por uma membrana. *In vivo*, esses corpos apoptóticos são eliminados por fagócitos. A apoptose requer a ativação da transcrição de genes específicos, incluindo a ativação de endonucleases, consequente degradação do DNA em fragmentos oligonucleossômicos e ativação de caspases (89).

A autofagia é um processo catabólico vital no qual as células degradam seu próprio conteúdo por meio dos lisossomos. Existem várias formas de autofagia, dependendo dos substratos que estão envolvidos e sendo processados e, na formação, ou não de vesículas de membrana dupla (94-96). A autofagia pode ocorrer após a TFD, sendo associada com maior sobrevivência em níveis baixos de fotodano para algumas células. Ainda, a autofagia pode se tornar uma via de morte celular se a apoptose é inibida ou quando as células tentam reciclar os constituintes danificados além de sua capacidade de recuperação (97). Devido à alta reatividade das EROs geradas (98-100) após a TFD, a autofagia é iniciada para remover organelas danificadas oxidativamente, como mitocôndrias e retículo endoplasmático que são alvos dos FS (101-103). Porém, a autofagia parece poder contribuir para a sobrevivência celular, e por outro lado pode também exercer uma função antitumorigênica. Uma combinação de inibidor de autofagia com TFD pode promover morte apoptótica, potencializando assim o efeito do tratamento (104). Portanto, a autofagia pode proteger células e ajudá-las a tolerar a TFD, no entanto, se houver um alto nível de autofagia, pode ocorrer a morte celular (105).

1.2.3.2 - Danos na vascularização do tumor

A viabilidade das células tumorais depende da quantidade de nutrientes fornecidos pelos vasos sanguíneos. Por sua vez, a formação e a manutenção dos vasos sanguíneos dependem de fatores de crescimento produzidos pelo tumor ou por células hospedeiras (106, 107). Assim, atingir a vasculatura do tumor é uma abordagem promissora para o tratamento

do câncer. Nos últimos 15 anos, uma série de trabalhos utilizando a TFD relataram um colapso microvascular (108-111), levando a hipóxia tecidual grave e anóxia (112-114). O colapso microvascular pode ser prontamente observado após a TFD (108, 112), levando a hipóxia tumoral pós-TFD grave e persistente (112). Os mecanismos subjacentes aos efeitos vasculares da TFD diferem muito quando se utilizam diferentes FS (115). A TFD também pode levar à constrição de vasos por meio da inibição da produção ou liberação de óxido nítrico pelo endotélio (10).

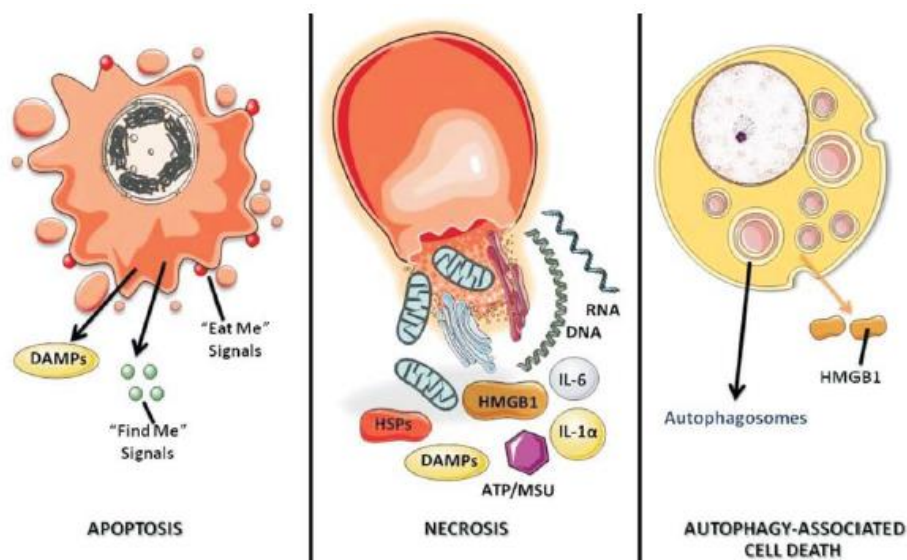


Figura 6 – Três principais vias de morte celular, seus perfis morfológicos e imunológicos (37).

1.2.3.3 - Ativação da resposta imune

É provável que o controle do tumor em longo prazo seja uma combinação de efeitos diretos da TFD sobre a lesão e sua vasculatura em combinação com a regulação do sistema imunológico. Quando a TFD induz a necrose de tumores e de sua vasculatura, uma resposta em cascata do sistema imunológico também é iniciada (116). A liberação de mediadores inflamatórios ocorre a partir da região tratada, que inclui várias citocinas, fatores de crescimento e proteínas. Essa liberação estimula vários glóbulos brancos a serem ativados, incluindo neutrófilos e macrófagos, que convergem para a região do tratamento. Esta ativação pode ser a responsável pela ocorrência da morte significativa de células tumorais por intermédio destas células imunes (117, 118).

Após a chegada ao local do tumor, os macrófagos fagocitam as células cancerosas que a TFD danificou e apresentam proteínas tumorais para os linfócitos T CD4 auxiliares, que

então ativam linfócitos T CD8. Essa reação imune ocorre não apenas no local da TFD, mas também pode ocorrer no tecido linfático regional e distante. As células T citotóxicas podem não só causar morte por necrose, mas também podem induzir apoptose. Clinicamente, os pacientes tratados com TFD apresentam níveis elevados de várias citocinas e avaliações histológicas de tumores tratados rotineiramente mostram infiltração de células imunológicas, novamente apontando para o efeito imunomodulador da TFD (72).


2 - CÂNCER CERVICAL

2.1- Epidemiologia mundial e no Brasil

O câncer cervical é uma doença evitável e curável se detectado precocemente e tratado adequadamente. Ainda assim continua sendo uma das causas mais comuns de morte relacionada ao câncer em mulheres em todo o mundo. O número anual de novos casos de câncer cervical foi projetado para aumentar de 570.000 para 700.000 entre 2018 e 2030 e o número anual de mortes projetado para aumentar de 311.000 para 400.000 mortes (119). Mundialmente, o câncer cervical é o quarto tipo mais comum de câncer em mulheres, excetuando-se os casos de câncer de pele não melanoma. Para o ano de 2018 foram estimados 569.847 novos casos e 311.365 mortes, sendo a quarta causa mais frequente de morte por câncer em mulheres (120).

No Brasil, o diagnóstico precoce tem avançado, de modo que na década de 1990, 70% dos casos diagnosticados eram da doença invasiva e atualmente, 44% dos casos são de lesão precursora do câncer (121). Ainda assim, excluindo o câncer de pele não melanoma, o câncer cervical é o terceiro mais incidente na população feminina, com estimativa de 16.710 novos casos para o ano de 2020, representando 7,5% de todos os casos de câncer entre as mulheres (Figura 7) (122).

Distribuição proporcional dos dez tipos de câncer mais incidentes estimados para 2020 por sexo, exceto pele não melanoma*

Localização primária	Casos	%			Localização primária	Casos	%
Próstata	65.840	29,2%			Mama feminina	66.280	29,7%
Cólon e Reto	20.540	9,1%			Cólon e Reto	20.470	9,2%
Traqueia, Brônquio e Pulmão	17.760	7,9%			Colo do útero	16.710	7,5%
Estômago	13.360	5,9%			Traqueia, Brônquio e Pulmão	12.440	5,6%
Cavidade Oral	11.200	5,0%			Glândula Tireoide	11.950	5,4%
Esôfago	8.690	3,9%			Estômago	7.870	3,5%
Bexiga	7.590	3,4%			Ovário	6.650	3,0%
Linfoma não Hodgkin	6.580	2,9%			Corpo do útero	6.540	2,9%
Laringe	6.470	2,9%			Linfoma não Hodgkin	5.450	2,4%
Leucemias	5.920	2,6%			Sistema Nervoso Central	5.230	2,3%

* Números arredondados para múltiplos de 10

Figura 7 - Distribuição proporcional dos dez tipos de câncer mais incidentes estimados para 2020 por sexo, exceto câncer de pele não melanoma no Brasil (122).

Apesar de avanços na prevenção, triagem, diagnóstico e tratamento nas últimas décadas, as disparidades globais da incidência e mortalidade pelo câncer cervical são significativas e sua prevalência entre as mulheres ainda continuam preocupantes (123).

2.2 - Lesões precursoras do câncer cervical e sua relação com o *Papillomavirus humano*

O câncer cervical apresenta história natural longa, começando com uma infecção persistente por um ou mais genótipos oncogênicos do *Papillomavirus humano* (HPV), seguido por alterações celulares precursoras, denominadas lesões intraepiteliais escamosas cervicais (SIL) e, finalmente, carcinoma invasor, caso as alterações celulares não sejam revertidas ou tratadas (124). A zona de transformação ou junção escamo-colunar é o sítio mais comum para o desenvolvimento do câncer cervical. Após a infecção das células basais pelo HPV, a progressão para o câncer invasivo ocorre predominantemente a partir das SIL de baixo grau (LSIL) para as de alto grau (HSIL) e destas para câncer cervical invasivo (125). A maioria das LSIL regridem em períodos relativamente curtos ou não progridem a HSIL, sendo que em torno de 57% dos casos de LSIL regridem, 11% progridem para HSIL e apenas 1% progride à neoplasia invasiva em decorrência principalmente da associação entre a infecção persistente por genótipos de HPV de alto risco oncogênico (HPV-AR) com fatores ambientais e genéticos envolvidos na carcinogênese (126). Cabe ressaltar que a lesão cervical não tem que passar obrigatoriamente por todas essas etapas para chegar ao câncer invasor. O período de evolução de uma lesão cervical inicial para a forma invasiva é de cerca de 10 a 20 anos (127) (Figura 8) Em virtude desta evolução longa composta por fases pré-clínicas, detectáveis e curáveis, é o câncer que apresenta um dos mais altos potenciais de prevenção e cura (128).

A infecção por HPV é iniciada quando a partícula viral penetra nas células basais do epitélio escamoso (Figura 8), pois este tipo celular é capaz de se dividir ativamente (130). As proteínas virais fazem com que estas células mantenham o processo de divisão celular em resposta ao início do processo de diferenciação, o que é necessário para que a progênie viral seja produzida. O estabelecimento e a manutenção dos genomas do HPV nas células infectadas estão associados à expressão dos genes precoces *E5*, *E6* e *E7*, que codificam suas respectivas oncoproteínas, assim como das proteínas de replicação *E1* e *E2*. Durante a divisão celular, as células basais deixam a camada basal, migram para a região suprabasal e começam a se diferenciar. Nesta fase, o genoma viral é dividido entre as células-filhas, que, ao migrarem para as camadas superiores do epitélio durante o processo de diferenciação,

continuam com o ciclo celular ativo. Nas camadas mais diferenciadas do epitélio, o DNA viral é empacotado em novos capsídios e a progênie do vírus é liberada a partir da camada superior do epitélio (131).

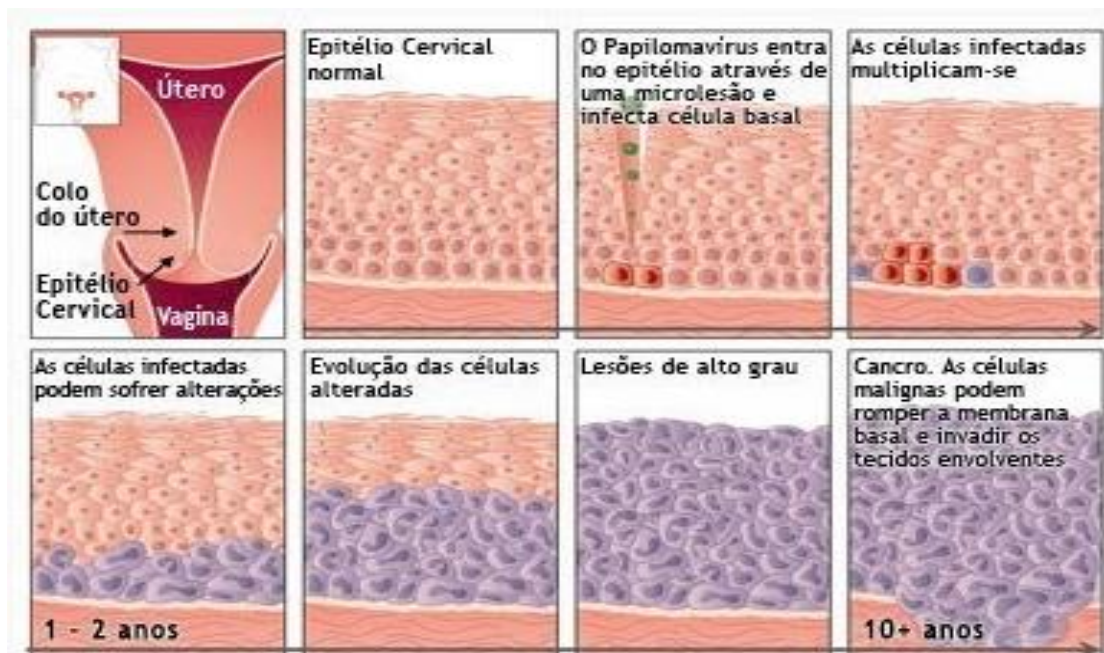


Figura 8 – Representação esquemática da carcinogênese cervical induzida por HPV (129).

O desenvolvimento do câncer cervical está associado à perda da regulação do ciclo produtivo do HPV, evento observado em infecções persistentes pelos HPV-AR, que tendem a integrar o seu genoma ao da célula hospedeira (132, 133). Durante o processo de integração, o genoma viral pode perder o gene *E4* e parte do gene *E2*, que exercem função de controle da transcrição dos demais genes virais. Como consequência da perda de função de *E2*, haverá um aumento da expressão dos genes *E6* e *E7*. Assim, o potencial oncogênico dos HPV depende da expressão de genes *E6/E7*, cujos produtos, as proteínas *E6* e *E7*, têm como alvo principal as proteínas p53 e pRb do genoma do hospedeiro, induzindo descontrole do ciclo celular (134, 135). Neste cenário, não haverá amadurecimento das células hospedeiras e nem produção de novas partículas virais (133, 135, 136). Assim, a capacidade dos HPV-AR de transformação celular é claramente associada à atividade das oncoproteínas *E6* e *E7*, mas essa transformação do epitélio do hospedeiro pode levar décadas (137, 138). Nas LSIL, a maior parte do genoma viral persiste na forma episossomal, mas nas HSIL estão frequentemente integrados ao genoma das células hospedeiras, sendo que a integração parece favorecer a transformação maligna (139, 140). Sendo assim, quando infectadas pelo HPV, as células escamosas do epitélio cervical podem apresentar alterações, de modo que seu ciclo celular se desregula, aumentando o número de mitoses e desenvolvendo lesões epiteliais de diferentes graus (LSIL e HSIL).

Estas lesões, em sua maioria regredem ou então, menos frequentemente, evoluem para formas malignas, ou seja, para o câncer cervical (135).

Nas duas últimas décadas, diversos estudos associaram à infecção genital pelo HPV como principal fator de risco para o desenvolvimento de câncer cervical, sendo este vírus responsável por 99,7% dos casos (141, 142). A infecção genital pelo HPV é a infecção sexualmente transmissível (IST) de origem viral mais comum no mundo sendo responsável por formas clínicas assintomáticas e/ou benignas e ainda, por formas malignas na região orofaríngea e genital (143). Infecções persistentes por genótipos de HPV-AR são o principal fator no desenvolvimento de câncer cervical. Os genótipos de HPV-AR são 16, 18, 31, 33, 35, 39, 45, 51, 52, 56, 58, 66, 68, 73, 69 e 82, sendo que mundialmente os mais frequentes são os genótipos 16 e 18, prevalecendo em aproximadamente 70% dos cânceres cervicais (144-147).

A grande maioria das mulheres infectadas pelo HPV são capazes de eliminar espontaneamente o vírus e somente uma minoria das infectadas irão manter o vírus com possibilidade de progressão (137). Os mecanismos de proteção mais importantes são os de supressão ou eliminação do HPV por meio da resposta imune mediada por células de defesa nos dois primeiros anos de exposição ao vírus (148). A infecção persistente por genótipos de HPV-AR é considerada como o fator mais importante para o desenvolvimento das lesões cervicais e progressão para o câncer cervical. Porém, considerando as elevadas taxas de regressão espontânea, não é suficiente para o desenvolvimento do câncer cervical (137). Alguns cofatores que podem contribuir na carcinogênese cervical têm sido descritos como por exemplo a elevada carga viral, número de gestações, uso de contraceptivos orais, tabagismo, imunossupressão, predisposição genética e infecção conjunta com outras ISTs (148).

2.3- Tratamentos de lesões precursoras e do câncer cervical invasivo

O tratamento apropriado das lesões precursoras (HSIL na citologia, neoplasias intraepiteliais cervicais-NIC graus 2 e 3 na histologia e adenocarcinoma in situ) é meta prioritária para a redução da incidência e mortalidade pelo câncer do colo uterino (149). As diretrizes brasileiras recomendam, após confirmação colposcópica ou histológica, o tratamento excisional das HSIL, por meio de exérese da zona de transformação (EZT) por eletrocirurgia (150). Quando a colposcopia é satisfatória, com achado anormal compatível com a citologia, restrito à ectocérvice ou até o primeiro centímetro do canal endocervical, o procedimento deve ser realizado ambulatorialmente, permitindo o tratamento imediato das lesões (151). O objetivo desta estratégia é facilitar o acesso das mulheres ao tratamento, diminuindo a

ansiedade, as possibilidades de perdas no seguimento e os custos da assistência (152). No caso de colposcopia insatisfatória, ou quando a lesão ultrapassa o primeiro centímetro do canal, o tratamento indicado é a conização, realizada preferencialmente por técnica eletrocirúrgica (149).

Entre os tratamentos mais comuns para o câncer cervical invasivo estão a cirurgia e a radioterapia. O tipo de tratamento dependerá de fatores como estadiamento da doença, o tamanho do tumor e fatores pessoais, como idade e desejo de ter filhos (153). Para os estágios iniciais do câncer cervical invasivo, pode-se usar a cirurgia ou radioterapia combinada com quimioterapia. Para os estágios posteriores, a radiação combinada com quimioterapia geralmente é o tratamento principal. A quimioterapia (por si só) costuma ser usada para tratar o câncer cervical avançado (154).

Porém, as opções de tratamento com efeitos citotóxicos para evitar o avanço do câncer cervical ainda são limitadas. A quimioterapia pode funcionar como um adjuvante, quando empregada logo após o tratamento primário do tumor por cirurgia ou radioterapia. Pode ser também um neoadjuvante, quando realizada antes do tratamento local, com o objetivo de reduzir o tamanho tumoral e propiciar condições adequadas para o tratamento cirúrgico e/ou radioterápico subsequente. Ainda, existe a quimio-radioterapia concomitante, que é administrada simultaneamente com a radioterapia para potencializar o efeito do tratamento, que pode aumentar a sobrevida da paciente. Porém, os efeitos colaterais tendem a ser piores (155).

Os quimioterápicos mais usados para tratamento do câncer cervical incluem cisplatina, carboplatina, paclitaxel, topotecano e gemcitabina. A cisplatina é o agente citotóxico mais efetivo contra o câncer cervical metastático, além disso, aumenta a sensibilidade à radioterapia (156). Os efeitos colaterais da quimioterapia dependem do tipo da droga, da dose administrada e do tempo de duração do tratamento. Estes efeitos são temporários e podem incluir especialmente náuseas e vômitos, perda de apetite, feridas na boca, perda de cabelo, inflamações na boca, infecção, hemorragia ou hematomas após pequenos cortes ou lesões e falta de ar (155).

Nos últimos anos, a taxa de sobrevivência por 5 anos para os pacientes com câncer cervical melhorou significativamente devido à aplicação de quimioradioterapia concomitante. No entanto, a recorrência local e metástases ainda são manifestações pós-tratamento comuns em pacientes com câncer cervical avançado. Uma vez que ocorre falha no pós-tratamento, o prognóstico torna-se pior: as taxas de sobrevivência de 1 ano para essas pacientes são menores que 20% (157). Além disso, vários efeitos colaterais são produzidos influenciando a

qualidade de vida da paciente (158). Apesar destes fatos alarmantes, ainda faltam métodos de tratamento eficazes.

As características de alta seletividade pelos tecidos tumorais, o risco reduzido de eventos adversos em comparação com métodos convencionais (cirurgia, radiação ou quimioterapia) e baixo risco de complicações graves podem tornar a TFD uma alternativa eficaz na abordagem para o tratamento do câncer cervical invasivo, neoplasias intraepiteliais cervicais e infecções cervicais por HPV, particularmente em mulheres jovens (159, 160).

2.4 - A TFD no tratamento de lesões cervicais

No Brasil, as NIC podem ser tratadas de forma não invasiva por meio da TFD utilizando um protocolo clínico inovador derivado de uma pesquisa que teve início em 2011, sob a coordenação do Prof. Dr. Vanderlei Bagnato, do Grupo de Óptica do Instituto de Física de São Carlos (IFSC/USP) (161). O protocolo utiliza um creme que contém uma substância chamada aminolevulinato de metila que é precursora de outra molécula, a protoporfirina IX (PpIX). Essa substância, após ser excitada por um LED vermelho presente em um sistema portátil e versátil produz EROs, eliminando as lesões em apenas 20 minutos de forma não invasiva, preservando o colo do útero das pacientes (162).

Em um relato de caso, Castro e colaboradores (163) descrevem o tratamento de uma paciente de 33 anos de idade com NIC grau 3 com o FS aminolevulinato de metila por via tópica e TFD. Para isso foram aplicados 2,5 g de um creme contendo o aminolevulinato de metila a 20% (p/p) durante a noite. Após esse período, o colo do útero foi iluminado duas vezes, com três semanas de intervalo, usando uma sonda com LEDs. A NIC 3 e o HPV-AR foram eliminados após 120 dias do segundo procedimento e não houve recorrência em 6 meses de acompanhamento, o que foi caracterizado com cura.

Stringasci e colaboradores (164) trataram uma paciente com condilomatose utilizando a TFD e o aminolevulinato de metila em creme a 20% (p/p) como FS. A paciente foi tratada por 6 semanas, com um total de seis sessões, com sete dias de intervalo entre cada sessão. Após o tratamento, o tecido apresentou ausência clínica de lesão e ausência aparente de cicatriz, com bom resultado estético e preservando a sensibilidade da região. No acompanhamento da paciente por onze meses não foi verificado recorrência das lesões. Condiloma ou verrugas genitais afetam os tecidos da área genital devido a infecções induzidas pelo HPV. Existem algumas terapias tópicas indicadas para o tratamento dessas lesões, mas todas apresentam uma alta taxa de recorrência. A TFD está se mostrando uma estratégia

interessante para o tratamento dessas lesões, sendo capaz também de tratar células infectadas pelo vírus em lesões subclínicas.

JUSTIFICATIVA

A infecção genital por HPV é a infecção sexualmente transmissível viral mais frequente em todo o mundo e está diretamente relacionada ao desenvolvimento do câncer cervical, que atualmente permanece com grande incidência mundial e constitui-se de um importante problema de saúde pública, causando significativa morbidade e mortalidade feminina. No Brasil, o câncer cervical é a terceira causa mais comum de câncer na população feminina, sendo a quarta causa de morte por câncer em mulheres. A infecção cervical persistente por HPV-AR é uma causa necessária para induzir à carcinogênese cervical. As opções de tratamento para obter efeitos citotóxicos em células neoplásicas e evitar, portanto, o avanço do câncer de cervical ainda são limitados e apresentam elevadas taxas de insucesso. Assim, ainda existe a necessidade de buscar novos tratamentos para esse tipo de câncer. Nesta perspectiva, diversos estudos já demonstraram a atividade da HIP após a fotoativação, provocando danos celulares em concentrações muito pequenas sobre diversas linhagens de células tumorais. Porém, até onde conhecemos, não existem estudos que avaliem a atividade antitumoral *in vitro* da HIP encapsulada com plurônio[®] P123 (HIP/P123) em linhagens celulares de câncer cervical. Considerando que poucos estudos tem abordado e explorado este tema, propomos a realização de ensaios *in vitro* para determinar a atividade e o mecanismo de ação da TFD utilizando como FS a HIP/P123 em modelo de neoplasia cervical.

OBJETIVOS

Objetivo Geral

Avaliar a atividade antitumoral *in vitro* e o mecanismo de ação da HIP/P123 frente a um painel abrangente de linhagens celulares de câncer cervical incluindo HeLa (HPV 18-positivo), SiHa (HPV 16-positivo), CaSki (HPV 16 e 18-positivo), e C33A (HPV-negativa), comparando com a linhagem celular epitelial humana não tumorigênica (HaCaT).

Objetivos específicos

- Avaliar as taxas de morte celular decorrentes da exposição das cinco linhagens celulares à TFD com HIP/P123;
- Identificar as alterações morfológicas celulares após o tratamento com TFD utilizando HIP/P123;
- Avaliar a citotoxicidade à longo prazo da TFD com HIP/P123 nas linhagens celulares de câncer cervical através do ensaio clonogênico;
- Verificar a internalização da HIP/P123 nas cinco linhagens por microscopia de fluorescência;
- Verificar a internalização da HIP/P123 nas cinco linhagens por citometria de fluxo;
- Verificar a localização subcelular da HIP/P123 nas linhagens celulares de câncer cervical por microscopia de fluorescência;
- Identificar as vias de morte celular induzidas pela exposição das células de câncer cervical tratadas com TFD com HIP/P123 por citometria de fluxo;
- Analisar a via de morte celular por necrose utilizando o ensaio da enzima lactato desidrogenase;
- Avaliar a fragmentação do DNA após o tratamento das cinco linhagens celulares com TFD com HIP/P123;
- Observar a produção de EROs nas cinco linhagens por microscopia de fluorescência após o tratamento das linhagens celulares com TFD com HIP/P123;
- Determinar a produção de EROs nas cinco linhagens por fluorimetria após o tratamento das cinco linhagens celulares com TFD com HIP/P123;
- Determinar a peroxidação lipídica nas cinco linhagens por fluorimetria após o tratamento com TFD com HIP/P123;

- Determinar os mecanismos do tipo I e II da TFD nas linhagens de câncer cervical após o tratamento com TFD com HIP/P123;
- Avaliar o efeito da TFD com HIP/P123 na migração e invasão das células neoplásicas cervicais pelo ensaio da ferida e utilizando os insertos com matrigel respectivamente;
- Determinar por ELISA os níveis de metaloproteinases de membrana do tipo 2 e 9 (MMP-2 e MMP-9) e do fator de crescimento endotelial vascular (VEGF);
- Determinar o potencial da TFD com HIP/P123 para o tratamento de diferentes tipos de câncer cervical.

Referências bibliográficas:

- (1) Van Straten D, Mashayekhi V, De Bruijn HS, Oliveira S, Robinson DJ. Oncologic photodynamic therapy: basic principles, current clinical status and future directions. *Cancers*. 2017; 9(2):19.
- (2) Levy JG. Photodynamic therapy. *Trends Biotechnol*. 1995; 13(1):14-8.
- (3) Wolf P. Photodynamic therapy in dermatology: state of the art. *J Eur Acad Dermatol Venereol*. 2001; 15(6):508-9.
- (4) Ghodasra DH, Demirci H. Photodynamic therapy for choroidal metastasis. *Am J Ophthalmol*. 2016; 161:104-9.
- (5) Kharkwal GB, Sharma SK, Huang YY, Dai T, Hamblin MR. Photodynamic therapy for infections: clinical applications. *Lasers Surg Med*. 2011; 43(7):755-67.
- (6) Castano AP, Demidova TN, Hamblin MR. Mechanisms in photodynamic therapy: part one—photosensitizers, photochemistry and cellular localization. *Photodiagnosis Photodyn Ther*. 2004; 1(4):279-93.
- (7) Raab O. Über die Wirkung fluorescirender Stoffe auf Infusorien. *Z Biol*. 1900; 39:524-46.
- (8) Von Tappeiner H. Ueber wirkung der photodynamischen (fluorescierenden) Stoffe auf Protozoan und Enzyme. *Dtsch Arch Klin Med*. 1904; 80:427-87.
- (9) Figge FH, Weiland GS, Manganiello LO. Cancer detection and therapy. Affinity of neoplastic, embryonic, and traumatized tissues for porphyrins and metalloporphyrins. *Proc of Soc Exp Biol Med*. 1948; 68(3):640-1.
- (10) Rassmussen-Taxdal D, Ward GE, Figge FH. Fluorescence of human lymphatic and cancer tissues following high doses of intravenous hematoporphyrin. *Cancer*. 1955; 8(1):78-81.
- (11) Lipson RL, Baldes EJ, Olsen AM. Hematoporphyrin derivative: a new aid for endoscopic detection of malignant disease. *J Thorac Cardiovasc Surg*. 1961; 42(5):623-9.
- (12) Lipson RL, Baldes EJ, Olsen AM. The use of a derivative of hematoporphyrin in tumor detection. *J Natl Cancer Inst*. 1961; 26(1):1-11.
- (13) Kessel D. Photodynamic therapy: a brief history. *J Clin Med*. 2019; 8(10):1581.
- (14) Dolmans DE, Fukumura D, Jain RK. Photodynamic therapy for cancer. *Nat Rev Cancer*. 2003; 3(5):380-7.
- (15) Baas P, Van Mansom I, Van Tinteren H, Stewart FA, Van Zandwijk N. Effect of N-acetylcysteine on photofrin-induced skin photosensitivity in patients. *Lasers Surg Med*. 1995; 16(4):359-67.
- (16) Nseyo UO, De Haven J, Dougherty TJ, Potter WR, Merrill DL, Lundahl SL, et al. Photodynamic therapy (PDT) in the treatment of patients with resistant superficial bladder cancer: a long term experience. *J Clin Laser Med Surg*. 1998; 16(1):61-8.
- (17) Corti L, Toniolo L, Boso C, Colaut F, Fiore D, Muzzio PC, et al. Long-term survival of patients treated with photodynamic therapy for carcinoma in situ and early non-small-cell lung carcinoma. *Lasers Surg Med*. 2007; 39(5):394-402.
- (18) Wolfsen HC. Carpe luz—seize the light: endoprevention of esophageal adenocarcinoma when using photodynamic therapy with porfimer sodium. *Gastrointest Endosc*. 2005; 62(4):499-503.
- (19) D'Cruz AK, Robinson MH, Biel MA. mTHPC-mediated photodynamic therapy in patients with advanced, incurable head and neck cancer: A multicenter study of 128 patients. *Head Neck*. 2004; 26(3):232-40.
- (20) Braathen LR, Szeimies RM, Basset-Seguín N, Bissonnette R, Foley P, Pariser D, et al. Guidelines on the use of photodynamic therapy for nonmelanoma skin cancer: an

international consensus. International Society for Photodynamic Therapy in Dermatology, 2005. *J Am Acad Dermatol.* 2007; 56(1):125-43.

(21) Michels S, Schmidt-Erfurth U. Photodynamic therapy with verteporfin: A new treatment in ophthalmology. *Semin Ophthalmol.* 2001; 16(4):201-6.

(22) Salah M, Samy N, Fadel M. Methylene blue mediated photodynamic therapy for resistant plaque psoriasis. *J Drugs Dermatol.* 2009; 8(1):42-9.

(23) Lu Y, Li L, Lin Z, Wang L, Lin L, Li M, et al. A new treatment modality for rheumatoid arthritis: combined photothermal and photodynamic therapy using Cu₇. 2S₄ nanoparticles. *Adv Healthc Mater.* 2018; 7(14):1800013.

(24) Sepúlveda AAL, Arenas Velásquez AM, Patiño Linares IA, de Almeida L, Fontana CR, Garcia C, et al. Efficacy of photodynamic therapy using TiO₂ nanoparticles doped with Zn and hypericin in the treatment of cutaneous Leishmaniasis caused by *Leishmania amazonensis*. *Photodiagnosis Photodyn Ther.* 2020; 30:101676.

(25) Zhang J, Zhang X, He Y, Wu X, Huang J, Huang H, et al. Photodynamic therapy for severe facial acne vulgaris with 5% 5-aminolevulinic acid vs 10% 5-aminolevulinic acid: A split-face randomized controlled study. *J Cosmet Dermatol.* 2020; 19(2):368-74.

(26) Al Nazeh A, Alshahrani A, Almoammar S, Kamran MA, Togoo RA, Alshahrani I. Application of photodynamic therapy against periodontal bacteria in established gingivitis lesions in adolescent patients undergoing fixed orthodontic treatment. *Photodiagnosis Photodyn Ther.* 2020; 31:101904.

(27) Dias LD, Bagnato VS. An update on clinical photodynamic therapy for fighting respiratory tract infections: a promising tool against COVID-19 and its co-infections. *Laser Phys Lett.* 2020; 17(8):083001.

(28) Dias LD, Blanco KC, Bagnato VS. COVID-19: Beyond the virus. The use of Photodynamic Therapy for the Treatment of Infections in the Respiratory Tract. *Photodiagnosis Photodyn Ther.* 2020; 31(101804):1-2.

(29) Bergh J. Quo vadis with targeted drugs in the 21st century? *J Clin Oncol.* 2009; 27(1):2-5

(30) Fojo T, Grady C. How much is life worth: cetuximab, non-small cell lung cancer, and the \$440 billion question. *J Natl Cancer Inst.* 2009; 101(15):1044-8.

(31) Hampton T. Targeted cancer therapies lagging. *JAMA.* 2006; 296(16):1951-2.

(32) Chakraborty S, Rahman T. The difficulties in cancer treatment. *Ecancermedalscience.* 2012; 6:ed16.

(33) Möller TR, Einhorn N, Lindholm C, Ringborg U, Svensson H. Radiotherapy and cancer care in Sweden. *Acta Oncol.* 2003; 42(5-6):366-75.

(34) Delaney G, Jacob S, Featherstone C, Barton M. The role of radiotherapy in cancer treatment: estimating optimal utilization from a review of evidence-based clinical guidelines. *Cancer.* 2005; 104(6):1129-37.

(35) Jones R. Cytotoxic chemotherapy: clinical aspects. *Medicine.* 2016; 44(1):25-9.

(36) Corrie PG. Cytotoxic chemotherapy: clinical aspects. *Medicine.* 2011; 39(12):717-22.

(37) Agostinis P, Berg K, Cengel KA, Foster TH, Girotti AW, Gollnick SO, et al. Photodynamic therapy of cancer: an update. *CA Cancer J Clin.* 2011; 61(4):250-81.

(38) Dougherty TJ, Gomer CJ, Henderson BW, Jori G, Kessel D, Korbélik M, et al. Photodynamic therapy. *J Natl Cancer Inst.* 1998; 90(12):889-905.

(39) Kalka K, Merk H, Mukhtar H. Photodynamic therapy in dermatology. *J Am Acad Dermatol.* 2000; 42(3):389-413.

(40) Oleinick NL, Morris RL, Belichenko I. The role of apoptosis in response to photodynamic therapy: what, where, why, and how. *Photochem Photobiol Sci.* 2002; 1(1):1-21.

(41) Macdonald IJ, Dougherty TJ. Basic principles of photodynamic therapy. *J Porphyr Phthalocyanines.* 2001; 5(02):105-29.

- (42) Ribeiro JN, Flores AV, Mesquita RC, Nicola JH, Nicola EMD. Terapia Fotodinâmica: uma luz na luta contra o câncer. *Physicae*. 2005; 5(1):1-10.
- (43) Silva AR. Preparação, caracterização e avaliação de nanosferas de PLGA (50:50) contendo In (III)-Meso-tetrafenilporfirina para aplicação em terapia fotodinâmica. [Tese] Campinas: Universidade Estadual de Campinas; 2007.
- (44) Calzavara-Pinton P, Venturini M, Sala R. Photodynamic therapy: update 2006 Part 1: Photochemistry and photobiology. *J Eur Acad Dermatol Venereol*. 2007; 21(3):293-302.
- (45) Nuno O, Torezan LAR. Terapia fotodinâmica em dermatologia. *Laser em Dermatologia - Conceitos Básicos e Aplicações*. 1ed. São Paulo: Roca; 2002.
- (46) Agostinis P, Vantieghem A, Merlevede W, de Witte PA. Hypericin in cancer treatment: more light on the way. *Int J Biochem Cell Biol*. 2002; 34(3):221-41.
- (47) Falk H, Schoppel G. On the synthesis of hypericin by oxidative trimethylemodin anthrone and emodin anthrone dimerization: Isohypericin. *Monatsh Chem*. 1992; 123(10):931-8.
- (48) Brockmann H, Haschad MN, Maier K, Pohl F. Über das Hypericin, den photodynamisch wirksamen Farbstoff aus *Hypericum perforatum*. *Naturwissenschaften*. 1939; 27(32):550-.
- (49) Ehrenberg B, Anderson JL, Foote CS. Kinetics and yield of singlet oxygen photosensitized by hypericin in organic and biological media. *Photochem Photobiol*. 1998; 68(2):135-40.
- (50) Jacobson JM, Feinman L, Liebes L, Ostrow N, Koslowski V, Tobia A, et al. Pharmacokinetics, safety, and antiviral effects of hypericin, a derivative of St. John's wort plant, in patients with chronic hepatitis C virus infection. *Antimicrob Agents Chemother*. 2001; 45(2):517-24.
- (51) Noell S, Mayer D, Strauss WS, Tatagiba MS, Ritz R. Selective enrichment of hypericin in malignant glioma: pioneering in vivo results. *Int J Oncol*. 2011; 38(5):1343-8.
- (52) Zheng Y, Yin G, Le V, Zhang A, Chen S, Liang X, et al. Photodynamic-therapy activates immune response by disrupting immunity homeostasis of tumor cells, which generates vaccine for cancer therapy. *Int J Biol Sci*. 2016; 12(1):120.
- (53) Galluzzi L, Vacchelli E, Pedro J-MB-S, Buqué A, Senovilla L, Baracco EE, et al. Classification of current anticancer immunotherapies. *Oncotarget*. 2014; 5(24):12472-508.
- (54) Kubin A, Wierrani F, Burner U, Alth G, Grunberger W. Hypericin-the facts about a controversial agent. *Curr Pharm Des*. 2005; 11(2):233-53.
- (55) Wirz A, Meier B, Sticher O. Solubility of hypericin in methanol and methanol-pyridine. *Pharmazie*. 2002; 57(8):543-5.
- (56) Kubin A, Loew H, Burner U, Jessner G, Kolbabeck H, Wierrani F. How to make hypericin water-soluble. *Pharmazie*. 2008; 63(4):263-9.
- (57) Saw CLL, Olivo M, Soo KC, Heng PWS. Delivery of hypericin for photodynamic applications. *Cancer Lett*. 2006; 241(1):23-30.
- (58) Tatischeff I, Alfsen A. A new biological strategy for drug delivery: eucaryotic cell-derived nanovesicles. *J Biomater Nanobiotechnol*. 2011; 2(05):494.
- (59) Kwon GS. *Polymeric Drug Delivery Systems*. 1 ed. Boca Raton: CRC Press; 2005.
- (60) Gohy J-F. Block Copolymer Micelles. In: Abetz V, editor. *Block Copolymers II*. Berlin, Heidelberg: Springer Berlin Heidelberg; 2005. p. 65-136.
- (61) Alexandridis P, Holzwarth JF, Hatton TA. Micellization of poly (ethylene oxide)-poly (propylene oxide)-poly (ethylene oxide) triblock copolymers in aqueous solutions: thermodynamics of copolymer association. *Macromolecules*. 1994; 27(9):2414-25.
- (62) Batrakova EV, Kabanov AV. Pluronic block copolymers: evolution of drug delivery concept from inert nanocarriers to biological response modifiers. *J Control Release*. 2008; 130(2):98-106.

- (63) Akash MSH, Rehman K. Recent progress in biomedical applications of Pluronic (PF127): pharmaceutical perspectives. *J Control Release*. 2015; 209:120-38.
- (64) Jindal N, Mehta S. Nevirapine loaded Poloxamer 407/Pluronic P123 mixed micelles: optimization of formulation and in vitro evaluation. *Colloids Surf B Biointerfaces*. 2015; 129:100-6.
- (65) Chen Y, Zhang W, Huang Y, Gao F, Sha X, Fang X. Pluronic-based functional polymeric mixed micelles for co-delivery of doxorubicin and paclitaxel to multidrug resistant tumor. *Int J Pharm*. 2015; 488(1):44-58.
- (66) Vilsinski BH, Gerola AP, Enumo JA, Campanholi KdSS, Pereira PCdS, Braga G, et al. Formulation of Aluminum Chloride Phthalocyanine in Pluronic™ P-123 and F-127 Block Copolymer Micelles: Photophysical properties and Photodynamic Inactivation of Microorganisms. *Photochem Photobiol*. 2015; 91(3):518-25.
- (67) Vilsinski BH, Aparicio JL, Pereira PCdS, Fávoro SL, Campanholi KSS, Gerola AP, et al. Physico-chemical properties of meso-tetrakis (p-methoxyphenyl) porphyrin (TMPP) incorporated into pluronic™ p-123 and f-127 polymeric micelles. *Química Nova*. 2014; 37(10):1650-6.
- (68) Montanha MC, Silva LL, Pangoni FBB, Cesar GB, Gonçalves RS, Caetano W, et al. Response surface method optimization of a novel Hypericin formulation in P123 micelles for colorectal cancer and antimicrobial photodynamic therapy. *J Photochem Photobiol B*. 2017; 170:247-55.
- (69) Damke G, Souza R, Montanha M, Damke E, Gonçalves R, Cesar G, et al. Selective photodynamic effects on breast cancer cells provided by P123 Pluronic®-based nanoparticles modulating hypericin delivery. *Anticancer Agents Med Chem*. 2020; 20(11):1352-1367
- (70) Sakita KM, Conrado PC, Faria DR, Arita GS, Capoci IR, Rodrigues-Vendramini FA, et al. Copolymeric micelles as efficient inert nanocarrier for hypericin in the photodynamic inactivation of *Candida* species. *Future Microbiol*. 2019; 14(6):519-31.
- (71) Zelickson B, Goldman M. Mechanisms of action of topical aminolevulinic acid. *Photodynamic Therapy*. Philadelphia: Elsevier Saunders; 2005.
- (72) Allison RR, Moghissi K. Photodynamic therapy (PDT): PDT mechanisms. *Clin Endosc*. 2013; 46(1):24.
- (73) Pazos M, Nader HB. Effect of photodynamic therapy on the extracellular matrix and associated components. *Braz J Med Biol Res*. 2007; 40(8):1025-35.
- (74) Taylor E, Brown S. The advantages of aminolevulinic acid photodynamic therapy in dermatology. *J Dermatol Treat*. 2002; 13(sup1):s3-s11.
- (75) Issa MCA, Manela-Azulay M. Terapia fotodinâmica: revisão da literatura e documentação iconográfica. *An Bras Dermatol*. 2010; 85(4):501-11.
- (76) Castano AP, Mroz P, Hamblin MR. Photodynamic therapy and anti-tumour immunity. *Nat Rev Cancer*. 2006; 6(7):535-45.
- (77) Chatterjee DK, Fong LS, Zhang Y. Nanoparticles in photodynamic therapy: an emerging paradigm. *Adv Drug Deliv Rev*. 2008; 60(15):1627-37.
- (78) Sharman WM, Allen CM, Van Lier JE. Photodynamic therapeutics: basic principles and clinical applications. *Drug Discov Today*. 1999; 4(11):507-17.
- (79) Sibata C, Colussi V, Oleinick N, Kinsella T. Photodynamic therapy: a new concept in medical treatment. *Braz J Med Biol Res*. 2000; 33(8):869-80.
- (80) Silva E, Santos E, Júnior E. Terapia fotodinâmica no tratamento do câncer de pele: conceitos, utilizações e limitações. *Rev Bras Farm*. 2009; 90(3):211-7.
- (81) Foote CS. Definition of type I and type II photosensitized oxidation. *Photochem Photobiol*. 1991; 54(5):659.

- (82) Beckman JS, Beckman TW, Chen J, Marshall PA, Freeman BA. Apparent hydroxyl radical production by peroxynitrite: implications for endothelial injury from nitric oxide and superoxide. *Proc Natl Acad Sci U S A*. 1990; 87(4):1620-4.
- (83) Beckman JS, Koppenol WH. Nitric oxide, superoxide, and peroxynitrite: the good, the bad, and ugly. *Am J Physiol*. 1996; 271(5):C1424-C37.
- (84) Beckman JS. Peroxynitrite versus Hydroxyl Radical: The Role of Nitric Oxide in Superoxide-Dependent Cerebral Injury. *Ann N Y Acad Sci*. 1994; 738(1):69-75.
- (85) Beckman JS, Chen J, Ischiropoulos H, Crow JP. Oxidative chemistry of peroxynitrite. *Methods Enzymol*. 1994; 233:229-40.
- (86) Henderson BW, Dougherty TJ. How does photodynamic therapy work? *Photochem Photobiol*. 1992; 55(1):145-57.
- (87) Dewhirst M, Kimura H, Rehmus S, Braun R, Papahadjopoulos D, Hong K, et al. Microvascular studies on the origins of perfusion-limited hypoxia. *Br J Cancer Suppl*. 1996; 27:S247.
- (88) Tromberg B, Orenstein A, Kimel S, Barker S, Hyatt J, Nelson J, et al. In vivo tumor oxygen tension measurements for the evaluation of the efficiency of photodynamic therapy. *Photochem Photobiol*. 1990; 52(2):375-85.
- (89) Castano AP, Demidova TN, Hamblin MR. Mechanisms in photodynamic therapy: part two—cellular signaling, cell metabolism and modes of cell death. *Photodiagnosis Photodyn Ther*. 2005; 2(1):1-23.
- (90) Kerr JF, Wyllie AH, Currie AR. Apoptosis: a basic biological phenomenon with wideranging implications in tissue kinetics. *Br J Cancer*. 1972; 26(4):239-57.
- (91) Peres CM, Curi R. Como cultivar células. 1ed. Rio de Janeiro: Guanabara Koogan; 2005.
- (92) Schwartz LM, Smith SW, Jones M, Osborne BA. Do all programmed cell deaths occur via apoptosis? *Proc Natl Acad Sci U S A*. 1993; 90(3):980-4.
- (93) Lawen A. Apoptosis—an introduction. *Bioessays*. 2003; 25(9):888-96.
- (94) Galluzzi L, Bravo-San Pedro JM, Levine B, Green DR, Kroemer G. Pharmacological modulation of autophagy: therapeutic potential and persisting obstacles. *Nat Rev Drug Discov*. 2017; 16(7):487.
- (95) Mizushima N. A brief history of autophagy from cell biology to physiology and disease. *Nat Cell Biol*. 2018; 20(5):521-7.
- (96) Dikic I, Elazar Z. Mechanism and medical implications of mammalian autophagy. *Nat Rev Mol Cell Biol*. 2018; 19(6):349-64.
- (97) Kessel D, Oleinick NL. Initiation of autophagy by photodynamic therapy. *Methods Enzymol*. 2009; 453:1-16.
- (98) Wang W, Moriyama L, Bagnato V. Photodynamic therapy induced vascular damage: an overview of experimental PDT. *Laser Phys. Lett*. 2012; 10(2):023001.
- (99) Wang H, Dong C, Zhao P, Wang S, Liu Z, Chang J. Lipid coated upconverting nanoparticles as NIR remote controlled transducer for simultaneous photodynamic therapy and cell imaging. *Int. J. Pharm*. 2014; 466(1-2):307-13.
- (100) Chernyak BV, Izyumov DS, Lyamzaev KG, Pashkovskaya AA, Pletjushkina OY, Antonenko YN, et al. Production of reactive oxygen species in mitochondria of HeLa cells under oxidative stress. *Biochim Biophys Acta*. 2006; 1757(5-6):525-34.
- (101) Sparsa A, Bellaton S, Naves T, Jauberteau M-O, Bonnetblanc J-M, Sol V, et al. Photodynamic treatment induces cell death by apoptosis or autophagy depending on the melanin content in two B16 melanoma cell lines. *Oncol Rep*. 2013; 29(3):1196-200.
- (102) Buytaert E, Dewaele M, Agostinis P. Molecular effectors of multiple cell death pathways initiated by photodynamic therapy. *Biochim Biophys Acta*. 2007; 1776(1):86-107.

- (103) Krestyn E, Kolarova H, Bajgar R, Tomankova K. Photodynamic properties of ZnTPPS4, ClAlPcS2 and ALA in human melanoma G361 cells. *Toxicol In Vitro*. 2010; 24(1):286-91.
- (104) Du L, Jiang N, Wang G, Chu Y, Lin W, Qian J, et al. Autophagy inhibition sensitizes bladder cancer cells to the photodynamic effects of the novel photosensitizer chlorophyllin e4. *J Photochem Photobiol B*. 2014; 133:1-10.
- (105) Liang L, Bi W, Tian Y. Autophagy in photodynamic therapy. *Trop J Pharm Res*. 2016; 15(4):885-9.
- (106) Carmeliet P, Jain RK. Angiogenesis in cancer and other diseases. *Nature*. 2000; 407(6801):249-57.
- (107) Jain RK, Carmeliet PF. Vessels of death or life. *Sci. Am*. 2001; 285(6):38-45.
- (108) Star WM, Marijnissen HP, van den Berg-Blok AE, Versteeg JA, Franken KA, Reinhold HS. Destruction of rat mammary tumor and normal tissue microcirculation by hematoporphyrin derivative photoradiation observed in vivo in sandwich observation chambers. *Cancer Res*. 1986; 46(5):2532-40.
- (109) Fingar VH, Wieman TJ, Haydon PS. The effects of thrombocytopenia on vessel stasis and macromolecular leakage after photodynamic therapy using photofrin. *Photochem Photobiol*. 1997; 66(4):513-7.
- (110) Fingar VH, Kik PK, Haydon PS, Cerrito PB, Tseng M, Abang E, et al. Analysis of acute vascular damage after photodynamic therapy using benzoporphyrin derivative (BPD). *Br J Cancer*. 1999; 79(11-12):1702-8.
- (111) Dolmans DE, Kadambi A, Hill JS, Waters CA, Robinson BC, Walker JP, et al. Vascular accumulation of a novel photosensitizer, MV6401, causes selective thrombosis in tumor vessels after photodynamic therapy. *Cancer Res*. 2002; 62(7):2151-6.
- (112) Henderson BW, Fingar VH. Relationship of tumor hypoxia and response to photodynamic treatment in an experimental mouse tumor. *Cancer Res*. 1987; 47(12):3110-4.
- (113) Chen Q, Chen H, Hetzel FW. Tumor oxygenation changes post-photodynamic therapy. *Photochem Photobiol*. 1996; 63(1):128-31.
- (114) Busch TM, Wileyto EP, Emanuele MJ, Del Piero F, Marconato L, Glatstein E, et al. Photodynamic therapy creates fluence rate-dependent gradients in the intratumoral spatial distribution of oxygen. *Cancer Res*. 2002; 62(24):7273-9.
- (115) Castano AP, Demidova TN, Hamblin MR. Mechanisms in photodynamic therapy: Part three-Photosensitizer pharmacokinetics, biodistribution, tumor localization and modes of tumor destruction. *Photodiagnosis Photodyn Ther*. 2005; 2(2):91-106.
- (116) Gollnick SO, Liu X, Owczarczak B, Musser DA, Henderson BW. Altered expression of interleukin 6 and interleukin 10 as a result of photodynamic therapy in vivo. *Cancer Res*. 1997; 57(18):3904-9.
- (117) Coutier S, Bezdetnaya L, Marchal S, Melnikova V, Belitchenko I, Merlin JL, et al. Foscan (mTHPC) photosensitized macrophage activation: enhancement of phagocytosis, nitric oxide release and tumour necrosis factor-alpha-mediated cytolytic activity. *Br J Cancer*. 1999; 81(1):37-42.
- (118) Gollnick SO, Evans SS, Baumann H, Owczarczak B, Maier P, Vaughan L, et al. Role of cytokines in photodynamic therapy-induced local and systemic inflammation. *Br J Cancer*. 2003; 88(11):1772-9.
- (119) Maillhot Vega RB, Balogun OD, Ishaq OF, Bray F, Ginsburg O, Formenti SC. Estimating child mortality associated with maternal mortality from breast and cervical cancer. *Cancer*. 2019; 125(1):109-17.
- (120) Bray F, Ferlay J, Soerjomataram I, Siegel RL, Torre LA, Jemal A. Global cancer statistics 2018: GLOBOCAN estimates of incidence and mortality worldwide for 36 cancers in 185 countries. *CA Cancer J Clin*. 2018; 68(6):394-424.

- (121) Vieira RC, Monteiro Jdo S, Manso EP, Dos Santos MR, Tsutsumi MY, Ishikawa EA, et al. Prevalence of type-specific HPV among female university students from northern Brazil. *Infect Agent Cancer*. 2015; 10:21.
- (122) Instituto Nacional do Câncer – INCA – Ministério da Saúde [Internet]. Tipos de câncer - Câncer do colo do útero 2020 [Acesso em 29 de novembro de 2020]. Disponível em: <https://www.inca.gov.br/tipos-de-cancer/cancer-do-colo-do-utero>.
- (123) Cohen PA, Jhingran A, Oaknin A, Denny L. Cervical cancer. *Lancet* (London, England). 2019; 393(10167):169-82.
- (124) Sankaranarayanan R, Thara S, Esmey PO, Basu P. Cervical cancer: screening and therapeutic perspectives. *Med Princ Pract*. 2008; 17(5):351-64.
- (125) Pinto AP, Crum CP. Natural history of cervical neoplasia: defining progression and its consequence. *Clin Obstet Gynecol*. 2000; 43(2):352-62.
- (126) Rosa MI, Medeiros LR, Rosa DD, Bozzeti MC, Silva FR, Silva BR. Human papillomavirus and cervical neoplasia. *Cad Saude Publica*. 2009; 25(5):953-64.
- (127) Koeneman MM, Kruitwagen RF, Nijman HW, Slangen BF, Van Gorp T, Kruse AJ. Natural history of high-grade cervical intraepithelial neoplasia: a review of prognostic biomarkers. *Expert Rev Mol Diagn*. 2015; 15(4):527-46.
- (128) Roden RB, Monie A, Wu TC. Opportunities to improve the prevention and treatment of cervical cancer. *Curr Mol Med*. 2007; 7(5):490-503.
- (129) ABC da Medicina. [Internet]. Câncer de Colo de útero e Infecção por HPV – Fisiopatologia e Vacina. [Acesso em 30 de novembro de 2020]. Disponível em: <https://abcdamedicina.com.br/cancer-de-colo-de-utero-e-infeccao-por-hpv-fisiopatologia-e-vacina.html>
- (130) Moody CA, Laimins LA. Human papillomavirus oncoproteins: pathways to transformation. *Nat Rev Cancer*. 2010; 10(8):550-60.
- (131) Chow LT, Broker TR, Steinberg BM. The natural history of human papillomavirus infections of the mucosal epithelia. *APMIS*. 2010; 118(6-7):422-49.
- (132) Bodily J, Laimins LA. Persistence of human papillomavirus infection: keys to malignant progression. *Trends in microbiol*. 2011; 19(1):33-9.
- (133) Tota JE, Chevarie-Davis M, Richardson LA, Devries M, Franco EL. Epidemiology and burden of HPV infection and related diseases: implications for prevention strategies. *Prev Med*. 2011; 53 Suppl 1:S12-21.
- (134) Lizano M, Berumen J, García-Carrancá A. HPV-related carcinogenesis: basic concepts, viral types and variants. *Arch Med Res*. 2009; 40(6):428-34.
- (135) Verteramo R, Pierangeli A, Calzolari E, Patella A, Recine N, Mancini E, et al. Direct sequencing of HPV DNA detected in gynaecologic outpatients in Rome, Italy. *Microbes Infect*. 2006; 8(9-10):2517-21.
- (136) Lehtinen M, Ault KA, Lyytikäinen E, Dillner J, Garland SM, Ferris DG, et al. Chlamydia trachomatis infection and risk of cervical intraepithelial neoplasia. *Sex Transm Infect*. 2011; 87(5):372-6.
- (137) Sudenga SL, Rositch AF, Otieno WA, Smith JS. Knowledge, attitudes, practices, and perceived risk of cervical cancer among Kenyan women: brief report. *Int J Gynecol Cancer*. 2013; 23(5):895-9.
- (138) Instituto Nacional do Câncer – INCA – Ministério da Saúde [Internet]. Diretrizes brasileiras para rastreamento do câncer de colo do útero. [Acesso em 29 de novembro de 2020] Disponível em: http://bvsmms.saude.gov.br/bvs/publicacoes/inca/rastreamento_cancer_colo_uterio.pdf
- (139) Muñoz N. Human papillomavirus and cancer: the epidemiological evidence. *J Clin Virol*. 2000; 19(1-2):1-5.

- (140) Silva J, Cerqueira F, Medeiros R. Chlamydia trachomatis infection: implications for HPV status and cervical cancer. *Arch Gynecol Obstet*. 2014; 289(4):715-23.
- (141) Faridi R, Zahra A, Khan K, Idrees M. Oncogenic potential of Human Papillomavirus (HPV) and its relation with cervical cancer. *Virol J*. 2011; 8:269.
- (142) de Sanjosé S, Diaz M, Castellsagué X, Clifford G, Bruni L, Muñoz N, et al. Worldwide prevalence and genotype distribution of cervical human papillomavirus DNA in women with normal cytology: a meta-analysis. *Lancet Infect Dis*. 2007; 7(7):453-9.
- (143) Shrestha S, Sudenga SL, Smith JS, Bachmann LH, Wilson CM, Kempf MC. The impact of highly active antiretroviral therapy on prevalence and incidence of cervical human papillomavirus infections in HIV-positive adolescents. *BMC Infect Dis*. 2010; 10:295.
- (144) World Health Organization. International Agency for Research on Cancer [Internet]. Globocan. [Acesso em 30 de novembro de 2020]. Disponível em: http://globocan.iarc.fr/Pages/fact_sheets_cancer.aspx.
- (145) Koh WJ, Greer BE, Abu-Rustum NR, Apte SM, Campos SM, Cho KR, et al. Uterine Sarcoma, Version 1.2016: Featured Updates to the NCCN Guidelines. *J Natl Compr Canc Netw*. 2015; 13(11):1321-31.
- (146) Kjær SK, Frederiksen K, Munk C, Iftner T. Long-term absolute risk of cervical intraepithelial neoplasia grade 3 or worse following human papillomavirus infection: role of persistence. *J Natl Cancer Inst*. 2010; 102(19):1478-88.
- (147) Schiffman M, Castle PE, Jeronimo J, Rodriguez AC, Wacholder S. Human papillomavirus and cervical cancer. *Lancet*. 2007; 370(9590):890-907.
- (148) Rosa MI, Fachel JM, Rosa DD, Medeiros LR, Igansi CN, Bozzetti MC. Persistence and clearance of human papillomavirus infection: a prospective cohort study. *Am J Obstet Gynecol*. 2008; 199(6):617.e1-7.
- (149) Instituto Nacional do Câncer – INCA – Ministério da Saúde [Internet]. Tratamento 2020 [Acesso em 01 de dezembro de 2020]. Disponível em: <https://www.inca.gov.br/controlado-cancer-do-colo-do-utero/acoes-de-controlado/tratamento>
- (150) Instituto Nacional do Câncer – INCA – Ministério da Saúde [Internet]. Diretrizes Brasileiras para o Rastreamento do Câncer do Colo do Útero 2016 [Acesso em 03 de dezembro de 2020]. Disponível em: <https://www.inca.gov.br/publicacoes/livros/diretrizes-brasileiras-para-o-rastreamento-do-cancer-do-colo-do-utero>
- (151) Kuttukaran A, Kekre A, Jose R, Seshadri L. See & treat protocol for evaluation & management of cervical intraepithelial neoplasia. *Indian J Med Res*. 2002; 116:106.
- (152) Sadan O, Yarden H, Schejter E, Bilavsky E, Bachar R, Lurie S. Treatment of high-grade squamous intraepithelial lesions: A “see and treat” versus a three-step approach. *Eur J Obstet Gynecol Reprod Biol*. 2007; 131(1):73-5.
- (153) American Cancer Society [Internet]. Cervical Cancer Stages. [Acesso em 03 de dezembro de 2020]. Disponível em: <http://www.cancer.org/cancer/cervicalcancer/detailedguide/cervical-cancer-staged>.
- (154) American Cancer Society [Internet]. Treating Cervical Cancer. [Acesso em 03 de dezembro de 2020]. Disponível em: <https://www.cancer.org/cancer/cervical-cancer/treating.html>
- (155) Martín-Martínez A, Molano F, Lloret M, Falcón-Vizcaino O, García-Hernández JA. Concurrent chemotherapy and radiotherapy for cervical cancer. *Eur J Gynaecol Oncol*. 2003; 24(2):160-2.
- (156) Yang H, Wu XL, Wu KH, Zhang R, Ju LL, Ji Y, et al. MicroRNA-497 regulates cisplatin chemosensitivity of cervical cancer by targeting transketolase. *Am J Cancer Res*. 2016; 6(11):2690-9.

- (157) Lorusso D, Petrelli F, Coinu A, Raspagliesi F, Barni S. A systematic review comparing cisplatin and carboplatin plus paclitaxel-based chemotherapy for recurrent or metastatic cervical cancer. *Gynecol. Oncol.* 2014; 133(1):117-23.
- (158) Khalil J, Bellefqih S, Sahli N, Afif M, Elkacemi H, Elmajjaoui S, et al. Impact of cervical cancer on quality of life: beyond the short term (Results from a single institution). *Gynecol Oncol Res Pract.* 2015; 2(1):7.
- (159) Istomin YP, Lapzevich TP, Chalau VN, Shliakhtsin SV, Trukhachova TV. Photodynamic therapy of cervical intraepithelial neoplasia grades II and III with Photolon. *Photodiagnosis Photodyn Ther.* 2010; 7(3):144-51.
- (160) Hillemanns P, Einstein MH, Iversen OE. Topical hexaminolevulinate photodynamic therapy for the treatment of persistent human papilloma virus infections and cervical intraepithelial neoplasia. *Expert Opin Investig Drugs.* 2015; 24(2):273-81.
- (161) Instituto de Física de São Carlos – Universidade de São Paulo [Internet]. Câncer de colo do útero – tudo sobre a doença e tratamento por TFD. [Acesso em 28 de novembro de 2020]. Disponível em: <https://www2.ifsc.usp.br/portal-ifsc/cancer-de-colo-do-utero/>.
- (162) Instituto de Física de São Carlos – Universidade de São Paulo [Internet]. LED pode tratar lesão que gera câncer de colo do útero. [Acesso em 28 de novembro de 2020]. Disponível em: <https://www5.usp.br/noticias/saude-2/led-pode-tratar-lesao-que-gera-cancer-de-colo-do-utero/>
- (163) de Castro CA, Lombardi W, Stringasci MD, Bagnato VS, Inada NM. High-risk HPV clearance and CIN 3 treated with MAL-PDT: A case report. *Photodiagnosis Photodyn Ther.* 2020; 31:101937.
- (164) Stringasci MD, Buzzá HH, de Arruda SS, Schiavone Crestana RH, Bagnato VS, Inada NM. HPV condylomatosis region treated with multiple sessions of MAL-PDT: A case report. *Photodiagnosis Photodyn Ther.* 2020; 31:101812.

CAPÍTULO II

**Artigo: “SELECTIVE PHOTODYNAMIC EFFECTS ON CERVICAL CANCER
CELLS PROVIDED BY P123 PLURONIC[®]-BASED NANOPARTICLES
MODULATING HYPERICIN DELIVERY”**



Contents lists available at ScienceDirect

Life Sciences

journal homepage: www.elsevier.com/locate/lifescie

Selective photodynamic effects on cervical cancer cells provided by P123 Pluronic®-based nanoparticles modulating hypericin delivery

Gabrielle Marconi Zago Ferreira Damke^a, Edilson Damke^a, Patrícia de Souza Bonfim-Mendonça^a, Bianca Altrão Ratti^b, Lyvia Eloiza de Freitas Meirelles^a, Vânia Ramos Sela da Silva^a, Renato Sonchini Gonçalves^c, Gabriel Batista César^c, Sueli de Oliveira Silva^b, Wilker Caetano^c, Noboru Hioka^c, Raquel Pantarotto Souza^a, Marcia Edilaine Lopes Consolaro^{a,*}

^a Department of Clinical Analysis and Biomedicine, Universidade Estadual de Maringá, Av. Colombo, 5790, 87025-210 Maringá, Paraná, Brazil

^b Department of Basic Health Sciences, Universidade Estadual de Maringá, Av. Colombo, 5790, 87025-210 Maringá, Paraná, Brazil

^c Department of Chemistry, Universidade Estadual de Maringá, Av. Colombo, 5790, 87025-210 Maringá, Paraná, Brazil



ARTICLE INFO

Keywords:
Photodynamic therapy
Cervical cancer
Hypericin
Pluronic P123

ABSTRACT

At present, cervical cancer is the fourth leading cause of cancer among women worldwide with no effective treatment options. In this study we aimed to evaluate the efficacy of hypericin (HYP) encapsulated on Pluronic® P123 (HYP/P123) photodynamic therapy (PDT) in a comprehensive panel of human cervical cancer-derived cell lines, including HeLa (HPV 18-positive), SiHa (HPV 16-positive), CaSki (HPV 16 and 18-positive), and C33A (HPV-negative), compared to a nontumorigenic human epithelial cell line (HaCaT). Were investigated: (i) cell cytotoxicity and phototoxicity, cellular uptake and subcellular distribution; (ii) cell death pathway and cellular oxidative stress; (iii) migration and invasion. Our results showed that HYP/P123 micelles had effective and selective time- and dose-dependent phototoxic effects on cervical cancer cells but not in HaCaT. Moreover, HYP/P123 micelles accumulated in endoplasmic reticulum, mitochondria and lysosomes, resulting in photodynamic cell death mainly by necrosis. HYP/P123 induced cellular oxidative stress mainly via type II mechanism of PDT and inhibited cancer cell migration and invasion mainly via MMP-2 inhibition. Taken together, our results indicate a potentially useful role of HYP/P123 micelles as a platform for HYP delivery to more specifically and effectively treat cervical cancers through PDT, suggesting they are worthy for in vivo preclinical evaluations.

1. Introduction

At present, cervical cancer is the fourth leading cause of cancer among women worldwide, despite the existence of highly effective prevention and screening methods [1,2]. Persistent high-risk human papillomavirus (HR-HPV) infection is the central factor in the development of cervical cancer, and HPV 16 and HPV 18 account for approximately 70% of all cases of this cancer [1–4]. Chemoradiotherapy is a standard treatment option for patients with unresectable and locally

advanced cervical cancer [5]. The 5-year survival rate of advanced cervical cancer has significantly improved due to the application of concurrent chemoradiotherapy in recent years. However, local recurrence and distant metastasis are still common post treatment manifestations in patients with advanced cervical cancer. Once post treatment failure occurs, prognosis becomes worse: the 1-year survival rates of patients with such failures are < 20% [6]. Moreover, various side effects are produced influencing patient's life quality [7]. Despite these alarming facts, efficient treatment methods are still lacking.

Abbreviations: ANOVA, analysis of variance; CMC, critical micellar concentration; DAPI, diamidino-2-phenylindole dihydrochloride; DM, D-mannitol; DMEM, Dulbecco's modified Eagle medium; DMSO, dimethyl sulfoxide; DPPP, diphenyl-1-pyrenylphosphine; DPPP-O, diphenyl-1-pyrenylphosphine oxide; ELISA, enzyme-linked immunosorbent assay; ER, endoplasmic reticulum; FBS, fetal bovine serum; FITC, fluorescein isothiocyanate; H₂DCFDA, 2',7'-dichlorodihydrofluorescein diacetate; H₂O₂, hydrogen peroxide; HR-HPV, high-risk human papillomavirus; HYP, hypericin; HYP/DMSO, HYP dissolved in DMSO; HYP/P123, hypericin encapsulated on Pluronic® P123; IC, inhibitory concentrations; ICD, immunogenic cell death; LED, light-emitting diode; MMP-2, matrix metalloproteinase-2; MMP-9, matrix metalloproteinase-9; MTT, 3-(4,5-dimethylthiazol-2-yl)-2,5-diphenyltetrazolium bromide; NUPESF, Research Nucleus in Photodynamic System; PBS, phosphate-buffered saline; PDT, photodynamic therapy; PEO, polyethylene oxide; PI, propidium iodide; PPO, polypropylene oxide; PS, photosensitizers; RFU, arbitrary units; ROS, reactive oxygen species; SA, sodium azide; SD, standard deviation; VEGF, vascular endothelial growth factor

* Corresponding author at: Universidade Estadual de Maringá, Av. Colombo, 5790, 87025-210 Maringá, Paraná, Brazil.

E-mail address: melconsolaro@gmail.com (M.E.L. Consolaro).

<https://doi.org/10.1016/j.lfs.2020.117858>

Received 6 April 2020; Received in revised form 22 May 2020; Accepted 25 May 2020

Available online 01 June 2020

0024-3205/ © 2020 Published by Elsevier Inc.

Since the first use of hematoporphyrin derivative together with red light irradiation to kill tumor cells in 1975, photodynamic therapy (PDT) has attracted extensive attention as a prospective strategy for cancer treatment [8]. The main elements of PDT are a photoactive drug, light in an appropriate wavelength, and molecular oxygen [9,10]. Light in an appropriate wavelength excites the photosensitizers (PS) to its triplet state interacting with the oxygen present in the tissue producing reactive oxygen species (ROS) by type I or type II mechanism. This interaction results in the production of free radicals [11] or singlet oxygen (1O_2) [12], respectively. Since the discovery of PDT, continuous efforts have been made to identify new ideal PS.

Some of these PS can be found in nature, such as hypericin (HYP), a phenanthroperylenequinone isolated mainly from plants of the genus *Hypericum perforatum* [13–15] which can be also chemically synthesized. This compound under light illumination (absorption peaks at 545 and 590 nm) [16] leads to antiproliferative and cytotoxic effects resulting in cell death by necrosis and/or apoptosis in different cancer cell lines. These properties, together with minimal toxicity in the absence of light, selectivity for some tumors, and a high clearance rate from the human organism together with antiproliferative and cytotoxic effects, shows that HYP is a promising PS for PDT of cancer [17–21]. However, as with most PS, HYP presents high hydrophobicity and form aggregates in aqueous media and body fluids [22,23]. The hydrophobic interactions can affect their photophysical (reducing 1O_2 generation), chemical (reduced solubility), and biological effects. It is thus essential to use delivery systems to overcome this shortcoming related to these PS [24,25]. One innovative nanomedicine-based technology for the delivery of hydrophobic compounds such as HYP reside in polymeric nanoparticles, which have been frequently studied as delivery systems for PDT [26,27]. Pluronic® copolymer P123 consist of triblock molecules of polyethylene oxide (PEO-hydrophilic region) and polypropylene oxide (PPO-hydrophobic region) with configuration $(EO)_x(PO)_y(EO)_x$ [26,28,29]. The micellization procedure of these amphiphilic monomers in aqueous media consists in the assembly of PPO groups to create the hydrophobic core of micelles, responsible for incorporating the hydrophobic drugs. Also, PEO groups are responsible for the stabilization of micelles in aqueous media, avoiding their adsorption and aggregation [30,31]. Furthermore, they are non-toxic and biocompatible, are stable in biological fluids because they are barely recognized by macrophages and do not bind to proteins, have a low critical micellar concentration (CMC) and favorable pharmacokinetics [31–34]. Consistent with these properties, our group has recently published important studies about the characteristics of the complexes of Pluronic with different PS, including HYP. Our most recent studies showed high efficiency of HYP-loaded Pluronic® P123 micelles for use in PDT against intestinal bacteria and colon carcinoma cells [35], and breast cancer cells [36].

Although HYP is a promising PS for PDT of cancer, little information is available regarding the effects of HYP-mediated PDT against cervical cancer, and the available data were mostly obtained in the HeLa cell line [37–47]. HeLa cells were derived from a case of adenocarcinoma of the uterine cervix in 1952 and contain integrated HPV 18 [48]. Notably, previous studies did not assessed the inhibitory activity of HYP in cell lines containing HPV 16 as SiHa and CasKi, which is the most prevalent genotype and the main causative agent of squamous cell cervical cancer (approximately 50% of total) [1,4,49]. Additionally, the antiproliferative activity of HYP has not been evaluated in cell lines derived from squamous cervical cancer cells (SiHa, CasKi and C33A), which is the most common type of cervical cancer worldwide (75%–85% of total) [50,51].

To continue our studies and to explore the capacity of HYP/P123 as a new therapeutic candidate for cervical cancer, in the present study we investigated the antitumoral effects of HYP encapsulated on Pluronic® P123 (HYP/P123) PDT in a comprehensive panel of human cervical cancer-derived cell lines, including HeLa (HPV 18-positive), SiHa (HPV 16-positive), CaSki (HPV 16 and 18-positive), and C33A (HPV-

negative), compared to a nontumorigenic human epithelial cell line (HaCaT). The objectives of this study were to investigate effects of HYP/P123 on HeLa, SiHa, CaSki, C33A, and HaCaT cells with respect to (i) cell cytotoxicity and phototoxicity, cellular uptake and subcellular distribution; (ii) cell death pathway and cellular oxidative stress; and (iii) migration and invasion. Our results demonstrated that HYP/P123 has a selective phototoxic effect: it induced necrosis in all cervical cancer cell lines, but not in HaCaT cells. Additionally, HYP/P123 PDT induced cellular oxidative stress mainly via type II mechanism of PDT and inhibited cancer cell migration and invasion mainly via MMP-2 inhibition. These results show that HYP/P123 PDT had a strong and selective antitumoral effect on cervical cancer cells immortalized by HPV 16, HPV 18, HPV 16 and 18 together, and without HPV, indicating its potential to be a powerful candidate in developing therapeutic agents for all cervical cancer types.

2. Materials and methods

2.1. Materials

HYP/P123 was supplied by the Research Nucleus in Photodynamic System (NUPESF), Chemistry Department, State University of Maringá/PR/Brazil. Pluronic® P123, dulbecco's modified Eagle medium (DMEM), amphotericin B, crystal violet solution, dimethyl sulfoxide (DMSO), diphenyl-1-pyrenylphosphine (DPPP) and sodium azide (SA) were purchased from Sigma Aldrich (St. Louis, MO, USA). Fetal bovine serum (FBS), penicillin/streptomycin, 3-(4,5-dimethylthiazol-2-yl)-2,5-diphenyltetrazolium bromide (MTT), MitoTracker®, LysoTracker®, ER-tracker®, NucBlue® Live ReadyProbes® Reagent, annexin-V/fluorescein isothiocyanate (FITC), propidium iodide (PI), Pierce lactate dehydrogenase (LDH) Cytotoxicity Assay Kit, agarose, 2',7'-dichlorodihydrofluorescein diacetate (H_2DCFDA), Matrix Metalloproteinase-2 (MMP-2) enzyme-linked immunosorbent assay (ELISA) kit, Matrix Metalloproteinase-9 (MMP-9) ELISA kit, vascular endothelial growth factor (VEGF) ELISA kit were purchased from Invitrogen (Waltham, MA, USA). Methanol, formaldehyde and hydrogen peroxide (H_2O_2) were purchased from Synth (Diadema, SP, Brazil). DNA QIAamp DNA mini kit was purchased from Qiagen (Hilden, NRW, Germany). D-mannitol (DM) was purchased from JP Pharmaceutical Industry S.A. (Ribeirão Preto, SP, Brazil). Matrigel was purchased from Corning (New York, NY, USA).

2.2. Synthesis and characterization of HYP

Formulations containing HYP (1,3,4,6,8,13-hexahidroxí-10,11-dimetilfenantro[1,10,9,8-opqra]perileno-7,14-diona, $C_{30}H_{16}O_8$, 98% purity) in nanostructures of Pluronic® P123 were kindly supplied by the NUPESF, Chemistry Department, State University of Maringá/PR/Brazil. HYP was synthesized and characterized by the NUPESF in accordance to the methodology described in a previous study [52–54].

2.3. Preparation of HYP-loaded Pluronic P123 micelles

Formulations containing HYP in nanostructures of Pluronic® P123 ($PEO_{20}-PPO_{65}-PEO_{20}$, $MW = 5750 \text{ gmol}^{-1}$) were prepared following the solid dispersion method [55]. The resulting formulation was lyophilized and hydrated before use to a concentration of 100 $\mu\text{mol/L}$ HYP/88 $\mu\text{mol/L}$ P123. Preparation and quality control of HYP/P123 formulation were previously determined by our research group and have been published in Montanha et al. [35], Damke et al. [36] and Sakita et al. [56].

2.4. Light source

A light-source device with 66 light-emitting diode (LED) units emitting white light at 6.3 J/cm^2 in a wavelength range from 450 to

750 nm was built to illuminate tissue culture plates containing the cells. The LED device covered the entire area of the tissue culture plates.

2.5. Cell lines and growth conditions

The human cell lines derived from invasive cervical cancer, HeLa (integrated HPV 18), SiHa (1 to 2 copies of HPV 16 integrated per cell) and CaSki (approximately 600 copies of HPV 16 integrated per cell, as well as sequences of HPV 18), and the spontaneously immortalized human epithelial cell line HaCaT (non-tumorigenic cells) were kindly donated by Dr. Luisa L. Villa, School of Medicine, University of São Paulo/SP/Brazil and Dr. Silvy S. Maria-Engler, Faculty of Pharmaceutical Sciences, University of São Paulo/SP/Brazil. The human cell line C33A (HPV negative) derived from invasive cervical cancer was purchased from the American Type Culture Collection (Rockville, MD, USA). The cell lines were maintained in a culture flask in DMEM supplemented with 10% FBS, 100 U/mL penicillin and 100 µg/mL streptomycin and 2.5 µg/mL amphotericin B solution at 37 °C in a humidified atmosphere with 5% CO₂.

2.6. Cytotoxicity and phototoxicity

Cell viability was determined by MTT assay [57]. The cell lines were seeded in 96-well tissue culture plates at a density of approximately 2.5×10^5 cells/mL. The cells were allowed to attach overnight at 37 °C in a humidified atmosphere with 5% CO₂. After 24 h the cells were treated with HYP/P123 at different concentrations (0.4, 0.6, 0.8, 1.0, 1.2, 1.4, 1.6, 1.8, 2.0 and 2.2 µmol/L of HYP) for 30 min in the absence of light to evaluate cytotoxicity.

To evaluate the phototoxicity, after incubation with the same concentrations of HYP/P123 for 30 min in the absence of light, the cells were exposed to a light source for 15 min. Then, they were incubated in the absence of light for 30 min. Cells treated with DMEM (NT) or P123 alone (1.94 µmol/L) were used as controls in all assays. After the treatment, the culture medium was removed, and the cells were washed with 100 µL of phosphate-buffered saline (PBS) and 50 µL of MTT solution (2 mg/mL) was added to each well, and the plates were incubated in the dark at 37 °C in a humidified atmosphere with 5% CO₂ for 4 h. At the end of incubation, the resulting formazan was dissolved in 150 µL of DMSO and the absorbance was measured at 570 nm using a microplate reader (Loccus, Cotia, SP, Brazil).

The inhibitory concentrations (IC), IC₃₀ (concentration that inhibited cell growth by 30% compared to NT), IC₅₀ (concentration that inhibited cell growth by 50% compared to NT) and IC₉₀ (concentration that inhibited cell growth by 90% compared to NT) values were obtained by nonlinear regression analysis of the data using GraphPad Prism 6.0 (GraphPad Software, San Diego, USA).

Additionally, the cells were seeded in a 24-well tissue culture plates at a density of 1.5×10^5 cells/mL. The cells were allowed to attach overnight at 37 °C in a humidified atmosphere with 5% CO₂. After 24 h, the cells were treated with 0.4, 1.4 and 2.2 µmol/L of HYP for 30 min in the absence of light, illuminated for 15 min and then incubated in the absence of light for 30 min. The cells treated only with DMEM were used as NT. The growth and morphology of the cells were observed immediately after treatment with an inverted microscope (EVOS® FL, Life Technologies, USA).

2.7. Clonogenic cell survival assay

HeLa, SiHa, CaSki and C33A cell lines were seeded in a 6-well tissue culture plates at a density of 600 cells/well. The cells were allowed to attach overnight at 37 °C in a humidified atmosphere with 5% CO₂. After 24 h, they were exposed to IC₃₀ and IC₅₀ values of HYP/P123 for 30 min in the absence of light, illuminated for 15 min, and then incubated in the absence of light for 30 min. Then, the cells were incubated in ideal conditions for 7 or 14 days (the medium was changed

after 7 days for cells that were exposed for 14 days). The cells treated only with DMEM were used as NT. The colonies formed were stained by crystal violet solution after fixation with methanol and counted manually [58].

2.8. Cellular uptake by fluorescent microscopy

The cell lines were seeded in a 24-well tissue culture plate at a density of 1.5×10^5 cells/mL. The cells were allowed to attach overnight at 37 °C in a humidified atmosphere with 5% CO₂. After 24 h, the cells were treated with 1 µmol/L HYP/P123 and 1 µmol/L HYP dissolved in DMSO (0.024%) (HYP/DMSO), incubated at 37 °C in a humidified atmosphere with 5% CO₂ for 30 min in the dark. To display fluorescence emitted by HYP inside the cell, an inverted fluorescence microscope with an RFP (red) filter (EVOS® FL, Life Technologies, USA) was used.

2.9. Cellular uptake by flow cytometry

Additionally, HYP/P123 uptake was analyzed by flow cytometry. Briefly, the cell lines were seeded in a 6-well tissue culture plate at a density of 2.5×10^5 cells/mL. The cells were allowed to attach overnight at 37 °C in a humidified atmosphere with 5% CO₂. After 24 h, the cells were treated with 1 µmol/L HYP/P123 and 1 µmol/L HYP/DMSO, incubated at 37 °C in a humidified atmosphere with 5% CO₂ for 30 min in the dark. After this time, the cells were removed by trypsinization, centrifuged at 1000 rpm for 7 min, resuspended and washed with PBS followed by centrifugation at 1000 rpm for 7 min. After the washing and centrifugation step, the pellet was resuspended in 200 µL of PBS and then the cells were analyzed on flow cytometer (BD FACS Calibur®, San Jose, CA, USA). The cells treated only with DMEM were used as NT [59].

2.10. Subcellular distribution

The cell lines were seeded in a 24-well tissue culture plate at a density of 1.5×10^5 cells/mL. They were allowed to attach overnight at 37 °C in a humidified atmosphere with 5% CO₂. After 24 h, the cells were incubated for 1 h with subcellular organelle probes specific for mitochondria (MitoTracker® excitation: 490 nm and emission: 516 nm), lysosomes (LysoTracker® excitation: 504 nm and emission: 511 nm), endoplasmic reticulum (ER-tracker® excitation: 504 nm and emission: 511 nm) and nucleus (NucBlue® Live ReadyProbes® excitation: 360 nm and emission: 460 nm) and for 30 min with HYP/P123 (5 µmol/L). To display the fluorescence emitted by HYP/P123 and the stained cell organelles, an inverted fluorescence microscope with DAPI (blue), RFP (red) and GFP (green) filters (EVOS® FL, Life Technologies, USA) was used.

2.11. Analysis of cell death pathways by flow cytometry

HeLa, SiHa, CaSki and C33A were seeded in 6-well tissue culture plates at a density of 2.5×10^5 cells/mL. The cells were allowed to attach overnight at 37 °C in a humidified atmosphere with 5% CO₂. After 24 h, they were exposed to IC₅₀ value of HYP/P123 for 30 min in the absence of light, illuminated for 15 min, and then incubated in the absence of light for 30 min. The cells treated only with DMEM were used as NT. After the treatment, the cells were trypsinized, centrifuged, washed and resuspended in annexin-binding buffer. After this, annexin-V/FITC and PI protocol were performed according to manufacturer's instructions.

2.12. Analysis of cell death by necrosis with lactate dehydrogenase (LDH) assay

The cells were seeded in 96-well tissue culture plates at a density of

2.5×10^5 cells/mL. They were allowed to attach overnight at 37 °C in a humidified atmosphere with 5% CO₂. After 24 h, the cells were exposed to IC₅₀ value of HYP/P123 for 30 min in the absence of light, illuminated for 15 min, and then incubated in the absence of light for 30 min. The cells treated only with DMEM were used as NT. After the treatment, the supernatant was collected and analyzed using a Pierce LDH Cytotoxicity Assay Kit, a colorimetric method, according to manufacturer's instructions. The absorbance was measured at 490 nm and 680 nm using a microplate reader (Loccus, Cotia, SP, Brazil).

2.13. DNA fragmentation

The cells were seeded in 6-well tissue culture plates at a density of 1.5×10^6 cells/mL. The cells were allowed to attach overnight at 37 °C in a humidified atmosphere with 5% CO₂. After 24 h, they were exposed to IC₅₀ value of HYP/P123 for 30 min in the absence of light, illuminated for 15 min, and then incubated in the absence of light for 30 min. The cells treated only with DMEM were used as NT. After all treatments, the cells were collected and DNA was extracted using a DNA QIAamp DNA mini kit. The extracted DNA was subjected to electrophoretic analysis in a 1.2% agarose gel to identify the DNA fragmentation [60].

2.14. Detection of total ROS by fluorescent microscopy

Total ROS production was first measured based on an increase in fluorescence caused by the conversion of a non-fluorescent dye H₂DCFDA (emission 515 nm, excitation 492 nm) to highly fluorescent 2',7'-dichlorofluorescein (DCF) [60]. The cells were seeded in 24-well tissue culture plates at a density of 1.5×10^5 cells/mL. The cells were allowed to attach overnight at 37 °C in a humidified atmosphere with 5% CO₂. After 24 h, they were exposed to 0.4 μmol/L of HYP/P123 for 30 min in the absence of light, illuminated for 15 min, and then incubated in the absence of light for 30 min. After this, the cells were washed with PBS, fixed with 4% formaldehyde solution for 15 min, washed again with PBS and treated with 20 μM H₂DCFDA solution for 15 min in room temperature protected from light. After the incubation time the cells were washed with PBS and then observed and imaged using an inverted fluorescence microscope (EVOS® FL, Life Technologies, USA).

2.15. Detection of total ROS by fluorimetric assay

The cells were seeded in 24-well tissue culture plates at a density of 2.5×10^5 cells/mL. The cells were allowed to attach overnight at 37 °C in a humidified atmosphere with 5% CO₂. After 24 h, they were exposed to IC₅₀ value of HYP/P123 for 30 min in the absence of light, illuminated for 15 min, and then incubated in the absence of light for 30 min. After the treatment, the cells were incubated with 10 μM H₂DCFDA, a permeable probe, in the dark for 30 min. Afterwards, the cells were trypsinized and resuspended in PBS. A solution containing 200 μM H₂O₂ was used as a positive control (PC). The cells treated only with DMEM were used as NT. Fluorescence intensity was analyzed at an excitation wavelength of 488 nm and an emission wavelength of 530 nm with a fluorescence microplate reader (Victor X3, PerkinElmer, Finland). Arbitrary units (RFU) were based directly on fluorescence intensity, and the fluorescence was normalized to the number of cells [61].

2.16. Lipid peroxidation (LPO) assay

The cells were seeded in 24-well tissue culture plates at a density of 2.5×10^5 cells/mL. The cells were allowed to attach overnight at 37 °C in a humidified atmosphere with 5% CO₂. After 24 h, they were exposed to IC₅₀ value of HYP/P123 for 30 min in the absence of light, illuminated for 15 min, and then incubated in the absence of light for 30 min.

After the treatment, the cells were incubated with 5 μM DPPP for 15 min in the dark at room temperature. Afterwards, the cells were trypsinized and resuspended in PBS. H₂O₂ (200 μM) was used as a PC. The cells treated only with DMEM were used as NT. Fluorescence was determined at an excitation wavelength of 355 nm and an emission wavelength of 460 nm with a fluorescence microplate reader (Victor X3, PerkinElmer, Finland). RFU were based directly on fluorescence intensity, and the fluorescence was normalized to the number of cells [61].

2.17. Evaluation of type I and type II mechanism of PDT

In order to visualize the photochemical mechanism of HYP/P123 PDT, sodium azide (SA) and D-mannitol (DM) specific scavengers of ¹O₂ and hydroxyl radicals respectively, were used to prevent the ROS formation [62,63]. The experiment was divided into three treatment groups: group 1 - IC₃₀ value of HYP/P123; group 2 - IC₃₀ value of HYP/P123 and 20 mmol/L SA solution; and group 3 - IC₃₀ value of HYP/P123 and 40 mmol/L DM solution. The cells were seeded in 96-well tissue culture plates at a density of 2.5×10^5 cells/mL. The cells were allowed to attach overnight at 37 °C in a humidified atmosphere with 5% CO₂. After 24 h, they were exposed to the treatments described in groups 1, 2 and 3 for 30 min in the absence of light, illuminated for 15 min, and then incubated in the absence of light for 30 min. After the treatment, a MTT assay was performed to determine cell viability [63].

2.18. Wound-healing migration assay

Wound-healing assay was performed as previously described [64]. HeLa, SiHa, CaSki and C33A cells were seeded in 6-well tissue culture plates at a density of 2.5×10^4 cells/mL. The cells were allowed to attach overnight at 37 °C in a humidified atmosphere with 5% CO₂. After 24 h, confluent monolayers of the cells were then mechanically scratched with a blue pipet tip (1000 μL), and cell debris was removed by washing with PBS. Then, the wounded monolayer was incubated with IC₃₀ and IC₅₀ values of HYP/P123 for 30 min in the absence of light, illuminated for 15 min, and then incubated in the absence of light for 30 min. The cells treated only with DMEM were used as NT. The cell migration into the scratched region was recorded using an inverted microscope (EVOS FL Cell Imaging System, Life Technologies, CA, USA) at 0, 24, 48, and 72 h. Wound closure after 24, 48, and 72 h was compared to the initial measurements.

2.19. Invasion assay

Transwell invasion chambers containing polycarbonate filters (8 μm, Costar Corp., Cambridge, MA) were coated on the upper surface with matrigel. HeLa, SiHa, CaSki and C33A cell lines (5×10^4 cells/mL) were suspended in serum-free DMEM and IC₃₀ and IC₅₀ values of HYP/P123 were added to the upper chamber. The lower chambers contained DMEM supplemented with 10% FBS. The cells not treated with HYP/P123 were used as a NT. All cells were incubated for 24 h at 37 °C in a humidified atmosphere with 5% CO₂. The cells on the upper surface of the filter were completely removed by wiping them with a cotton swab. The cells that had invaded through the matrigel and reached the lower surface of the filter were fixed in methanol, stained with a crystal violet solution, and counted under a light microscope at 20× magnification. The mean number of cells in 10 fields was calculated, and the assay was performed in triplicate [65].

2.20. Enzyme-linked immunosorbent (ELISA) assay for MMP-2 and MMP-9

The levels of MMP-2 and MMP-9 after the treatment were quantified using an ELISA kit (Invitrogen, MA, USA). HeLa, SiHa, CaSki and C33A cells were seeded in 24-well tissue culture plates at a density of

2.5×10^5 cells/mL. The cells were allowed to attach overnight at 37 °C in a humidified atmosphere with 5% CO₂. After 24 h, the cells were exposed to IC₅₀ value of HYP/P123 for 30 min in the absence of light, illuminated for 15 min, and then incubated in the absence of light for 30 min. After the treatment, supernatants were collected, centrifuged and analyzed according to the manufacturer's instructions. The cells treated only with DMEM were used as NT. The absorbance was measured at 450 nm using a microplate reader (Loccus, Cotia, SP, Brazil).

2.21. ELISA assay for human vascular endothelial growth factor (VEGF)

The levels of VEGF after the treatment were quantified using an ELISA kit (Invitrogen, MA, USA). HeLa, SiHa, CaSki and C33A cells were seeded in 24-well tissue culture plates at a density of 2.5×10^5 cells/mL. The cells were allowed to attach overnight at 37 °C in a humidified atmosphere with 5% CO₂. After 24 h, they were exposed to IC₅₀ value of HYP/P123 for 30 min in the absence of light, illuminated for 15 min, and then incubated in the absence of light for 30 min. After the treatment, supernatants were collected, centrifuged and analyzed according to the manufacturer's instructions. The cells treated only with DMEM were used as NT. The absorbance was measured at 450 nm using a microplate reader (Loccus, Cotia, SP, Brazil).

2.22. Statistical analysis

Significant differences among means were calculated using analysis of variance (ANOVA) followed by Tukey–Kramer multiple comparisons test, except for viability experiments, where Student's t-distribution was used for data analyses. At least three independent experiments were performed to express the means \pm standard deviation (SD). GraphPad Prism 6.0 software (GraphPad, San Diego, CA, USA) was used to analyze the data. *P* values < 0.05 were considered statistically significant.

3. Results and discussion

3.1. HYP/P123-mediated PDT inhibits cervical cancer cells proliferation but not inhibits HaCaT cells

To study the effects of HYP/P123 PDT on tumor cells as well as on normal cells, we exposed four cervical cancer cell lines, HeLa (integrated HPV 18), SiHa (integrated HPV 16), CaSki (integrated HPV 16 and HPV 18), and C33A (without HPV), as well as a human immortalized keratinocyte (HaCaT) cell line (control cells), to increasing doses of HYP/P123 in the absence of light (Fig. 1A) or under light illumination (Fig. 1B), which were evaluated through MTT assay. When the cytotoxicity of HYP/P123 was evaluated in the absence of light (Fig. 1A), there was no decreasing in cell viability in all cell lines evaluated. Also, the solution containing only P123 copolymer did not showed any cytotoxic effect to the cells in the presence and absence of light. The same occurred on all the cell lines exposed to the light without the presence of HYP/P123 (NT) indicating that the illumination itself does not cause cytotoxic effects to the tested cells (Fig. 1B). Damage caused by HYP/P123 in the presence of light (Fig. 1B) showed selective action in cancer cells from the lowest concentration tested (0.40 μ mol/L; *P* < 0.05), as it was not able to significantly reduce HaCaT cell viability at the tested concentrations. Taken together, these data indicate that HYP/P123 PDT exerted concentration-dependent cytotoxic effects on all cervical cancer cell lines tested, with an IC₅₀ of 1.06 μ mol/L for HeLa, 0.8 μ mol/L for SiHa, 1.48 μ mol/L for CaSki, and 0.35 μ mol/L for C33A cells. For the HaCaT cells, the IC₃₀, IC₅₀ and IC₉₀ values were > 2.2 μ mol/L. The IC₃₀, IC₅₀ and IC₉₀ values are shown in Fig. 1C. These data highlight the selective effect of HYP/P123 micelles on cancer cells, similar to other *in vitro* [66–70] and *in vivo* [71] studies, which reported its low intrinsic toxicity and differential effects in normal versus cancer cells. Additionally, our data are in agreement with our previous study in which HYP/P123 micelles PDT showed the

selective effect on breast cancer cells but not on normal breast cells [36]. Finally, it is well known that functions of the HPV oncogenes E6 and E7 are crucial for HPV-induced cervical carcinogenesis and for the support of the viral life cycle, in which they are able to combine with tumor suppressor p53 and retinoblastoma (Rb) respectively and act cooperatively to facilitate cell immortalization, genomic instability and malignant conversion [2,4]. Considering that HYP/P123 PDT exerted concentration-dependent cytotoxic effects on cancer cells immortalized by HPV 16, HPV 18, HPV 16 and 18 together, and without HPV, this treatment does not seem to downregulate the expression of HPV E6/E7 oncogenes, but this evidence still need to be more studied.

The cell growth inhibition induced by HYP/P123 PDT was further verified by microscopy. The results presented in Fig. 1D show that the growth of HeLa, SiHa, CaSki, and C33A cells was effectively inhibited after exposure to concentrations of 0.4, 1.4 e 2.2 μ mol/L HYP/P123 in the presence of light. Whereas HaCaT cell growth was unaffected. HYP/P123 PDT also induced pronounced morphological changes when the cervical cancer cell lines were exposed to 0.4–2.2 μ mol/L HYP/P123 concentrations after illumination. The cells exhibited retraction of cytoplasmic expansion and detachment from the plate due to cell death. Morphological changes were not observed in HaCaT cells exposed to the same concentrations of HYP/P123 on the same length of time after illumination.

To further examine the ability of a cell to proliferate indefinitely, thereby retaining the reproductive ability to form a large colony or a clone after HYP/P123 PDT, a clonogenic cell survival assay was performed [58,72]. For this purpose, we exposed all cervical cancer cell lines to subtoxic doses of HYP/P123 (IC₃₀ and IC₅₀). It was observed a significant reduction in a dose-time-dependent manner in colonies formation of all cervical cancer cell lines after illumination for 7 and 14 days incubation with IC₃₀ and IC₅₀ compared to NT (*P* < 0.05). Also, there was a decrease in the number and size of the colonies circumference after incubation for 7 and 14 days (Fig. 2). These results indicated that HYP/P123 exposure to the light exerted long-term dose-dependent phototoxic effects on cervical cancer cells, which reflects the decrease in long-term cell proliferation.

Overall, these results show that HYP/P123 micelles decreased colony formation at HYP subtoxic doses and had a selective dose- and time-dependent cytotoxic effect on cervical cancer cells, highlighting their potential for PDT of cervical cancer.

3.2. HYP/P123 was actively and selectively internalized by all tumor cell lines

The presence of intracellular HYP was first observed through the emitted fluorescence in the RFV (red) filter, as seen in Fig. 3A and B. It was possible to observe that the intensity of the emitted fluorescence by HYP on all cancer cell lines treated with HYP/P123 micelles was higher. The same was not observed in HaCaT. In addition, fluorescence was observed mainly in the cytoplasm of tumor cells (Fig. 3B). When the cells were treated with HYP/DMSO, it was not possible to verify red fluorescence inside the cells even in the tumor cells and HaCaT (Fig. 3A). Next, the internalization of HYP/P123 was analyzed using flow cytometry. The fluorescence intensity presented by the tumor cells treated with HYP/P123 was higher than that presented when the cells were incubated with HYP/DMSO (Fig. 3C). On the other hand, the fluorescence profile presented by the HaCaT was very different from that presented by the tumor cells. More specifically, it is possible to observe in the Fig. 3C that HaCaT cells incubated with DMEM or treated with HYP/DMSO presented very similar fluorescence intensity. However, an increase in the fluorescence was observed when these cells were treated with HYP/P123, but this fluorescence intensity was similar to the intensity presented by the tumor cells when incubated with HYP/DMSO. Taken together, these data demonstrate that the HYP/P123 exhibit a higher capacity to permeate the cytoplasmic membrane and to internalize preferably in the cytoplasm of all cervical cancer

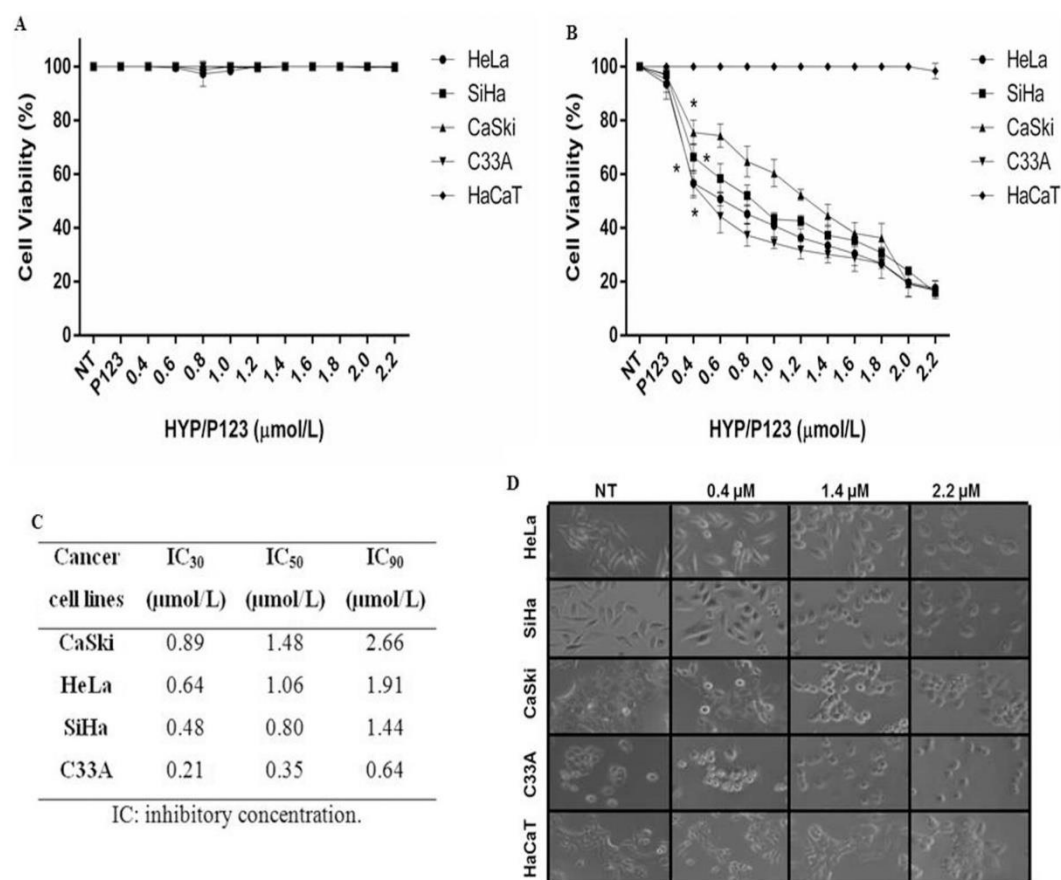


Fig. 1. Cytotoxic and phototoxic effects of HYP/P123 on cervical cancer cell lines (HeLa, SiHa, CaSki, and C33A) and on a human keratinocyte cell line (HaCaT). (A) Dose-response curves indicating the viability of the cervical cancer cell lines and the HaCaT cells (control cells) not changed following exposure to HYP/P123 (0.4–2.2 $\mu\text{mol/L}$) in the absence of light compared to non-treated (NT) cells. (B) Dose-response curves indicating the viability of the cervical cancer cell lines and the HaCaT cells following exposure to HYP/P123 (0.4–2.2 $\mu\text{mol/L}$) in the presence of light. A statistically significant difference in cell viability was observed between the HeLa, SiHa, CaSki, and C33A cells. (*) represent statistically significant ($P < 0.05$) differences between the treated and NT cancer cell lines. Each line represents the mean \pm SD of three independent experiments conducted in triplicate. (C) Approximate IC₃₀, IC₅₀ and IC₉₀ values determined according to the cell viability (MTT assay) obtained in B. For the HaCaT cells, the IC₃₀, IC₅₀ and IC₉₀ values were $> 2.2 \mu\text{mol/L}$. (D) Differential effects on cell morphology induced by HYP/P123 in the presence of light. Cell photomicrographs were taken at $20\times$ magnification. Note that the HaCaT cells do not show morphological changes.

cells, proving their selective activity toward cancer cells. Thus, the entry of HYP into the cervical cancer cells was facilitated by the P123, which was previously described to act as a delivery method to facilitate transport across the cytoplasmic membranes or the target binding site [24]. The exact mechanisms of cellular uptake of HYP are still unclear and require further investigation [73]. Whether the cellular uptake of HYP relies mainly on passive processes like temperature-dependent diffusion and solubility [74,75] or through membrane transport pathway (such as endocytosis or pinocytosis) [76] is still unsettled [77]. The association between transport behavior of HYP and determinants of its subcellular localization therefore require further investigation.

3.3. HYP/P123 leads to HYP distribution in the endoplasmic reticulum, mitochondria, and lysosomes in all tumor cell lines

The subcellular localization of HYP after incubation with HYP/P123 micelles was analyzed through specific organelle probes for mitochondria (MitoTracker[®]), lysosomes (LysoTracker[®]), endoplasmic reticulum (ER-tracker[®]), and nucleus (NucBlue[®]), using fluorescence imaging. The overlap of the images shows a change of the color in the region in which HYP is located in the organelles. As seen in Fig. 4, all

tumor cell lines presented high fluorescence intensity after HYP/P123 exposure which coincides with the fluorescence of the ER, mitochondria, and lysosomes. These data are in agreement with other studies that revealed that HYP accumulates in the membranes of the ER, the Golgi apparatus, lysosomes and mitochondria [14,19,78,79]. Additionally, all tumor cell lines presented a weak or absent fluorescence of HYP that coincides with the fluorescence of the nucleus, which is also in agreement with other studies [19].

The cellular uptake and subcellular localization of HYP might be affected by its lipophilicity, incubation concentrations and/or interaction with serum lipoproteins [14,59,80]. In relation to lipophilicity, the subcellular location of the PS is directly related to its chemical nature. Hydrophobic and hydrophilic PS with > 2 negative charges in their molecules differs in their ability to diffuse through the plasma membrane and relocate into intracellular membranes. Hydrophobic PS exhibit these abilities whereas hydrophilic PS due to being too polar are captured by endocytosis [81]. Considering these concepts, our results indicate that the problem of HYP hydrophobicity [22,23] was overcome with the Pluronic[®] P123 encapsulation. Pluronic[®] P123 plays a key role in the encapsulation capacity of the PS but also in its delivery, facilitating passive transcellular diffusion across the biomembrane

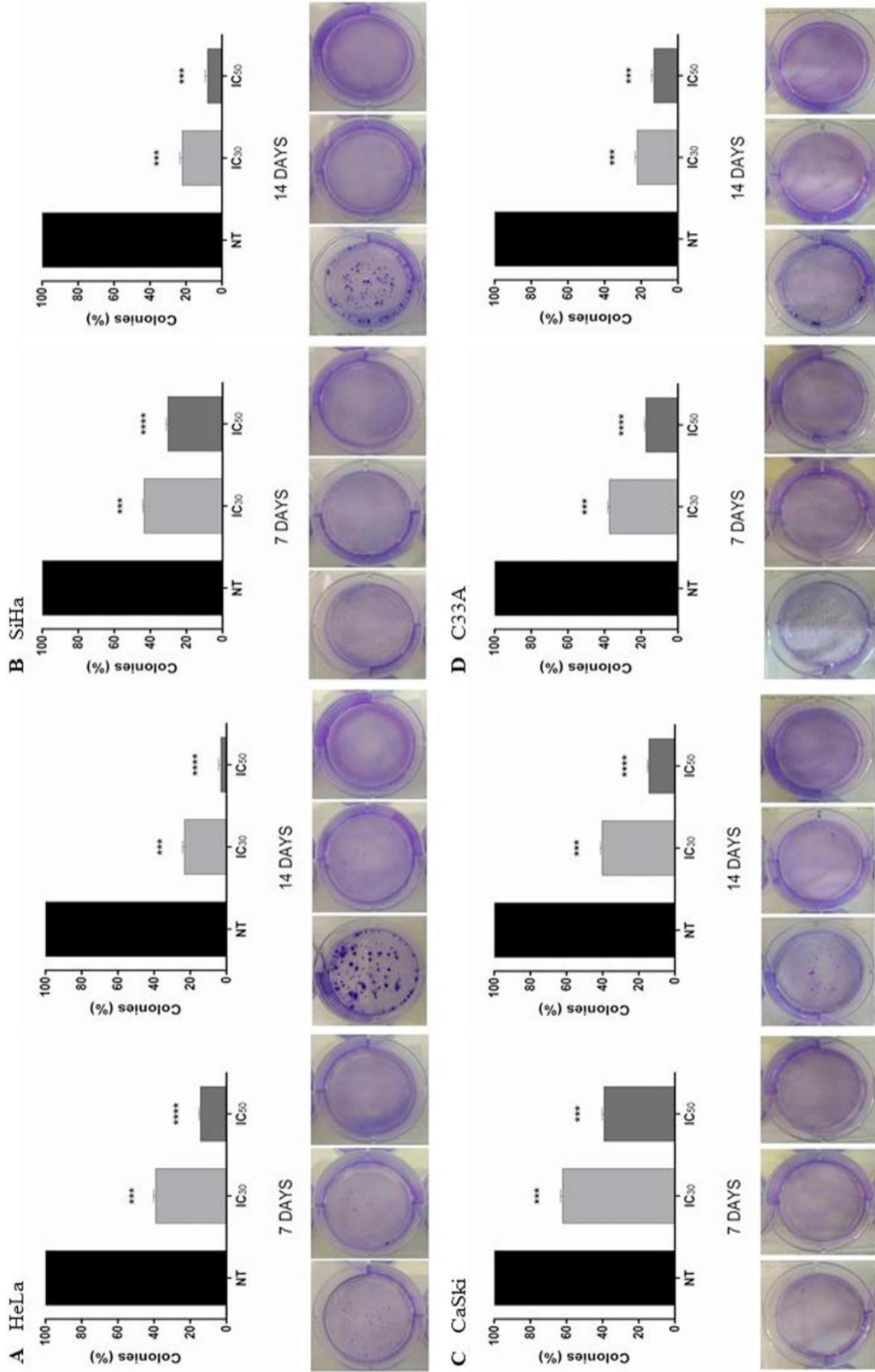


Fig. 2. The effect of HYP/P123 PDT exposure on the clonogenicity of cervical cancer cell lines at 7 and 14 days followed by culture with DMEM. The graph indicates that the recovery diminished with increasing times of exposure in cervical cancer cell lines. Data are shown as the mean values \pm SD of three independent experiments conducted in triplicate. Photos indicate that exposure to HYP/P123 PDT reduced colony formation by 7 and 14 days in HeLa (A), SiHa (B), CaSki (C), and C33A (D) cell lines. The (***) (****) marks statistical significance when comparing treated cell groups (IC₃₀ and IC₅₀) with NT for 7 or 14 days. $P < 0.05$ was considered significant.

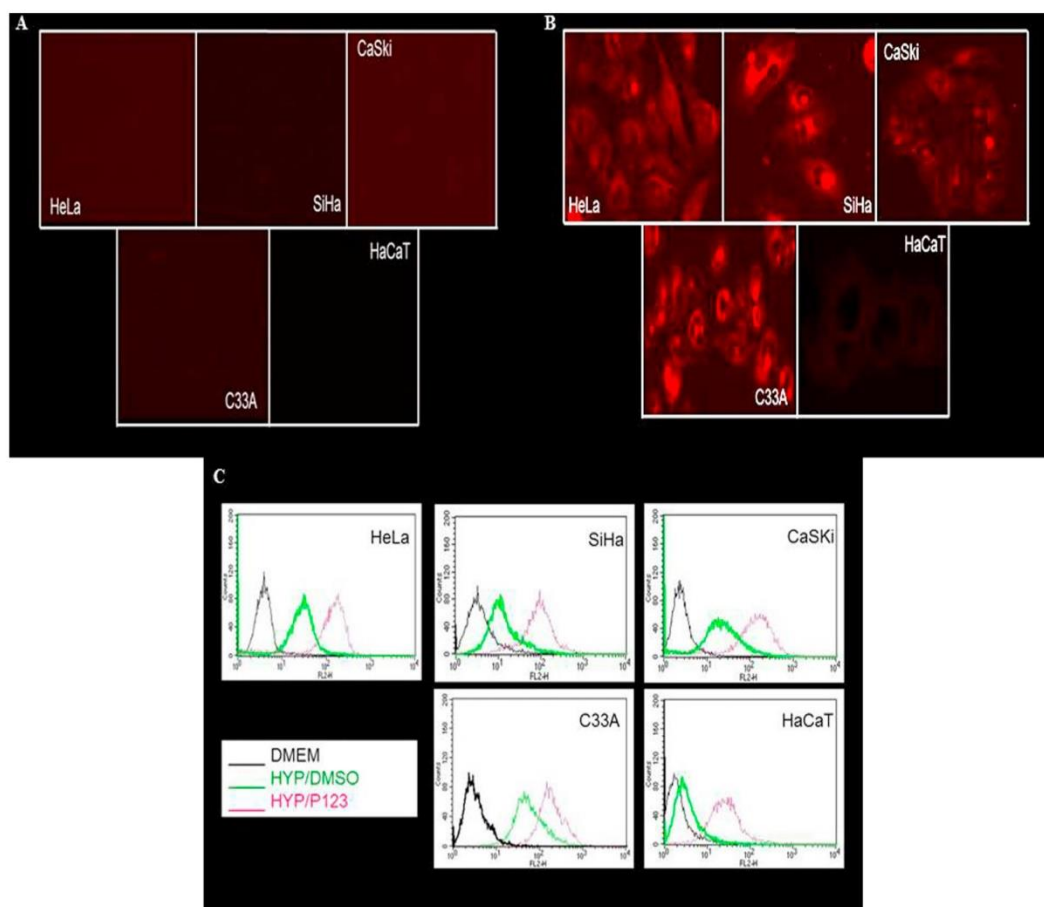


Fig. 3. Cellular uptake of HYP/123 in HeLa, CaSki, SiHa and C33A tumor cells and in HaCaT cell line (control cells) determined by fluorescence microscopy and by flow cytometry. (A) Cellular uptake of cell lines treated with HYP/DMSO determined by fluorescence microscopy with RFV (red) filter (20 \times magnification). It was not possible to verify red fluorescence inside the cells even in the tumor cells and HaCaT. (B) Cellular uptake of cell lines treated with HYP/123 determined by fluorescence microscopy with RFV (red) filter (20 \times magnification). All tumor cell lines showed high fluorescence intensity but in HaCaT no fluorescence was observed. (C) HYP/123 cellular uptake of cell lines determined by flow cytometry. Data are shown as the mean values of three independent experiments conducted in triplicate. (For interpretation of the references to color in this figure legend, the reader is referred to the web version of this article.)

microenvironment via lipophilic domains [82–84]. Other advantages have been described in addition to stabilizing, protecting, and improving the biodistribution of the encapsulated drug [29]. Our data showing the subcellular localization of HYP after incubation with HYP/P123 micelles in HeLa, SiHa, CaSki and C33A cell lines reinforce the advantages of Pluronic® P123 for encapsulation of HYP as an option for future studies in the treatment of cervical cancer.

The occurrence of necrosis or apoptosis following HYP PDT depends on HYP subcellular location [77]. Generally, photoactive compounds localizing in the mitochondria or the ER promote apoptosis, within a certain threshold of oxidative stress, while PDT with photosensitizers targeting either the plasma membrane or lysosomes, can either delay or block the apoptotic program predisposing the cells to necrosis [85]. Therefore, considering that HYP was sub-localized in the ER, mitochondria and lysosomes, we evaluated the type of cell death pathway involved in cells treated with HYP/P123 PDT.

3.4. HYP/P123-mediated PDT induces predominantly necrotic death in cervical cancer cells

Upon light-activation, HYP is efficient primarily in the generation of

singlet oxygen (1O_2 ; type II mechanism) and superoxide anion (O_2^- ; type I mechanism) [86,87], which can ultimately lead to necrosis [40,88,89], apoptosis [78,89], autophagy-associated cell death [90,91] or even to immunogenic cell death (ICD) [92]. As described above, HYP/P123 PDT induces a significant decrease in all cervical cancer cell lines viability and was sublocalized in the ER, mitochondria and lysosomes. To determine the type and extent of cell lines death, we first analyzed whether HYP/P123 PDT could induce apoptosis and/or necrosis in cervical cancer cells via an Annexin V-FITC/PI assay using flow cytometry. Annexin-V/FITC conjugate and PI were used for assessing the percentage of viable, early apoptotic, late apoptotic/necrotic and necrotic cells. It is based on the principle that normal cells are hydrophobic in nature as they express phosphatidyl serine in the inner membrane (side facing the cytoplasm) and when the cells undergo apoptosis, the inner membrane flips to become the outer membrane, thus exposing phosphatidyl serine. The exposed phosphatidyl serine is detected by Annexin V, and PI stains the necrotic cells, which have leaky DNA content that help to differentiate the apoptotic and necrotic cells [93].

Fig. 5 shows the distribution of cell populations after the cell lines exposure to IC_{50} value of HYP/P123 with illumination. Cells treated

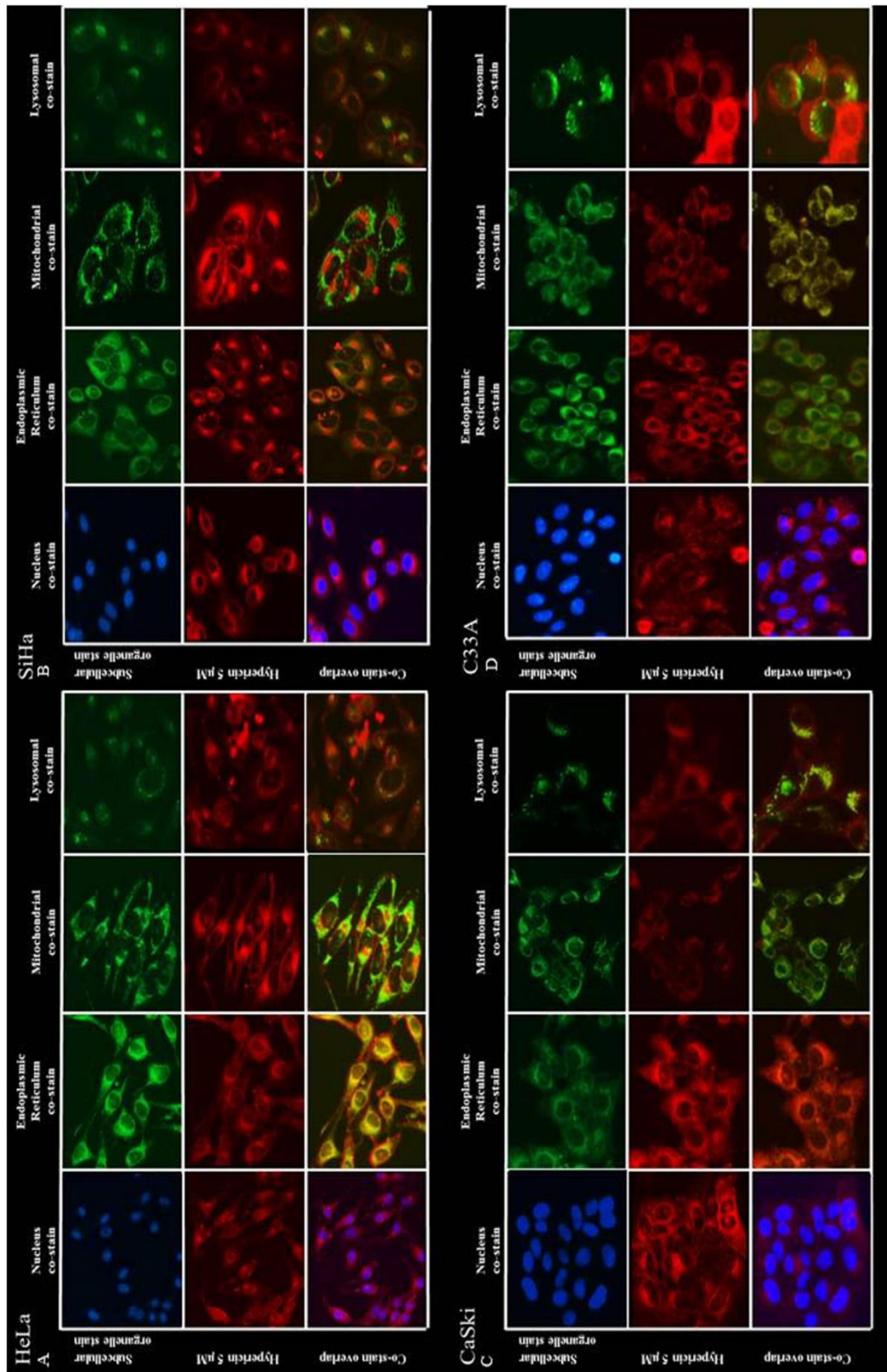


Fig. 4. HYP subcellular localization after treatment with HYP/P123 (5 µmol/L, HYP/P123) micelles in cervical cancer cell lines incubated for 30 min and co-stained with specific organelle probes for mitochondria (MitoTracker[®]), endoplasmic reticulum (ER-tracker[®]), lysosomes (LysoTracker[®]) and nucleus (NucBlue[®]), and using fluorescence imaging. (A) HeLa, (B) SiHa, (C) CaSki and (D) C33A cell lines. Cell photomicrographs were taken at 20 × magnification.

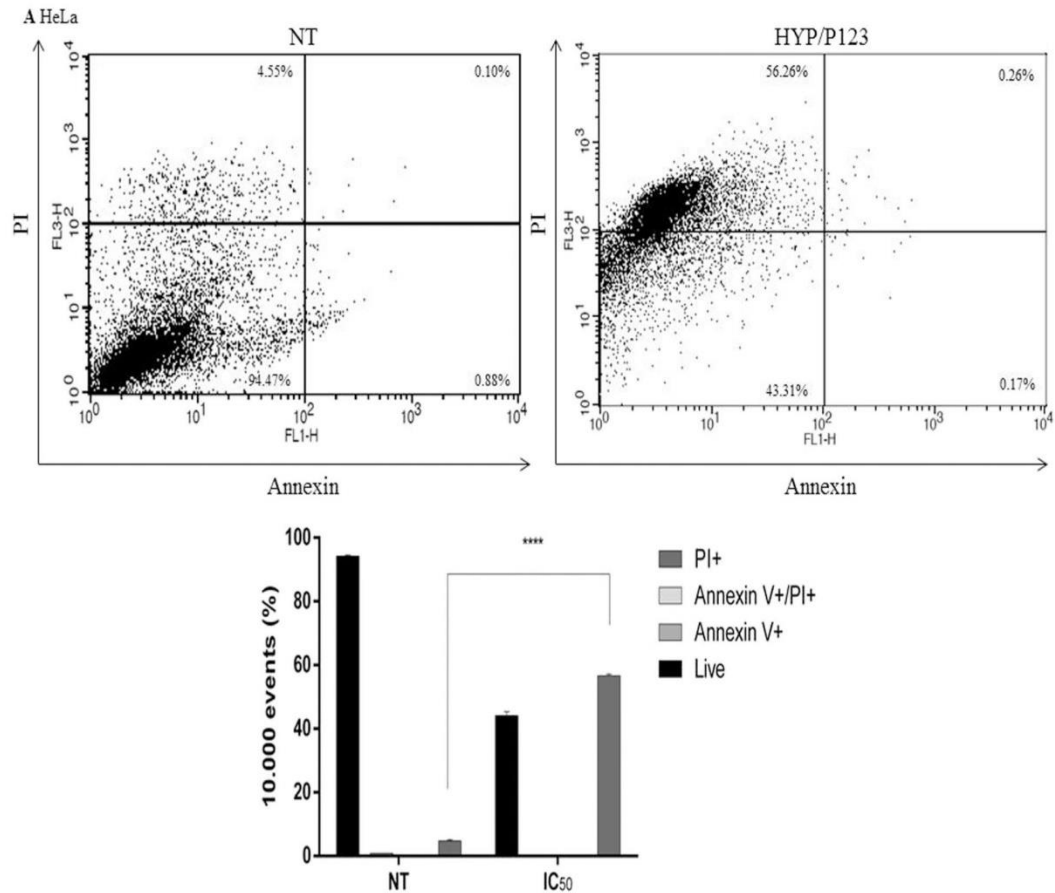


Fig. 5. Death pathway analysis via an Annexin V-FITC/PI assay using flow cytometry on cervical cancer cell lines HeLa (A), SiHa (B), CaSki (C) and C33A (D) exposed to IC₅₀ value of HYP/P123 PDT. Cells treated only with DMEM were used as NT. Dot plot shows intensity of Annexin V-FITC fluorescence on the X-axis and PI fluorescence on the Y-axis. The graph indicates the percentage of live cells in comparison to apoptotic (Annexin V⁺), late apoptotic (Annexin V⁺/PI⁺) and necrotic cells (PI⁺); each bar represents the mean \pm SD of three independent experiments conducted in triplicate. One-way ANOVA with a multiple comparison test (Tukey-Kramer multiple comparisons test) was used for data analysis to identify potentially causal associations between variables. The (*) (****) marks statistical significance when comparing treated cells with NT. $P < 0.05$ was considered significant.

only with DMEM were used as NT. A dot-plot of annexin-V-FITC versus PI showed four separate clusters: viable cells (lower left quadrant), early apoptotic cells (upper left quadrant), late apoptotic cells (upper right quadrant), and necrotic cells (lower right quadrant). As can be seen in Fig. 5A–D, the main death pathway after HYP/P123 PDT in all cancer cell lines was necrosis but apoptosis was also detected in some cancer cell lines. More specifically, HeLa and C33A showed significant association with the cluster characteristic of necrotic cells (Fig. 5A and D, respectively). SiHa and CaSki were associated with necrotic cells and also with late apoptotic cells (Fig. 5B and C respectively). Additionally, SiHa presented a weak association with early apoptosis (Fig. 5B).

The HYP subcellular distribution in the lysosomes observed by us is compatible with the death pathway by necrosis since it has already been determined that the activation of photosensitizers on lysosomes may disrupt the lysosomal membrane and result in the release of lysosomal proteases that may lead to necrosis [94]. On the other hand, the subcellular distribution of HYP in the ER and mitochondria observed in the cervical cancer cell lines suggests a death pathway due to apoptosis. Early apoptotic cells were significantly detected only on SiHa cells. This can be explained, at least in part, by the following evidence. Depending on the strength of the photodynamic process (e.g., light dose and dye concentration) HYP may inflict severe damage to the

mitochondria leading to a bioenergetic collapse which favors necrotic cell death, or diminish their defenses against cell death pathways, perturbing mitochondrial membrane integrity [95]. Still, it is well known that necrosis is the major cell death morphology induced by PDT with compounds localized in the plasma membrane [96–98]. This is likely due to a rapid loss of plasma membrane integrity, incapability to maintain ion fluxes across the plasma membrane and fast depletion of intracellular ATP, following photosensitization [99,100]. However, in certain PDT paradigms, necrosis and not secondary necrosis consequent to apoptotic cell death, appears to be the preferential mode of cell death also for photosensitizers originally found in the plasma membrane or subsequently relocated to other subcellular compartments. This suggests that signaling pathways that orchestrate necrosis rather than apoptosis may exist. Although a biochemical pathway mediating necrosis following PDT has not been identified yet, certain factors, such as Ca²⁺ overload, the origin and type of generated ROS, may be decisive to promote a necrotic cell death pathway [101].

Furthermore, our results are consistent with other studies, as follows. Studies with murine and human tumor cell lines presented a shift from apoptotic to necrotic cell death pathway produced by the increase of HYP concentration and/or the increase of light exposure [102–104]. Necrosis was described by Mikes et al. [40] as a predominant death

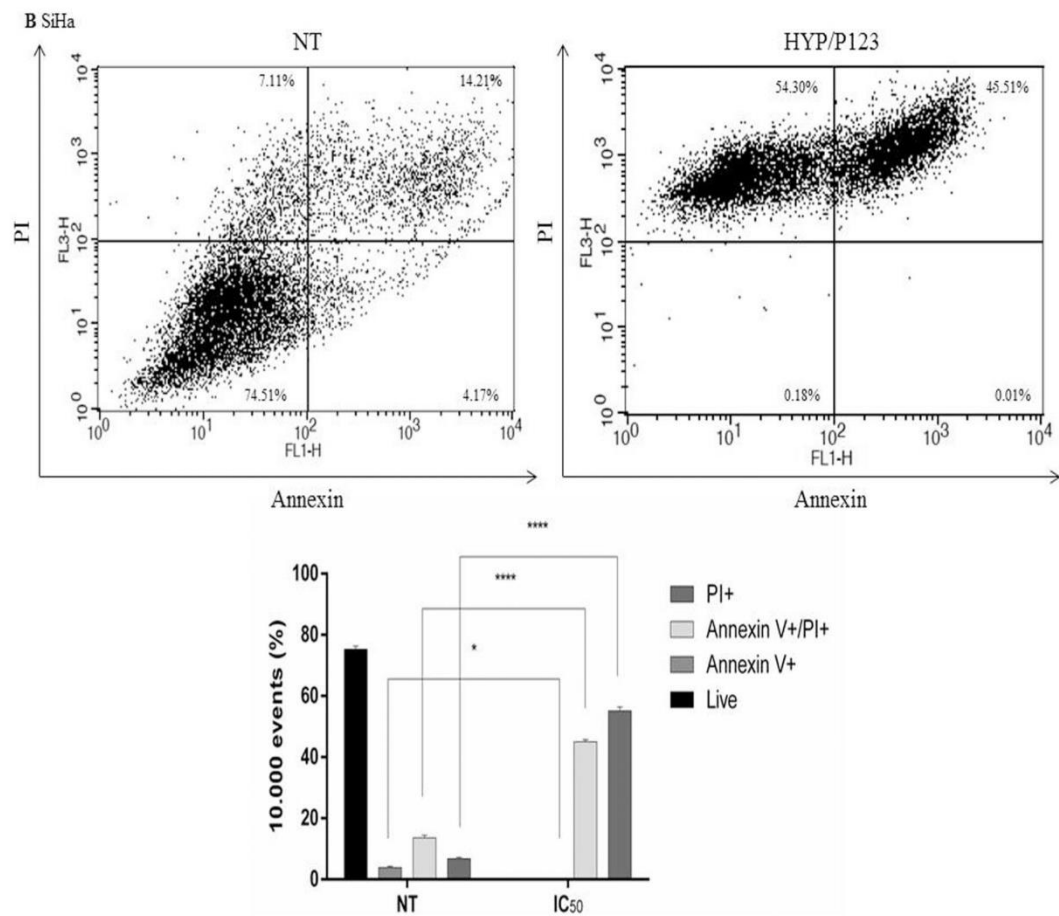


Fig. 5. (continued)

pathway in the human colon adenocarcinoma HT-79 cell line after treatment with HYP alone. Lavie et al. [105] showed changes in the apoptotic pathway for necrosis when they treated promyelocytic leukemia HL-60 cells by increasing the extracellular concentration of HYP.

Considering the results described above that showed death mainly by necrosis in all cancer cell lines, we evaluated the cell death by necrosis pathway by other assays. Although there are many assays for the detection of apoptosis, relatively few assays are available for measuring specifically necrosis. A key signature for necrotic cells is the permeabilization of plasma membrane. This event can be quantified in tissue culture settings by measuring the release of the enzyme LDH [106]. LDH is a stable cytoplasmic enzyme that is found in almost all cells and is released into extracellular space and in cell culture supernatant when the plasma membrane is damaged [107]. Therefore, we further evaluated the necrosis death pathway by the LDH assay. As shown in Fig. 6A, higher levels of LDH were quantified in all cervical cancer cell lines medium than in the NT (HeLa, SiHa, and CaSki, $P = 0.001$; C33A, $P = 0.0012$) but not in HaCaT cells ($P > 0.9999$) after HYP/P123 PDT (IC_{50}).

Next, we evaluated the effect of HYP/P123 exposure in the presence of light by DNA fragmentation that is a classic signal of apoptotic cells. DNA fragmentation was not observed after HYP/P123 PDT (Fig. 6B). These results contribute to reinforce the results obtained in the analysis of the cell death pathway, in which necrosis was the predominant cell death pathway. The results also showed that although was detected early apoptosis in SiHa by flow cytometry, this was not the main death

pathway in these cells. Similar to other cell lines, SiHa also did not presented DNA fragmentation, showing that death by early apoptosis was not a significant death pathway. Still, the absence of DNA fragmentation in all cervical cancer cell lines is also in accordance with the results of HYP subcellular distribution, in which HYP fluorescence on the nucleus was weak/absent. These results may be due, at least in part, to the weak HYP-DNA interaction, which leads to a very low probability of HYP genotoxicity [108–111].

3.5. HYP/P123-mediated PDT induces oxidative stress in cervical cancer cell lines but not in HaCaT

We began studying the mechanistic action of HYP/P123-mediated PDT by examining the production of total ROS. To accomplish this, ROS production was measured based on an increase in the fluorescence. This was caused by the conversion of a nonfluorescent dye H_2DCFDA to highly fluorescent DCF [60] after HYP/P123-mediated PDT exposure to $0.4 \mu\text{mol/L}$ of HYP/P123 in the cervical cancer cell lines and HaCaT cells with illumination. Fig. 7A shows the bright field images and their corresponding fluorescence images of the cells treated with HYP/P123 PDT, that confirm the successful delivery of HYP/P123 and production of intracellular total ROS via PDT. The cervical cancer cells presented intense fluorescence in their cytoplasm while the HaCaT, a non-tumor cell line, did not.

Next, we assessed the production of total ROS by fluorimetric assay (Fig. 7C). Our results showed that HYP/P123 PDT significantly

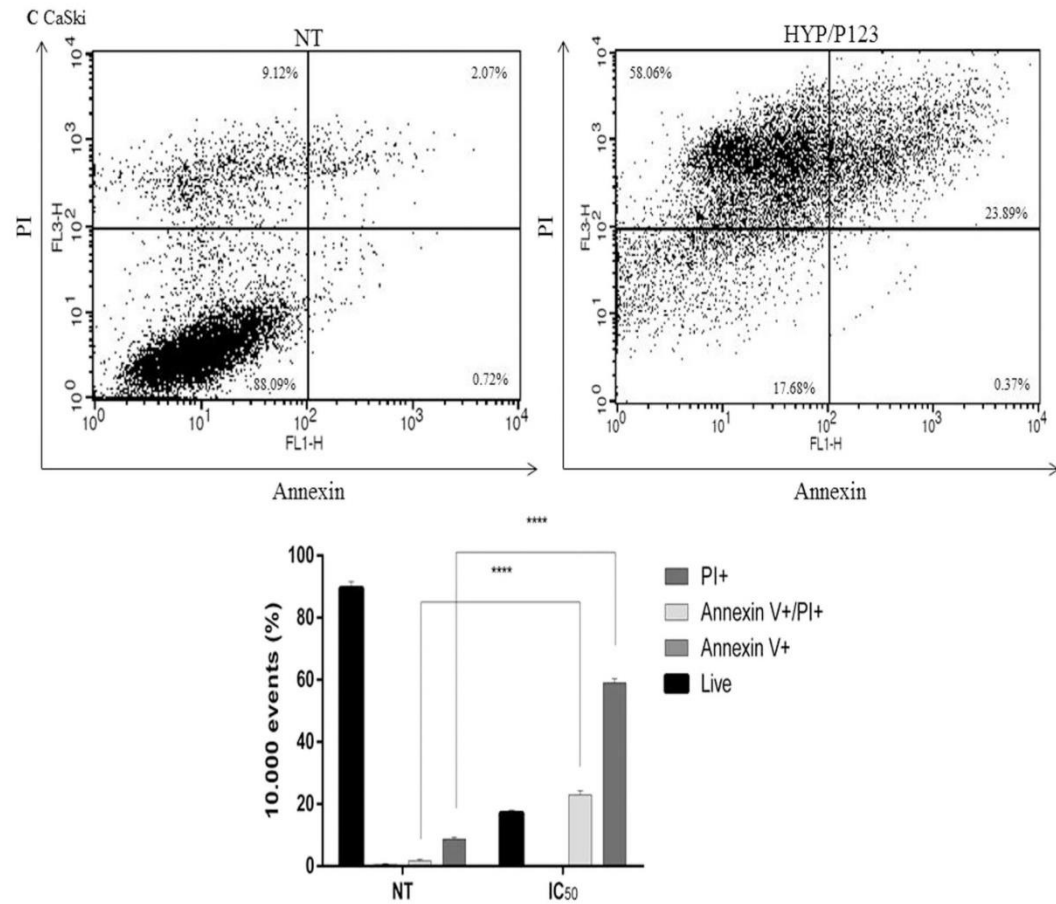


Fig. 5. (continued)

increased total ROS production in all cervical cancer cell lines compared with NT ($P < 0.0001$ for HeLa, SiHa, CaSki and C33A). This increase in total ROS production was similar to that induced by the PC cells treated only with H_2O_2 . Moreover, total ROS production was not changed in the HaCaT cells after exposure to HYP/P123-mediated PDT ($P > 0.9999$); rather, the HaCaT cells maintained ROS levels similar to the NT.

Following, we evaluated the effect of HYP/P123 PDT on LPO that can be used as an indicator of cellular oxidative stress. LPO can be defined as a cascade of biochemical events resulting from the action of free radicals on the unsaturated lipids of cell membranes. This process primarily generates alkyl, peroxy, and alkoxy radicals, leading to the destruction of unsaturated lipid structure, the failure of mechanisms that exchange metabolites, and the induction of cell death [112]. The extent of lipid peroxidation was determined based on the amount of DPPH, which is essentially non-fluorescent until it is oxidized to a phosphine oxide (DPPP-O) by peroxides [113]. Our results showed that HYP/P123 PDT significantly increased LPO in all cervical cancer cell lines compared with the NT ($P < 0.0001$ for HeLa, SiHa, CaSki, and C33A). LPO was not changed in HaCaT cells after exposure to HYP/P123 PDT ($P = 0.9999$) (Fig. 7B). The high total ROS production and increased LPO in all cervical cancer cells but not in HaCaT reinforce the selective action of HYP/P123 PDT on cervical cancer cells.

Finally, considering that total ROS formation in PDT can occur through two mechanisms known as type I and type II, we evaluated these mechanisms. In type I mechanism occurs the formation of superoxide, hydroxyl radicals, among others. Already in type II

mechanism occurs the formation of closely reactive specie, known as 1O_2 that plays an important role in PDT [62,63]. In order to visualize the photochemical mechanism of HYP/P123 PDT, SA and DM specific scavengers of 1O_2 and hydroxyl radicals respectively, were used to prevent the ROS formation and to establish the type of PDT. After adding SA and DM during the treatment, ROS originated from PDT would be quenched, resulting in lower PDT action and subsequently increasing cell viability [63]. As shown in the Fig. 7D, the cell viability of the two groups tested with SA or DM was higher than those treated only with HYP/P123 IC_{30} values. Although cell viability was increased in both groups treated with scavengers, it was possible to note a slightly higher increase in the group treated with SA, suggesting that the formation of 1O_2 was higher than the other ROS. These data show that the type II mechanism of PDT is predominant in the cervical cancer cells treated with HYP/P123 PDT. It has previously been determined that both mechanisms can occur simultaneously and the ratio between them depends on the PS and the nature of the substrate molecules [114–117]. However, direct and indirect evidence supports a prevalent role for 1O_2 in the molecular processes initiated by PDT [118] as detected by us. Additionally, it has been suggested that the type II mechanism is the one to play a major role in the biological photoactivity of HYP [74,86] which is also in line with our results.

Taken together, our data reinforce again the selectivity of PDT action using the HYP/P123 increasing cellular oxidative stress in all cervical cancer cell lines but not in normal cells mainly via type II mechanism of PDT.

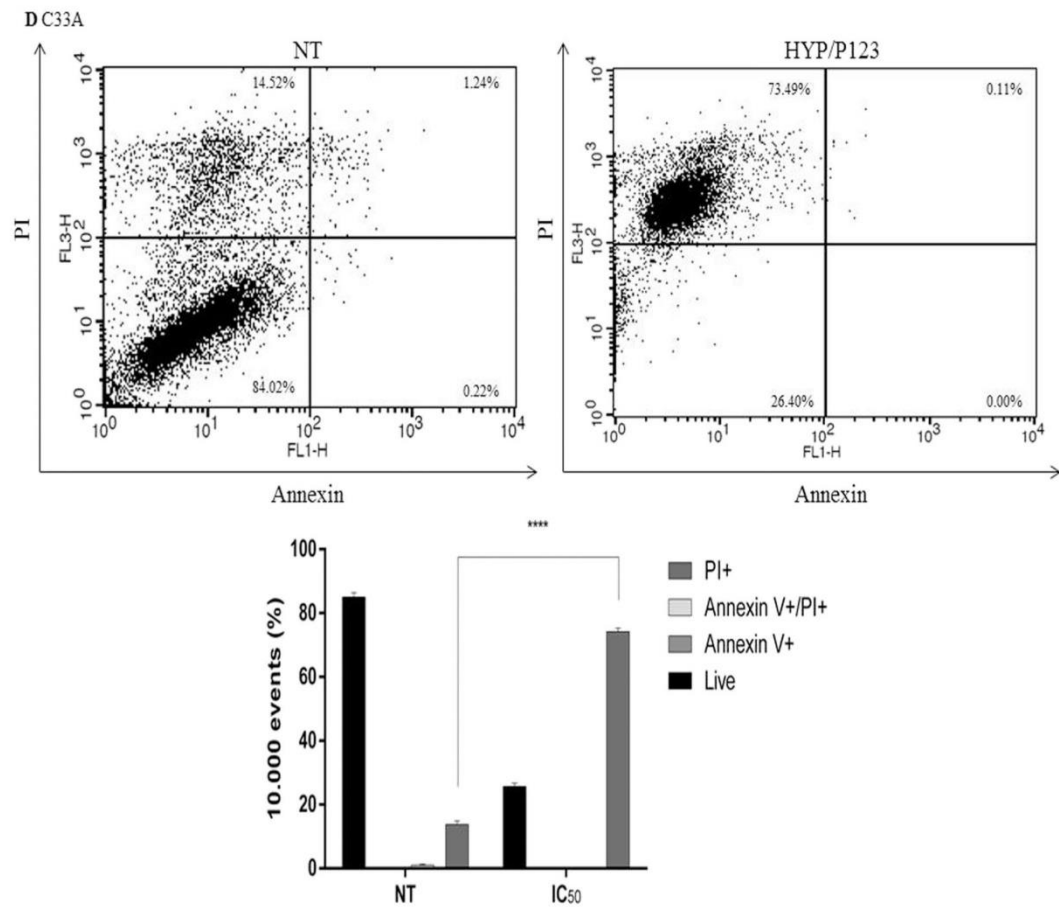


Fig. 5. (continued)

3.6. HYP/P123-mediated PDT inhibits cervical cancer cells migration and invasion

To further examine the effect of HYP/P123 PDT on cervical cancer cells migration, a wound-healing assay was performed. As shown in Fig. 8A–D, HYP/P123 (IC₃₀ and IC₅₀) effectively inhibited cells' basal migratory ability in HeLa, SiHa, CaSki and C33A at all times tested ($P < 0.0001$ at 24 h, 48 h, and 72 h for all cell lines) after PDT. Total wound closure was only observed in NT cells within 72 h for SiHa and CaSki, and within 48 h for HeLa and C33A, highlighting the effect of the HYP/P123 in preventing the migration of tumor cells, possibly by decreasing their ability to form metastases.

We next evaluated the effect of HYP/P123 PDT on cervical cancer cells migration and invasion abilities by the number of cells that migrated through a reconstituted matrigel layer to the bottom surface of a porous membrane in a transwell chamber assay. As shown in Fig. 8E, both concentrations of HYP/P123 (IC₃₀ and IC₅₀ of each cancer cell line) reduced the number of cells in the bottom surface of the transwell chamber, indicating a decrease in the invasiveness of all four cancer cell lines. There was a further significant reduction in cell invasion observed at the IC₃₀ and IC₅₀ of HYP/P123 in HeLa ($P = 0.0018$ and $P = 0.0008$, respectively), SiHa ($P = 0.0021$ and $P = 0.0005$, respectively), CaSki ($P = 0.0025$ and $P = 0.0012$, respectively), and C33A ($P = 0.0015$ and $P = 0.0001$, respectively) cells compared to the NT cells. These data shows the potential of HYP/P123 PDT in the decrease of the invasiveness of cervical cancer cells.

The processes of tumor growth, invasion and metastasis involve several complex biological phenomena: cell proliferation, proteolytic digestion and migration through components of the cell matrix [119]. In squamous carcinoma as the cervix, invasion and metastasis are regulated by a complex system characterized by neoplastic and stromal cell interaction. These processes are a consequence of basement membrane and extracellular matrix degradation by various enzymes, mainly matrix metalloproteinases (MMPs). The latter are zinc-dependent enzymes, with low expression in normal tissues but over-expressed in malignant neoplasms [120]. Of all MMPs, MMP-2 and MMP-9 (gelatinases) have been consistently associated with aggressiveness, metastatic potential, and poor prognosis in malignant neoplasms [119,120]. So, our next step was to assess the levels of MMP-2 and MMP-9 produced by cervical cancer cell lines after exposure to HYP/P123 PDT. ELISA was used to quantify this production in cervical cancer cells supernatants [121]. After the treatment with HYP/P123 PDT we noticed a significant decrease in MMP-2 levels in HeLa ($P = 0.001$), SiHa ($P = 0.0152$), CaSki ($P = 0.0081$) and C33A ($P = 0.0100$) (Fig. 9A). MMP-2 is the most abundant MMP, secreted by many cell types including tumor cells as cervical cancer [122]. Therefore, HYP/P123 PDT presented a potent effect on inhibition of invasion and metastasis via MMP-2 production inhibition.

Regarding MMP-9, there was a significant reduction in the production of this enzyme in HeLa ($P = 0.0016$), SiHa and CaSki ($P < 0.0001$ for both) cells. In the C33A cells, although it was observed a reduction in the production, it was not statistically significant ($P =$

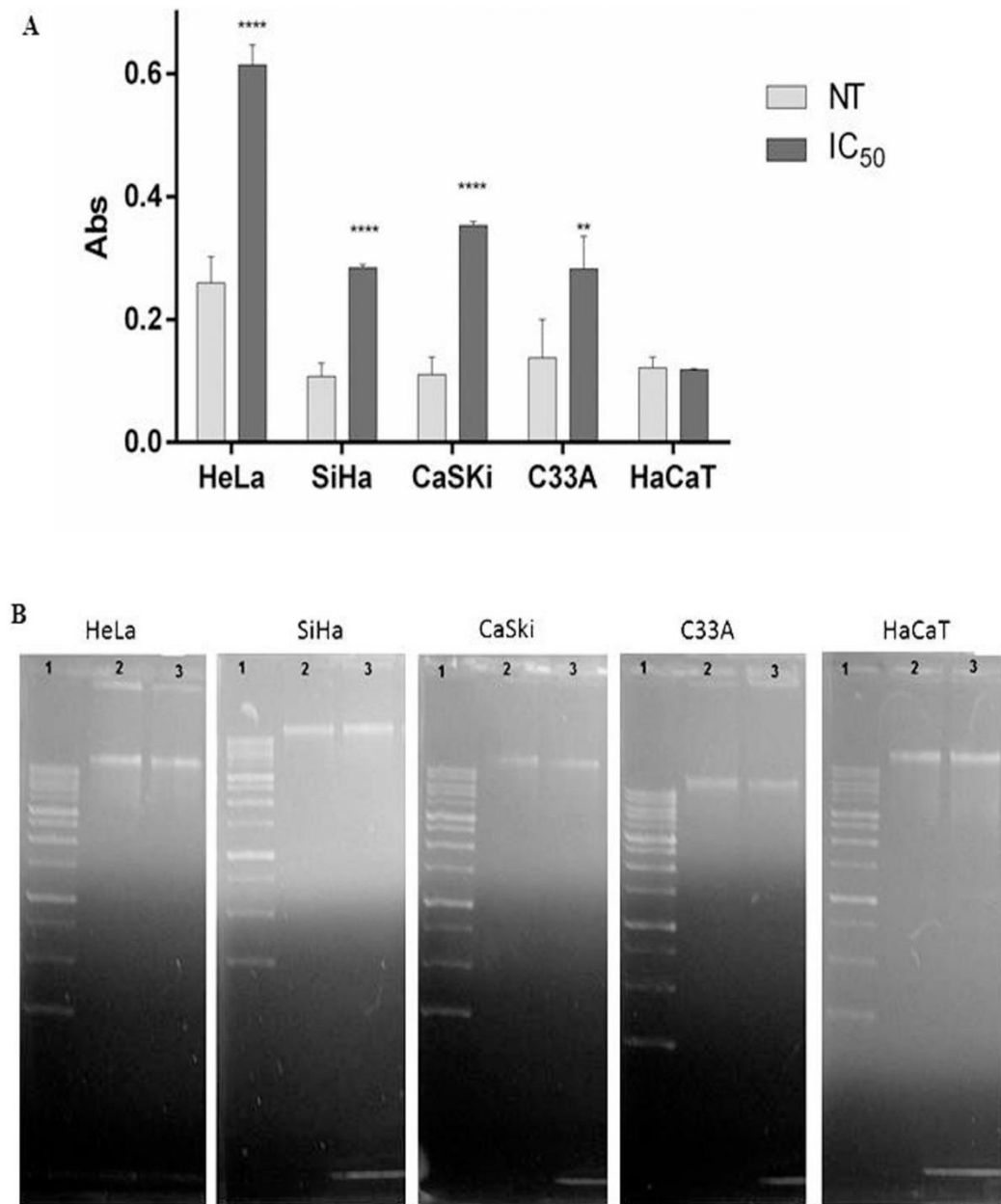


Fig. 6. Analysis of cell death pathways induced by HYP/P123-mediated PDT. (A) Permeabilization of the plasma membrane by measuring the release of the intracellular enzyme LDH. Each bar represents the mean \pm SD of three independent experiments conducted in triplicate. One-way ANOVA with a multiple comparison test (Tukey–Kramer multiple comparisons test) was used for data analysis to identify potentially causal associations between variables. The (**) (****) marks statistical significance when comparing treated cell groups (IC₅₀) with NT. $P < 0.05$ was considered significant. (B) DNA fragmentation assay. Agarose gel electrophoresis of HeLa, SiHa, CaSki, C33A and HaCaT treated with IC₅₀ values or NT. Lane 1: 1Kb DNA ladder, lane 2: NT and lane 3: cells treated with IC₅₀ values.

0.9417) (Fig. 9B). The data regarding HeLa, SiHa and CaSki are in agreement with Du et al. [123] which reported the down-regulation of MMP-9 following HYP PDT in well-differentiated human nasopharyngeal cancer cells infected by the Epstein Barr virus. On the other hand, our data of MMP-9 are in accordance with Stupáková et al. [124] that found that MMP-9 was not inhibited at all in glioma cells by photoactivated HYP.

Like other types of pre-malignant lesions and carcinoma,

angiogenesis is associated with high-grade cervical dysplasia and with invasive squamous carcinoma of the cervix. VEGF is known to be one of the most important inducers of angiogenesis and is upregulated in carcinoma of the cervix. Additionally, HPV 16 E6 oncoprotein activates the VEGF gene promoter [125]. Considering these evidences, we evaluated whether treatment with HYP/P123 PDT influences the production of VEGF in HeLa, SiHa, Caski and C33A cell lines. As shown in Fig. 9C, after treatment with HYP/P123 PDT, the VEGF production was

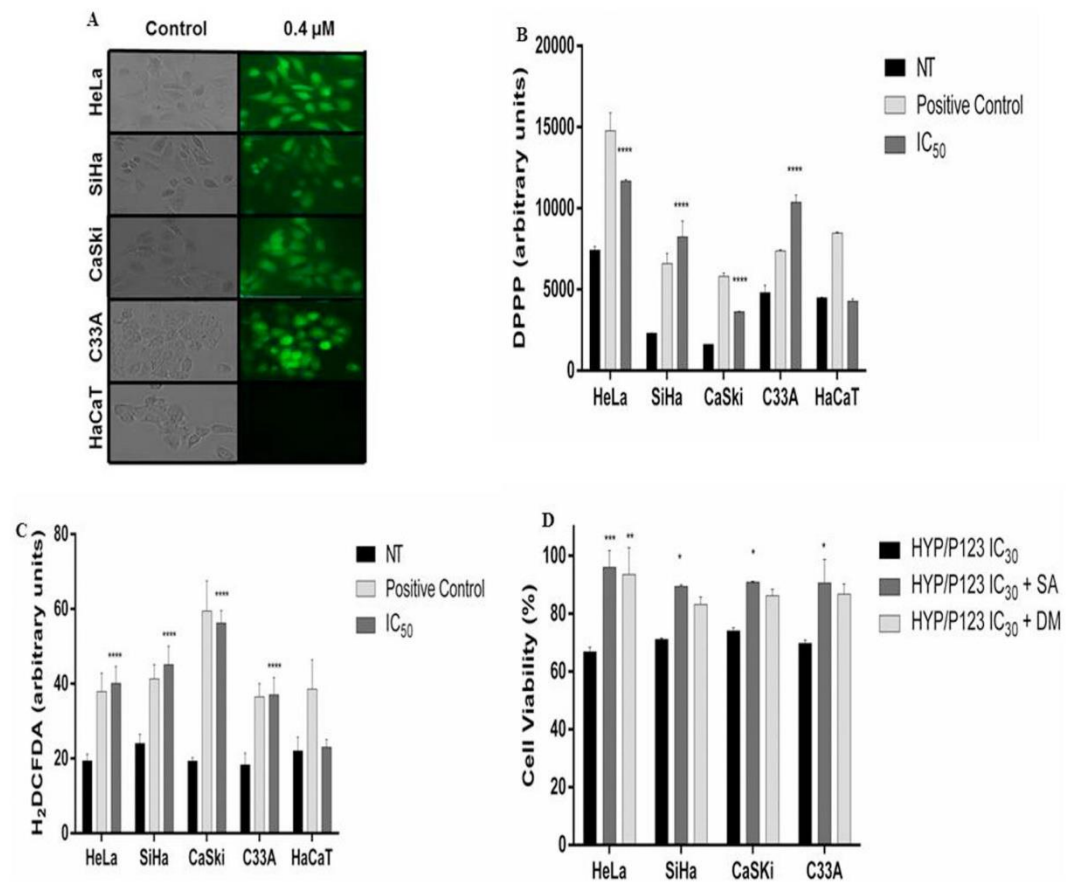


Fig. 7. Oxidative stress induced by HYP/P123-mediated PDT exposure in the cervical cancer cell lines and HaCaT cells with illumination. (A) Total ROS production: the bright field images and their corresponding fluorescence images of cells treated with HYP/P123 PDT. (B) Cellular oxidative stress determination by LPO which the amount of DPPP, that is essentially non-fluorescent until oxidation to DPPP-O by peroxides. HYP/P123 PDT significantly increased DPPP-O in all cervical cancer cell lines but not in HaCaT. (C) Production of total ROS by fluorimetric assay. (D) Determination of type I and type II mechanism of PDT. The cell viability of the two groups tested with SA and DM was higher than those treated only with HYP/P123 IC₃₀ values. Each bar represents the mean \pm SD of three independent experiments conducted in triplicate. One-way ANOVA with a multiple comparison test (Tukey–Kramer multiple comparisons test) was used for data analyses to identify potentially causal associations between variables. The (*) (**) (***) marks statistical significance when comparing treated cell groups with NT. $P < 0.05$ was considered significant.

decreased in HeLa and SiHa ($P < 0.0001$ for both) and CaSki ($P = 0.0006$). Zhang et al. [126] also described that photoactivated HYP inhibit the activation of the VEGF-A in human umbilical vein endothelial cells (HUVECs).

On the other hand, although VEGF production after treatment with HYP/P123 PDT in the C33A cell line is almost nil, there was no statistical significance ($P = 0.2892$). This may be due to the basal production of VEGF in this cell line be very low even in the untreated cells compared to the levels of the untreated HeLa, SiHa and CaSki cell lines. In support of this hypothesis, Yuan et al. [127] described that VEGF was highly expressed in tumor tissues of cervical cancer patients with HPV infection and the high levels of VEGF predict unfavorable prognosis of cervical cancer. It is interesting to note that there was no significant reduction in both VEGF and MMP-9 production in the C33A cell line after exposure to HYP/P123 PDT. This cell line is negative for HPV DNA. In HeLa, SiHa and CaSki, which are positive for HPV 18, 16, and 16 and 18, respectively, a significant reduction in the production of MMP-9 and VEGF was observed. These evidences points to the hypothesis that the effect of HYP/P123 PDT in reducing the production of MMP-9 and VEGF is related to positivity for HR-HPV. However, the mechanisms by which this happen still need to be elucidated.

4. Conclusion

Following our previous works, in this study, we aimed to evaluate the efficacy of HYP encapsulated on Pluronic®P123 (HYP/P123) PDT in a comprehensive panel of human cervical cancer-derived cell lines, including HeLa (HPV 18-positive), SiHa (HPV 16-positive), CaSki (HPV 16 and 18-positive), and C33A (HPV-negative), compared to a non-tumorigenic human epithelial cell line (HaCaT). Our results showed that HYP/P123 micelles had effective and selective time- and dose-dependent phototoxic effects on cervical cancer cells but little damage to normal cells (HaCaT). Additionally, HYP/P123 micelles had selective internalization in all cervical cancer cell lines but not in HaCaT, indicating their potential to permeate the membrane of these cells. Moreover, HYP/P123 micelles accumulated in endoplasmic reticulum, mitochondria and lysosomes organelles, resulting in photodynamic cell death mainly by necrosis. HYP/P123 micelles were able to inhibit the formation of cellular colonies, suggesting a possible ability to prevent the recurrence of cervical cancer. We also showed that HYP/P123 micelles inhibited the migration and invasion of tumor cells, possibly by decreasing their ability to form metastases mainly via MMP-2 inhibition. Taken together, the results presented here indicate that HYP/P123

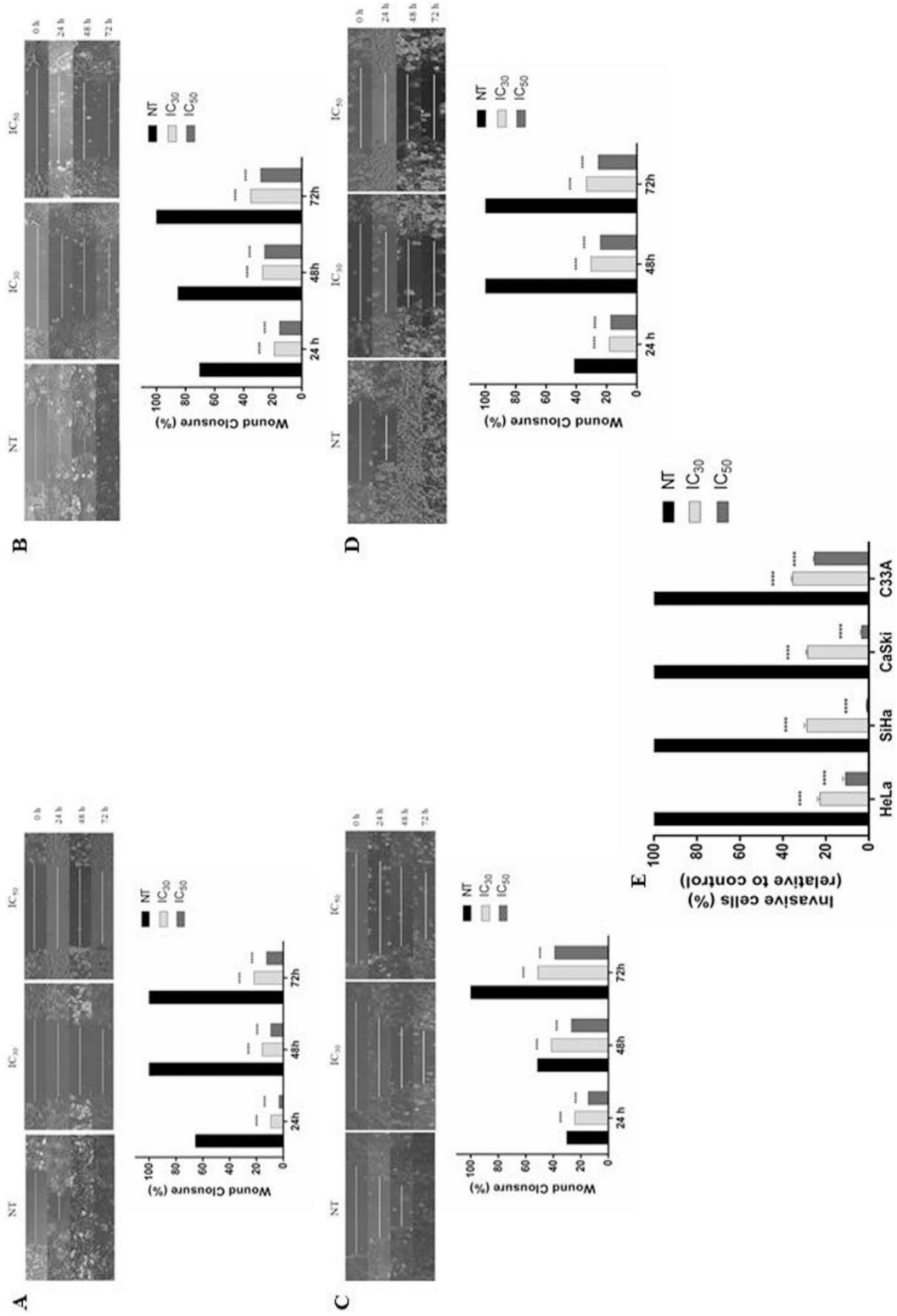


Fig. 8. Effects of HYP/P123 treatment on cell migration and invasion. Cell migration analysis using a wound-healing assay. HeLa (A), SiHa (B), CaSki (C), and C33A (D) cells after scratching in the absence (NT) and presence of HYP/P123. The results were calculated by comparing wound closure after 24, 48, and 72 h with the measurements taken at the initial time. (E) Cell invasion analysis using transwell chambers. Cervical cancer cell lines (HeLa, SiHa, CaSki, and C33A) were seeded onto matrigel coated filters in transwell chambers. After 24 h of PDT IC_{30} and IC_{50} of each cell line, the number of cells on the bottom side of the filter was quantified and expressed as percentage. The values are presented as the mean \pm SD of three independent experiments conducted in triplicate. The (****) marks statistical significance when comparing treated cell groups with NT. $P < 0.05$ was considered significant.

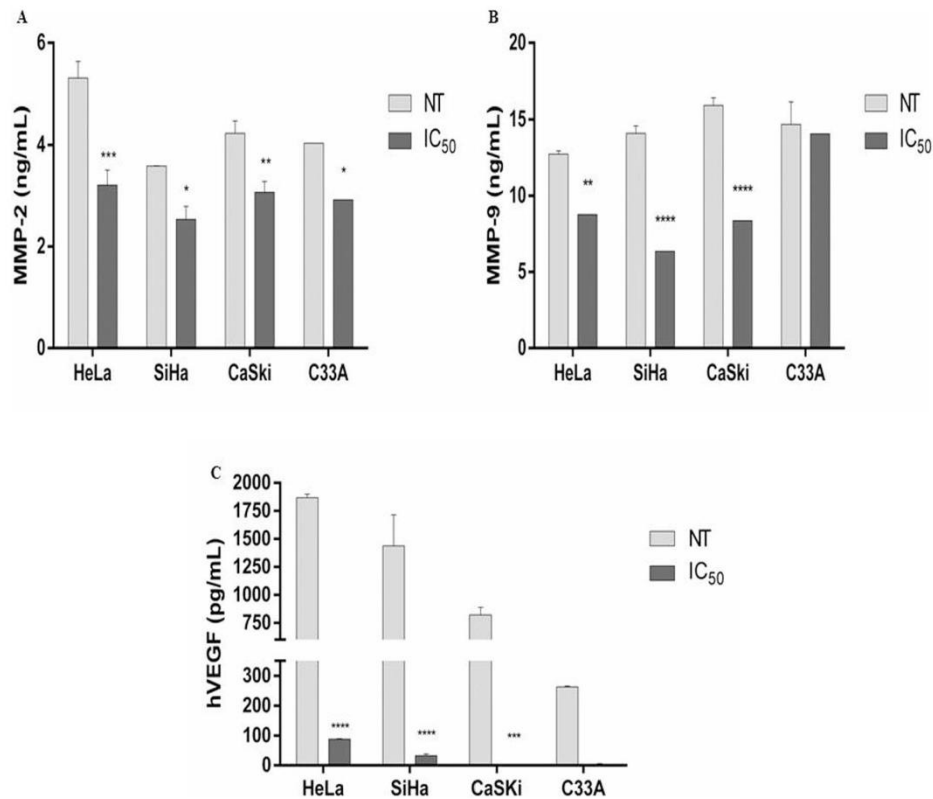


Fig. 9. The levels of MMP-2, MMP-9 and VEGF in HeLa, SiHa, CaSki and C33A with HYP/P123-mediated PDT. (A) MMP-2 production. (B) MMP-9 production. (C) VEGF production. Data are shown as the mean values \pm SD of three independent experiments conducted in triplicate. The (*) (**) (***) (****) marks statistical significance when comparing treated cells with NT. $P < 0.05$ was considered significant.

PDT had a strong and selective antitumoral effect on cervical cancer cells immortalized by HPV 16, HPV 18, HPV 16 and 18 together, and without HPV, indicating its potential to be a powerful candidate in developing therapeutic agents for all cervical cancer types. Additionally, indicate a potentially useful role of HYP/P123 micelles as a platform for HYP delivery to more specifically and effectively treat cervical cancers through PDT, suggesting they are worthy for in vivo preclinical evaluations.

Declaration of competing interest

The authors declare that they have no known competing financial interests or personal relationships that could have appeared to influence the work reported in this paper.

Acknowledgments

This work was supported by grants from Conselho Nacional de Desenvolvimento Científico e Tecnológico/CNPq (grant number

409382/2018-3, Brazil).

Author contributions

Conceptualization: Gabrielle Marconi Zago Ferreira Damke and Marcia Edilaine Lopes Consolaro; Methodology: Gabrielle Marconi Zago Ferreira Damke, Edilson Damke, Bianca Altrão Ratti, Renato Sonchini Gonçalves, Gabriel Batista César, Lyvia Eloiza de Freitas Meirelles and Sueli de Oliveira Silva; Data curation: Patrícia de Souza Bonfim-Mendonça, Wilker Caetano, Noboru Hioka and Raquel Pantarotto Souza; Supervision: Marcia Edilaine Lopes Consolaro; Writing original draft: Gabrielle Marconi Zago Ferreira Damke and Marcia Edilaine Lopes Consolaro; Review and editing: Gabrielle Marconi Zago Ferreira Damke, Edilson Damke, Bianca Altrão Ratti, Renato Sonchini Gonçalves, Gabriel Batista César, Vânia Ramos Sela da Silva and Sueli de Oliveira Silva.

References

- [1] F. Bray, J. Ferlay, I. Soerjomataram, R.L. Siegel, L.A. Torre, A. Jemal, Global

- cancer statistics 2018: GLOBOCAN estimates of incidence and mortality worldwide for 36 cancers in 185 countries, *CA Cancer J. Clin.* 68 (6) (2018) 394–424, <https://doi.org/10.3322/caac.21492>.
- [2] W.J. Koh, B.E. Greer, N.R. Abu-Rustum, S.M. Apte, S.M. Campos, K.R. Cho, C. Chu, D. Cohn, M.A. Crispens, D.S. Dizon, Uterine sarcoma, version 1.2016, *J. Natl. Compr. Cancer Netw.* 13 (11) (2015) 1321–1331, <https://doi.org/10.6004/jnccn.2015.0162>.
- [3] S.K. Kjær, K. Frederiksen, C. Munk, T. Iftner, Long-term absolute risk of cervical intraepithelial neoplasia grade 3 or worse following human papillomavirus infection: role of persistence, *J. Natl. Cancer Inst.* 102 (19) (2010) 1478–1488, <https://doi.org/10.1093/jnci/djq356>.
- [4] M. Schiffman, P.E. Castle, J. Jeronimo, A.C. Rodriguez, S. Wacholder, Human papillomavirus and cervical cancer, *Lancet* 370 (9590) (2007) 890–907, [https://doi.org/10.1016/S0140-6736\(07\)61416-0](https://doi.org/10.1016/S0140-6736(07)61416-0).
- [5] S.W. Li, W. Yuan, B. Zhao, Z.K. He, X. Guo, W.X. Xia, L.H. Xu, Positive effect of HPV status on prognostic value of blood lymphocyte-to-monocyte ratio in advanced cervical carcinoma, *Cancer Cell Int.* 16 (1) (2016) 54–68, <https://doi.org/10.1186/s12935-016-0334-1>.
- [6] D. Lorusso, F. Petrelli, A. Coiru, F. Raspagliesi, S. Barni, A systematic review comparing cisplatin and carboplatin plus paclitaxel-based chemotherapy for recurrent or metastatic cervical cancer, *Gynecol. Oncol.* 133 (1) (2014) 117–123, <https://doi.org/10.1016/j.ygyno.2014.01.042>.
- [7] J. Khalil, S. Bellefqih, N. Sahli, M. Afif, H. Elkacemi, S. Elmajaoui, T. Kebdani, N. Benjaafar, Impact of cervical cancer on quality of life: beyond the short term (results from a single institution), *Gynecol. Oncol. Res. Pract.* 2 (1) (2015) 7–13, <https://doi.org/10.1186/s40661-015-0011-4>.
- [8] T.J. Dougherty, G.B. Grindey, R. Fiel, K.R. Weishaupt, D.G. Boyle, Photodynamic therapy. II. Cure of animal tumors with hematoporphyrin and light 23, *J. Natl. Cancer Inst.* 55 (1) (1975) 115–121, <https://doi.org/10.1093/jnci/55.1.115>.
- [9] C.A. Robertson, D.H. Evans, H. Abrahamse, Photodynamic therapy (PDT): a short review on cellular mechanisms and cancer research applications for PDT, *J. Photochem. Photobiol. B* 96 (1) (2009) 1–8, <https://doi.org/10.1016/j.jphotobiol.2009.04.001>.
- [10] P. Calzavara-Pinton, M. Venturini, R. Sala, Photodynamic therapy: update 2006 part 1: photochemistry and photobiology, *J. Eur. Acad. Dermatol. Venerol.* 21 (3) (2007) 293–302, <https://doi.org/10.1111/j.1468-3083.2006.01902.x>.
- [11] J. Fuchs, J. Thiele, The role of oxygen in cutaneous photodynamic therapy, *Free Rad. Biol. Med.* 24 (5) (1998) 835–847, [https://doi.org/10.1016/S0891-5849\(97\)00370-5](https://doi.org/10.1016/S0891-5849(97)00370-5).
- [12] M. Ochsner, Photophysical and photobiological processes in the photodynamic therapy of tumours, *J. Photochem. Photobiol. B* 39 (1) (1997) 1–18, [https://doi.org/10.1016/S1011-1344\(96\)07428-3](https://doi.org/10.1016/S1011-1344(96)07428-3).
- [13] K.T. de Oliveira, J.M. de Souza, N.R. da Silva Gobo, F. Fávora de Assis, T.J. Brocksom, Coneitos Fundamentais e Aplicações de Fotossensibilizadores do Tipo Porphirinas, Clorinas e Ftalocianinas em Terapias Fotônicas, *Rev. Virtual de Quím.* 7 (1) (2014) 310–335, <https://doi.org/10.5935/1984-6835.20150016>.
- [14] M.C. Galanou, T.A. Theodossiou, D. Tsiourvas, Z. Sideratou, C.M. Paleos, Interactive transport, subcellular relocation and enhanced phototoxicity of hypericin encapsulated in guanidylated liposomes via molecular recognition, *Photochem. Photobiol.* 84 (5) (2008) 1073–1083, <https://doi.org/10.1111/j.1751-1097.2008.00392.x>.
- [15] L.F. Huang, W. Zeng-Hui, C. Shi-Lin, Hypericin: chemical synthesis and biosynthesis, *Chin. J. Nat. Med.* 12 (2) (2014) 81–88, [https://doi.org/10.1016/S1875-5364\(14\)60014-5](https://doi.org/10.1016/S1875-5364(14)60014-5).
- [16] P.S. Chung, C.K. Rhee, R.E. Saxton, D.J. Castro, M.B. Paiva, J. Soudant, A. Mathey, C. Foote, Hypericin uptake in rabbits and nude mice transplanted with human squamous cell carcinomas: study of a new sensitizer for laser phototherapy, *Laryngoscope* 104 (12) (1994) 1471–1476, <https://doi.org/10.1288/00005537-199412000-00008>.
- [17] R. Ebermann, G. Alth, M. Kreitner, A. Kubin, Natural products derived from plants as potential drugs for the photodynamic destruction of tumor cells, *J. Photochem. Photobiol. B* 36 (2) (1996) 95–97, [https://doi.org/10.1016/S1011-1344\(96\)07353-8](https://doi.org/10.1016/S1011-1344(96)07353-8).
- [18] H. Falk, From the photosensitizer hypericin to the photoreceptor stentorin—the chemistry of phenanthroperylene quinones, *Angew. Chem. Int. Ed. Engl.* 38 (21) (1999) 3116–3136, [https://doi.org/10.1002/\(SICI\)1521-3773\(19991102\)38:21<3116::AID-ANIE3116>3.0.CO;2-S](https://doi.org/10.1002/(SICI)1521-3773(19991102)38:21<3116::AID-ANIE3116>3.0.CO;2-S).
- [19] P. Agostinis, A. Vantieghem, W. Merlevede, P.A. de Witte, Hypericin in cancer treatment: more light on the way, *Int. J. Biochem. Cell Biol.* 34 (3) (2002) 221–241, [https://doi.org/10.1016/S1357-2725\(01\)00126-1](https://doi.org/10.1016/S1357-2725(01)00126-1).
- [20] T. Kiesslich, B. Krammer, K. Plaetzer, Cellular mechanisms and prospective applications of hypericin in photodynamic therapy, *Curr. Med. Chem.* 13 (18) (2006) 2189–2204, <https://doi.org/10.2174/09298670677935267>.
- [21] A. Karioti, A.R. Bilia, Hypericins as potential leads for new therapeutics, *Int. J. Mol. Sci.* 11 (2) (2010) 562–594, <https://doi.org/10.3390/ijms11020562>.
- [22] A. Wirz, B. Meier, O. Sticher, Solubility of hypericin in methanol and methanol-pyridine, *Pharmazie* 57 (8) (2002) 543–545.
- [23] A. Kubin, H. Loew, U. Burner, G. Jessner, H. Kolbabeck, F. Wierrani, How to make hypericin water-soluble, *Pharmazie* 63 (4) (2008) 263–269, <https://doi.org/10.1691/ph.2008.7292>.
- [24] C.L.L. Saw, M. Olivo, K.C. Soo, P.W.S. Heng, Delivery of hypericin for photodynamic applications, *Cancer Lett.* 241 (1) (2006) 23–30, <https://doi.org/10.1016/j.canlet.2005.10.020>.
- [25] I. Tatischeff, A. Alfsen, A new biological strategy for drug delivery: eucaryotic cell-derived nanovesicles, *J. Biomater. Nanobiotechnol.* 2 (05) (2011) 494–499, <https://doi.org/10.4236/jbnb.2011.225060>.
- [26] G.S. Kwon, *Polymeric Drug Delivery Systems*, 1 ed., CRC Press, Boca Raton, 2005.
- [27] J.F. Gohy, Block copolymer micelles, in: V. Abetaz (Ed.), *Block Copolymers II*, Springer, Berlin Heidelberg, 2005, pp. 65–136.
- [28] P. Alexandridis, J.F. Holzwarth, T.A. Hatton, Micellization of poly (ethylene oxide)-poly (propylene oxide)-poly (ethylene oxide) triblock copolymers in aqueous solutions: thermodynamics of copolymer association, *Macromolecules* 27 (9) (1994) 2414–2425, <https://doi.org/10.1021/ma00087a009>.
- [29] E.V. Batrakova, A.V. Kabanov, Pluronic block copolymers: evolution of drug delivery concept from inert nanocarriers to biological response modifiers, *J. Control. Release* 130 (2) (2008) 98–106, <https://doi.org/10.1016/j.jconrel.2008.04.013>.
- [30] M.S.H. Akash, K. Rehman, Recent progress in biomedical applications of Pluronic (PF127): pharmaceutical perspectives, *J. Control. Release* 209 (2015) 120–138, <https://doi.org/10.1016/j.jconrel.2015.04.032>.
- [31] N. Jindal, S. Mehta, Nevirapine loaded Pluronic 407/Pluronic P123 mixed micelles: optimization of formulation and in vitro evaluation, *Colloids Surf. B Biointerfaces* 129 (2015) 100–106, <https://doi.org/10.1016/j.colsurfb.2015.03.030>.
- [32] Y. Chen, W. Zhang, Y. Huang, F. Gao, X. Sha, X. Fang, Pluronic-based functional polymeric mixed micelles for co-delivery of doxorubicin and paclitaxel to multi-drug resistant tumor, *Int. J. Pharm.* 488 (1) (2015) 44–58, <https://doi.org/10.1016/j.ijpharm.2015.04.048>.
- [33] B.H. Vilsinski, A.P. Gerola, J.A. Enumo, K.d.S.S. Campanholi, P.C.d.S. Pereira, G. Braga, N. Hioka, E. Kimura, A.L. Tessler, W. Caetano, Formulation of aluminum chloride phthalocyanine in Pluronic™ P-123 and F-127 block copolymer micelles: photophysical properties and photodynamic inactivation of microorganisms, *Photochem. Photobiol.* 91 (3) (2015) 518–525, <https://doi.org/10.1111/php.12421>.
- [34] B.H. Vilsinski, J.L. Aparicio, P.C.d.S. Pereira, S.L. Fávora, K.S.S. Campanholi, A.P. Gerola, A.L. Tessler, N. Hioka, W. Caetano, Physico-chemical properties of meso-tetrakis (p-methoxyphenyl) porphyrin (TMPP) incorporated into pluronic™ p-123 and f-127 polymeric micelles, *Quim. Nova* 37 (10) (2014) 1650–1656, <https://doi.org/10.5935/0100-4042.201402073>.
- [35] M.C. Montanha, L.L. Silva, F.B.B. Pangoni, G.B. Cesar, R.S. Gonçalves, W. Caetano, N. Hioka, T.T. Tominaga, M.E.L. Consolaro, A. Diniz, E. Kimura, Response surface method optimization of a novel hypericin formulation in P123 micelles for breast cancer and antimicrobial photodynamic therapy, *J. Photochem. Photobiol. B* 170 (2017) 247–255, <https://doi.org/10.1016/j.jphotobiol.2017.04.008>.
- [36] G. Damke, R. Souza, M. Montanha, E. Damke, R. Gonçalves, G. Cesar, E. Kimura, W. Caetano, N. Hioka, M. Consolaro, Selective photodynamic effects on breast cancer cells provided by P123 Pluronic®-based nanoparticles modulating hypericin delivery, *Anti Cancer Agents Med. Chem.* (1) (2018) 1–12, <https://doi.org/10.2174/1871520618666181102091010>.
- [37] N. Hendrickx, C. Volanti, U. Moens, O.M. Setermes, P. de Witte, J.R. Vandenhede, J. Piette, P. Agostinis, Up-regulation of cyclooxygenase-2 and apoptosis resistance by p38 MAPK in hypericin-mediated photodynamic therapy of human cancer cells, *J. Biol. Chem.* 278 (52) (2003) 52231–52239, <https://doi.org/10.1074/jbc.M307591200>.
- [38] N. Hendrickx, M. Dewaele, E. Buytaert, G. Marsboom, S. Janssens, M. Van Boven, J.R. Vandenhede, P. de Witte, P. Agostinis, Targeted inhibition of p38 α MAPK suppresses tumor-associated endothelial cell migration in response to hypericin-based photodynamic therapy, *Biochem. Biophys. Res. Commun.* 337 (3) (2005) 928–935, <https://doi.org/10.1016/j.bbrc.2005.09.135>.
- [39] A.A. Kamuhabwa, J.D. Di Mavungu, L. Baert, M.-A. D'Hallewin, J. Hoogmartens, P.A. de Witte, Determination of hypericin in human plasma by high-performance liquid chromatography after intravesical administration in patients with transitional cell carcinoma of the bladder, *Eur. J. Pharm. Biopharm.* 59 (3) (2005) 469–474, <https://doi.org/10.1016/j.ejpb.2004.09.013>.
- [40] J. Mikeš, J. Kleban, V. Sačková, V. Horváth, E. Jamborová, A. Vaculová, A. Kozubík, J. Hofmanová, P. Fedorčák, Necrosis predominates in the cell death of human colon adenocarcinoma HT-29 cells treated under variable conditions of photodynamic therapy with hypericin, *Photochem. Photobiol. Sci.* 6 (7) (2007) 758–766, <https://doi.org/10.1039/b700350a>.
- [41] T. Breitenbach, M.K. Kuimova, P. Gbur, S. Hatz, N.B. Schack, B.W. Pedersen, J.D. Lambert, L. Poulsen, P.R. Ogilby, Photosensitized production of singlet oxygen: spatially-resolved optical studies in single cells, *Photochem. Photobiol. Sci.* 8 (4) (2009) 442–452, <https://doi.org/10.1039/b809049a>.
- [42] F. Lavielle, S. Deshayes, F. Gonnet, E. Larquet, S.G. Kruglik, N. Boisset, R. Daniel, A. Alfsen, I. Tatischeff, Nanovesicles released by Dictyostelium cells: a potential carrier for drug delivery, *Int. J. Pharm.* 380 (1–2) (2009) 206–215, <https://doi.org/10.1016/j.ijpharm.2009.06.039>.
- [43] T.T. Vuong, C. Vever-Bizet, S. Bonneau, G. Bourg-Heckly, Hypericin incorporation and localization in fixed HeLa cells for various conditions of fixation and incubation, *Photochem. Photobiol. Sci.* 10 (4) (2011) 561–568, <https://doi.org/10.1039/c0pp00324g>.
- [44] A. Barras, L. Boussekey, E. Courtade, R. Boukherroub, Hypericin-loaded lipid nanocapsules for photodynamic cancer therapy in vitro, *Nanoscale* 5 (21) (2013) 10562–10572, <https://doi.org/10.1039/c3nr02724d>.
- [45] R. Penjweini, S. Deville, O. Haji Maghsoudi, K. Notelaers, A. Ethirajan, M. Ameloot, Investigating the effect of poly-L-lactic acid nanoparticles carrying hypericin on the flow-biased diffusive motion of HeLa cell organelles, *J. Pharm. Pharmacol.* 71 (1) (2019) 104–116, <https://doi.org/10.1111/jphp.12779>.
- [46] E. Chen, X. Chen, X. Yuan, S. Wei, L. Zhou, J. Zhou, J. Shen, One-pot method to prepare a theranostic nanosystem with magnetic resonance imaging function and anticancer activity through multiple mechanisms, *Dalton Trans.* 46 (16) (2017) 5151–5158, <https://doi.org/10.1039/c7dt00489c>.
- [47] M.N. Moritz, J.L. Goncalves, I.A. Linares, J.R. Perussi, K.T. de Oliveira, Semi-

- synthesis and PDT activities of a new amphiphilic chlorin derivative, *Photodiagn. Photodyn. Ther.* 17 (2017) 39–47, <https://doi.org/10.1016/j.pdpdt.2016.10.005>.
- [48] S.M. Ju, J.G. Kang, J.S. Bae, H.O. Pae, Y.S. Lyu, B.H. Jeon, The flavonoid apigenin ameliorates cisplatin-induced nephrotoxicity through reduction of p53 activation and promotion of PI3K/Akt pathway in human renal proximal tubular epithelial cells, *Evid. Based Complement. Alternat. Med.* 2015 (2015) 1–9, <https://doi.org/10.1155/2015/186436>.
- [49] F. Lindenmeyer, H. Li, S. Menashi, C. Soria, H. Lu, Apigenin acts on the tumor cell invasion process and regulates protease production, *Nutr. Cancer* 39 (1) (2001) 139–147, https://doi.org/10.1207/S15327914nc391_19.
- [50] S. Shukla, A. Mishra, P. Fu, G.T. MacLennan, M.I. Resnick, S. Gupta, Up-regulation of insulin-like growth factor binding protein-3 by apigenin leads to growth inhibition and apoptosis of 22Rv1 xenograft in athymic nude mice, *FASEB J.* 19 (14) (2005) 2042–2044, <https://doi.org/10.1096/fj.05-3740fj>.
- [51] S. Shukla, G.T. MacLennan, P. Fu, S. Gupta, Apigenin attenuates insulin-like growth factor-1 signaling in an autochthonous mouse prostate cancer model, *Pharm. Res.* 29 (6) (2012) 1506–1517, <https://doi.org/10.1007/s11095-011-0625-0>.
- [52] R.S. Gonçalves, B.R. Rabello, G.B. Cesar, P.C. Pereira, M.A. Ribeiro, E.C. Meurer, N. Hioka, C.V. Nakamura, M.L. Bruschi, W. Caetano, An efficient multigram synthesis of hypericin improved by a low power LED based photoreactor, *Org. Process. Res. Dev.* 21 (12) (2017) 2025–2031, <https://doi.org/10.1021/acs.oprd.7b00317>.
- [53] R.S. Gonçalves, E.L. Silva, N. Hioka, C.V. Nakamura, M.L. Bruschi, W. Caetano, An optimized protocol for anthraquinones isolation from *Rhamnus frangula* L., *Nat. Prod. Res.* 32 (3) (2018) 366–369, <https://doi.org/10.1080/14786419.2017.1356836>.
- [54] R.S. Gonçalves, G.B. César, P.M. Barbosa, N. Hioka, C.V. Nakamura, M.L. Bruschi, W. Caetano, Optimized protocol for multigram preparation of emodin anthrone, a precursor in the hypericin synthesis, *Nat. Prod. Res.* 33 (8) (2019) 1196–1199, <https://doi.org/10.1080/14786419.2018.1457661>.
- [55] X. Zhang, J.K. Jackson, H.M. Burt, Development of amphiphilic diblock copolymers as micellar carriers of taxol, *Int. J. Pharm.* 132 (1) (1996) 195–206, [https://doi.org/10.1016/0378-5173\(95\)04386-1](https://doi.org/10.1016/0378-5173(95)04386-1).
- [56] K.M. Sakita, P.C. Conrado, D.R. Faria, G.S. Arita, I.R. Capoci, F.A. Rodrigues-Vendramini, N. Peralisi, G.B. Cesar, R.S. Gonçalves, W. Caetano, Copolymeric micelles as efficient inert nanocarrier for hypericin in the photodynamic inactivation of *Candida* species, *Future Microbiol.* 14 (6) (2019) 519–531, [https://doi.org/10.1016/0378-5173\(95\)04386-1](https://doi.org/10.1016/0378-5173(95)04386-1).
- [57] R.A.M. Terry L Riss, Andrew L Niles, Sarah Duellman, Hélène A Benink, Tracy J. Worzella, Lisa Minor, Cell viability assays, in: A.G.G. Sitta Sittampalam, Kyle Brimacombe, Michelle Arkin, Douglas Auld, Chris Austin, Jonathan Baell, Bruce Bejcek, Jose M.M. Caaveiro, Thomas D.Y. Chung, Nathan P. Coussens, Jayme L. Dahlin, Viswanath Devanaryan, Timothy L. Foley, Marcie Glicksman, Matthew D. Hall, Joseph V. Haas, Samuel R.J. Hoare, James Ingles, Philip W. Iversen, Steven H. Kahl, Stephen C. Kales, Susan Kirshner, Madhu Lal-Nag, Zhuyin Li, James McGee, Owen McManus, Terry Riss, O. Joseph Trask, Jr. Jeffrey R. Weidner, Mary Jo Wildey, Menghang Xia, Xu Xin (Eds.), *Assay Guidance Manual*, Eli Lilly & Company and the National Center for Advancing Translational Sciences, Bethesda, 2016.
- [58] N.A. Franken, H.M. Rodermond, J. Stap, J. Haveman, C. Van Bree, Clonogenic assay of cells in vitro, *Nat. Protoc.* 1 (5) (2006) 2315–2319, <https://doi.org/10.1038/nprot.2006.339>.
- [59] S. Kascakova, Z. Nadova, A. Mateasik, J. Mikes, V. Huntuosova, M. Refregiers, F. Sureau, J.-C. Maurizioot, P. Miskovsky, D. Jancura, High level of low-density lipoprotein receptors enhance hypericin uptake by U-87 MG cells in the presence of LDL, *Photochem. Photobiol.* 84 (1) (2008) 120–127, <https://doi.org/10.1111/j.1751-1097.2007.00207.x>.
- [60] G. Nam, S. Rangasamy, H. Ju, A.A.S. Samson, J.M. Song, Cell death mechanistic study of photodynamic therapy against breast cancer cells utilizing liposomal delivery of 5, 10, 15, 20-tetrakis (benzo [b] thiophene) porphyrin, *J. Photochem. Photobiol. B* 166 (2017) 116–125, <https://doi.org/10.1016/j.jphotobiol.2016.11.006>.
- [61] N. Miranda, H. Volpato, J.H. da Silva Rodrigues, W. Caetano, T. Ueda-Nakamura, S. de Oliveira Silva, C.V. Nakamura, The photodynamic action of pheophorbide a induces cell death through oxidative stress in *Leishmania amazonensis*, *J. Photochem. Photobiol. B* 174 (2017) 342–354, <https://doi.org/10.1016/j.jphotobiol.2017.08.016>.
- [62] J. Ribeiro, R. Jorge, Determinação do mecanismo de destruição de células mediado por meso-tetramesitylporfina, octaetilporfina, octaetilporfina de vanilil e luz visível, *Eclet. Quím.* 30 (2005) 7–13, <https://doi.org/10.1590/S0100-46702005000100001>.
- [63] J. Cheng, W. Li, G. Tan, Z. Wang, S. Li, Y. Jin, Synthesis and in vitro photodynamic therapy of chlorin derivative 131-ortho-trifluoromethyl-phenylhydrazono modified pyropheophorbide-a, *Biomed. Pharmacother.* 87 (2017) 263–273, <https://doi.org/10.1016/j.biopha.2016.12.081>.
- [64] C.-C. Liang, A.Y. Park, J.-L. Guan, In vitro scratch assay: a convenient and inexpensive method for analysis of cell migration in vitro, *Nat. Protoc.* 2 (2) (2007) 329–333, <https://doi.org/10.1038/nprot.2007.30>.
- [65] K. Tomin, R.H. Goldfarb, P. Albertsson, In vitro assessment of human natural killer cell migration and invasion, *Natural Killer Cells: Methods Mol. Biol.* 1441 (2016) 65–74, https://doi.org/10.1007/978-1-4939-3684-7_6.
- [66] D. Feinweber, T. Verwanger, O. Brüggemann, I. Teasdale, B. Kramer, Applicability of new degradable hypericin-polymer-conjugates as photosensitizers: principal mode of action demonstrated by in vitro models, *Photochem. Photobiol. Sci.* 13 (11) (2014) 1607–1620, <https://doi.org/10.1039/c4pp00251b>.
- [67] S. Noell, D. Mayer, W.S. Strauss, M.S. Tatagiba, R. Ritz, Selective enrichment of hypericin in malignant glioma: pioneering in vivo results, *Int. J. Oncol.* 38 (5) (2011) 1343–1348, <https://doi.org/10.3892/ijo.2011.968>.
- [68] J. Vandepitte, B. Van Cleynenbreugel, E. Lerut, H. Van Poppel, P. de Witte, Biodistribution and photodynamic effects of PVP-hypericin using multi-cellular spheroids composed of normal human urothelial and T24 transitional cell carcinoma cells, *J. Biomed. Opt.* 16 (1) (2011) 018001–1–018001-6, doi:<https://doi.org/10.1117/1.3533316>.
- [69] M. Roelants, B. Van Cleynenbreugel, E. Lerut, H. Van Poppel, P.A. de Witte, Human serum albumin as key mediator of the differential accumulation of hypericin in normal urothelial cell spheroids versus urothelial cell carcinoma spheroids, *Photochem. Photobiol. Sci.* 10 (1) (2011) 151–159, <https://doi.org/10.1039/c0pp00109k>.
- [70] L. Xu, X. Zhang, W. Cheng, Y. Wang, K. Yi, Z. Wang, Y. Zhang, L. Shao, T. Zhao, Hypericin-photodynamic therapy inhibits the growth of adult T-cell leukemia cells through induction of apoptosis and suppression of viral transcription, *Retrovirology* 16 (1) (2019) 1–13, <https://doi.org/10.1186/s12977-019-0467-0>.
- [71] B. Chen, P.A. de Witte, Photodynamic therapy efficacy and tissue distribution of hypericin in a mouse P388 lymphoma tumor model, *Cancer Lett.* 150 (1) (2000) 111–117, [https://doi.org/10.1016/S0304-3835\(99\)00381-X](https://doi.org/10.1016/S0304-3835(99)00381-X).
- [72] A. Munshi, M. Hobbs, R.E. Meyn, Clonogenic cell survival assay, in: R.D. Blumenthal (Ed.), *Chemosensitivity*, Springer, Belleville, 2005, pp. 21–28.
- [73] Z. Jendželovská, R. Jendželovský, B. Kuchárová, P. Fedoročko, Hypericin in the light and in the dark: two sides of the same coin, *Front. Plant Sci.* 7 (2016) 1–20, <https://doi.org/10.3389/fpls.2016.00560>.
- [74] C. Thomas, R.S. Pardini, Oxygen dependence of hypericin-induced phototoxicity to EMT6 mouse mammary carcinoma cells, *Photochem. Photobiol.* 55 (6) (1992) 831–837, <https://doi.org/10.1111/j.1751-1097.1992.tb08531.x>.
- [75] S. Sattler, U. Schaefer, W. Schneider, J. Hoelzl, C.M. Lehr, Binding, uptake, and transport of hypericin by Caco-2 cell monolayers, *J. Pharm. Sci.* 86 (10) (1997) 1120–1126, <https://doi.org/10.1021/js970004a>.
- [76] G. Siboni, H. Weitman, D. Freeman, Y. Mazur, Z. Malik, B. Ehrenberg, The correlation between hydrophilicity of hypericins and helianthron: internalization mechanisms, subcellular distribution and photodynamic action in colon carcinoma cells, *Photochem. Photobiol. Sci.* 1 (7) (2002) 483–491, <https://doi.org/10.1039/b202884k>.
- [77] Y.-F. Ho, M.-H. Wu, B.-H. Cheng, Y.-W. Chen, M.-C. Shih, Lipid-mediated preferential localization of hypericin in lipid membranes, *Biochim. Biophys. Acta* 1788 (6) (2009) 1287–1295, <https://doi.org/10.1016/j.bbmem.2009.01.017>.
- [78] S.M. Ali, M. Olivo, Bio-distribution and subcellular localization of Hypericin and its role in PDT induced apoptosis in cancer cells, *Int. J. Oncol.* 21 (3) (2002) 531–540, <https://doi.org/10.3892/ijo.21.3.531>.
- [79] J. Mikeš, M. Hýždlová, L. Kočí, R. Jendželovský, J. Kovač, A. Vaculová, J. Hofmanová, A. Kozubík, P. Fedoročko, Lower sensitivity of FHC fetal colon epithelial cells to photodynamic therapy compared to HT-29 colon adenocarcinoma cells despite higher intracellular accumulation of hypericin, *Photochem. Photobiol. Sci.* 10 (4) (2011) 626–632, <https://doi.org/10.1039/c0pp00359j>.
- [80] I. Crnolatac, A. Huygens, A. Van Aerschot, R. Bussion, J. Rozenski, P.A. de Witte, Synthesis, in vitro cellular uptake and photo-induced antiproliferative effects of lipophilic hypericin acid derivatives, *Bioorg. Med. Chem.* 13 (23) (2005) 6347–6353, <https://doi.org/10.1016/j.bmc.2005.09.003>.
- [81] N. Nakajima, N. Kawashima, A basic study on hypericin-PDT in vitro, *Photodiagn. Photodyn. Ther.* 9 (3) (2012) 196–203, <https://doi.org/10.1016/j.pdpdt.2012.01.008>.
- [82] S. Hezaveh, S. Samanta, A. De Nicola, G. Milano, D. Roccatano, Understanding the interaction of block copolymers with DMPC lipid bilayer using coarse-grained molecular dynamics simulations, *J. Phys. Chem. B* 116 (49) (2012) 14333–14345, <https://doi.org/10.1021/jp306565e>.
- [83] M. Johnsson, M. Silfvander, G. Karlsson, K. Edwards, Effect of PEO – PPO – PEO triblock copolymers on structure and stability of phosphatidylcholine liposomes, *Langmuir* 15 (19) (1999) 6314–6325, <https://doi.org/10.1021/la990288+>.
- [84] M.A. Firestone, A.C. Wolf, S. Seifert, Small-angle X-ray scattering study of the interaction of poly (ethylene oxide)-b-poly (propylene oxide)-b-poly (ethylene oxide) triblock copolymers with lipid bilayers, *Biomacromolecules* 4 (6) (2003) 1539–1549, <https://doi.org/10.1021/bm034134r>.
- [85] D. Kessel, Y. Luo, Y. Deng, C. Chang, The role of subcellular localization in initiation of apoptosis by photodynamic therapy, *Photochem. Photobiol.* 65 (3) (1997) 422–426, <https://doi.org/10.1111/j.1751-1097.1997.tb08581.x>.
- [86] C. Thomas, R.S. MacGill, G.C. Miller, R.S. Pardini, Photoactivation of hypericin generates singlet oxygen in mitochondria and inhibits succinoxidase, *Photochem. Photobiol.* 55 (1) (1992) 47–53, <https://doi.org/10.1111/j.1751-1097.1992.tb04208.x>.
- [87] Z. Diwu, J.W. Lown, Photosensitization with anticancer agents 17. EPR studies of photodynamic action of hypericin: formation of semiquinone radical and activated oxygen species on illumination, *Free Rad. Biol. Med.* 14 (2) (1993) 209–215, [https://doi.org/10.1016/0891-5849\(93\)90012-j](https://doi.org/10.1016/0891-5849(93)90012-j).
- [88] H.-Y. Du, M. Olivo, B.K.-H. Tan, B.-H. Bay, Hypericin-mediated photodynamic therapy induces lipid peroxidation and necrosis in nasopharyngeal cancer, *Int. J. Oncol.* 23 (5) (2003) 1401–1405, <https://doi.org/10.3892/ijo.23.5.1401>.
- [89] J. Mikeš, R. Jendželovský, V. Sačková, I. Uhrinová, M. Kello, L. Kuliková, P. Fedoročko, The role of p53 in the efficiency of photodynamic therapy with hypericin and subsequent long-term survival of colon cancer cells, *Photochem. Photobiol. Sci.* 8 (11) (2009) 1558–1567, <https://doi.org/10.1039/b9pp00021f>.
- [90] E. Buytaert, G. Callewaert, N. Hendrickx, L. Scorrano, D. Hartmann, L. Missiaen, J.R. Vandenheede, I. Heirman, J. Grooten, P. Agostinis, Role of endoplasmic reticulum depletion and multidomain proapoptotic BAX and BAK proteins in

- shaping cell death after hypericin-mediated photodynamic therapy, *FASEB J.* 20 (6) (2006) 756–758, <https://doi.org/10.1096/fj.05-4305fje>.
- [91] N. Rubio, I. Coupienne, E. Di Valentin, I. Heirman, J. Grooten, J. Piette, P. Agostinis, Spatiotemporal autophagic degradation of oxidatively damaged organelles after photodynamic stress is amplified by mitochondrial reactive oxygen species, *Autophagy* 8 (9) (2012) 1312–1324, <https://doi.org/10.4161/autophagy.20763>.
- [92] A.D. Garg, D.V. Krysko, T. Verfaillie, A. Kaczmarek, G.B. Ferreira, T. Marysael, N. Rubio, M. Firczuk, C. Mathieu, A.J. Roebroek, A novel pathway combining calreticulin exposure and ATP secretion in immunogenic cancer cell death, *EMBO J.* 31 (5) (2012) 1062–1079, <https://doi.org/10.1038/emboj.2011.497>.
- [93] I. Lakshmanan, S.K. Batra, Protocol for apoptosis assay by flow cytometry using annexin V staining method, *Bio Protoc* 3 (6) (2013) 1–4, <https://doi.org/10.21769/bioprotoc.374>.
- [94] J. Reiners Jr., J. Caruso, P. Mathieu, B. Chelladurai, X.-M. Yin, D. Kessel, Release of cytochrome c and activation of pro-caspase-9 following lysosomal photodamage involves bid cleavage, *Cell Death Differ.* 9 (9) (2002) 934–944, <https://doi.org/10.1038/sj.cdd.4401048>.
- [95] T.A. Theodosiou, J.S. Hothersall, P.A. De Witte, A. Pantos, P. Agostinis, The multifaceted phototoxic profile of hypericin, *Mol. Pharm.* 6 (6) (2009) 1775–1789, <https://doi.org/10.1021/mp900166q>.
- [96] N.L. Oleinick, R.L. Morris, I. Belichenko, The role of apoptosis in response to photodynamic therapy: what, where, why, and how, *Photochem. Photobiol. Sci.* 1 (1) (2002) 1–21, <https://doi.org/10.1039/b108586g>.
- [97] P. Agostinis, E. Buytaert, H. Breysens, N. Hendrickx, Regulatory pathways in photodynamic therapy induced apoptosis, *Photochem. Photobiol. Sci.* 3 (8) (2004) 721–729, <https://doi.org/10.1039/b315237e>.
- [98] R.D. Almeida, B.J. Manadas, A.P. Carvalho, C.B. Duarte, Intracellular signaling mechanisms in photodynamic therapy, *Biochim. Biophys. Acta* 1704 (2) (2004) 59–86, <https://doi.org/10.1016/j.bbcan.2004.05.003>.
- [99] Y.J. Hsieh, C.C. Wu, C.J. Chang, J.S. Yu, Subcellular localization of Photofrin® determines the death phenotype of human epidermoid carcinoma A431 cells triggered by photodynamic therapy: when plasma membranes are the main targets, *J. Cell. Physiol.* 194 (3) (2003) 363–375, <https://doi.org/10.1002/jcp.10273>.
- [100] C. Fabris, G. Valduga, G. Miotto, L. Borsetto, G. Jori, S. Garbisa, E. Reddi, Photosensitization with zinc (II) phthalocyanine as a switch in the decision between apoptosis and necrosis, *Cancer Res.* 61 (20) (2001) 7495–7500.
- [101] E. Buytaert, M. Dewaele, P. Agostinis, Molecular effectors of multiple cell death pathways initiated by photodynamic therapy, *Biochim. Biophys. Acta* 1776 (1) (2007) 86–107, <https://doi.org/10.1016/j.bbcan.2007.07.001>.
- [102] A. Vantieghem, Y. Xu, W. Declercq, P. Vandenaabee, G. Denecker, J.R. Vandenhede, W. Merlevede, P.A. De Witte, P. Agostinis, Different pathways mediate cytochrome c release after photodynamic therapy with hypericin, *Photochem. Photobiol.* 74 (2) (2001) 133–142, [https://doi.org/10.1562/0031-8655\(2001\)074<0133:dpmccr>2.0.co;2](https://doi.org/10.1562/0031-8655(2001)074<0133:dpmccr>2.0.co;2).
- [103] A. Vantieghem, Z. Assefa, P. Vandenaabee, W. Declercq, S. Courtois, J.R. Vandenhede, W. Merlevede, P. de Witte, P. Agostinis, Hypericin-induced photosensitization of HeLa cells leads to apoptosis or necrosis: involvement of cytochrome c and procaspase-3 activation in the mechanism of apoptosis, *FEBS Lett.* 440 (1) (1998) 19–24, [https://doi.org/10.1016/s0014-5793\(98\)01416-1](https://doi.org/10.1016/s0014-5793(98)01416-1).
- [104] A.R. Kamuhabwa, P.M. Agostinis, M.A. D'Hallewin, L. Baert, P.A. De Witte, Cellular photodestruction induced by hypericin in AY-27 rat bladder carcinoma cells, *Photochem. Photobiol.* 74 (2) (2001) 126–132, [https://doi.org/10.1562/0031-8655\(2001\)074<0126:CPIBHI>2.0.CO;2](https://doi.org/10.1562/0031-8655(2001)074<0126:CPIBHI>2.0.CO;2).
- [105] G. Lavie, C. Kaplinsky, A. Toren, I. Aizman, D. Meruelo, Y. Mazur, M. Mandel, A photodynamic pathway to apoptosis and necrosis induced by dimethyl tetrahydroxyhelianthone and hypericin in leukaemic cells: possible relevance to photodynamic therapy, *Br. J. Cancer* 79 (3–4) (1999) 423, <https://doi.org/10.1038/sj.bjc.6690066>.
- [106] F.K.-M. Chan, K. Moriwaki, M.J. De Rosa, Detection of necrosis by release of lactate dehydrogenase activity, *Methods Mol. Biol.* 979 (2013) 65–70, https://doi.org/10.1007/978-1-62703-290-2_7.
- [107] P. Kumar, A. Nagarajan, P.D. Uchil, Analysis of cell viability by the lactate dehydrogenase assay, *Cold Spring Harbor Protoc.* 2018 (6) (2018) 465–468, <https://doi.org/10.1101/pdb.prot095497>.
- [108] P. Miskovsky, F. Sureau, L. Chinsky, P.Y. Turpin, Subcellular distribution of hypericin in human cancer cells, *Photochem. Photobiol.* 62 (3) (1995) 546–549, <https://doi.org/10.1111/j.1751-1097.1995.tb02382.x>.
- [109] S. Okpanyi, H. Lidzba, B. Scholl, H. Miltenburger, Genotoxicity of a standardized Hypericum extract, *Arzneimittelforschung* 40 (8) (1990) 851–855.
- [110] P. Miskovsky, L. Chinsky, G.V. Wheeler, P.-Y. Turpin, Hypericin site specific interactions within polynucleotides used as DNA model compounds, *J. Biomol. Struct. Dyn.* 13 (3) (1995) 547–552, <https://doi.org/10.1080/07391102.1995.10508865>.
- [111] S. Sánchez-Cortés, P. Miskovsky, D. Jancura, A. Bertoluzza, Specific interactions of antiretrovirally active drug hypericin with DNA as studied by surface-enhanced resonance Raman spectroscopy, *J. Phys. Chem.* 100 (5) (1996) 1938–1944, <https://doi.org/10.1021/jp951980q>.
- [112] M. Morita, Y. Naito, T. Yoshikawa, E. Niki, Plasma lipid oxidation induced by peroxyinitrite, hypochlorite, lipoxygenase and peroxy radicals and its inhibition by antioxidants as assessed by diphenyl-1-pyrenylphosphine, *Redox Biol.* 8 (2016) 127–135, <https://doi.org/10.1016/j.redox.2016.01.005>.
- [113] Y. Okimoto, A. Watanabe, E. Niki, T. Yamashita, N. Noguchi, A novel fluorescent probe diphenyl-1-pyrenylphosphine to follow lipid peroxidation in cell membranes, *FEBS Lett.* 474 (2–3) (2000) 137–140, [https://doi.org/10.1016/s0014-5793\(00\)01587-8](https://doi.org/10.1016/s0014-5793(00)01587-8).
- [114] B.W. Henderson, T.J. Dougherty, How does photodynamic therapy work? *Photochem. Photobiol.* 55 (1) (1992) 145–157, <https://doi.org/10.1111/j.1751-1097.1992.tb04222.x>.
- [115] K. Berg, P.K. Selbo, A. Weyergang, A. Dietze, L. Prasmackaite, A. Bonsted, B. Engesaeter, E. Angell-Petersen, T. Warloe, N. Frandsen, Porphyrin-related photosensitizers for cancer imaging and therapeutic applications, *J. Microsc.* 218 (2) (2005) 133–147, <https://doi.org/10.1111/j.1365-2818.2005.01471.x>.
- [116] D.E. Dolmans, D. Fukumura, R.K. Jain, Photodynamic therapy for cancer, *Nat. Rev. Cancer* 3 (5) (2003) 380–387, <https://doi.org/10.1038/nrc1071>.
- [117] T.J. Dougherty, C.J. Gomer, B.W. Henderson, G. Jori, D. Kessel, M. Korbelik, J. Moan, Q. Peng, Photodynamic therapy, *J. Natl. Cancer Inst.* 90 (12) (1998) 889–905, <https://doi.org/10.1093/jnci/90.12.889>.
- [118] M. Niedre, M.S. Patterson, B.C. Wilson, Direct near-infrared luminescence detection of singlet oxygen generated by photodynamic therapy in cells in vitro and tissues in vivo, *Photochem. Photobiol.* 75 (4) (2002) 382–391, [https://doi.org/10.1562/0031-8655\(2002\)075<0382:DNILDO>2.0.CO;2](https://doi.org/10.1562/0031-8655(2002)075<0382:DNILDO>2.0.CO;2).
- [119] L. Nakopoulou, I. Giannopoulou, K. Stefanaki, E. Panayotopoulou, I. Tsimpa, P. Alexandrou, J. Mavrommatis, S. Katsarou, P. Davaris, Enhanced mRNA expression of tissue inhibitor of metalloproteinase-1 (TIMP-1) in breast carcinomas is correlated with adverse prognosis, *J. Pathol.* 197 (3) (2002) 307–313, <https://doi.org/10.1002/path.1129>.
- [120] A.C. Pereira, E.D.d. Carmo, V. Silveira, S.U. Amadei, L.E.B. Rosa, O papel das MMP-2 e 9 no desenvolvimento do carcinoma epidermóide, *Rev. Bras. Cancerol.* 52 (3) (2006) 257–262.
- [121] R. Zhao, T. Zhang, B. Ma, X. Li, Antitumor activity of *Portulaca oleracea* L. polysaccharide on HeLa cells through inducing TLR4/NF- κ B signaling, *Nutr. Cancer* 69 (1) (2017) 131–139, <https://doi.org/10.1080/01635581.2017.1248294>.
- [122] A. Chatterjee, J. Chakrabarti, A. Mitra, N. Chattopadhyay, Membrane-associated MMP-2 in human cervical cancer, *J. Environ. Pathol. Toxicol. Oncol.* 22 (2) (2003) 8, <https://doi.org/10.1615/jenvpathtoxconcol.v22.i2.20>.
- [123] H.Y. Du, M. Olivo, R. Mahendran, Q. Huang, H.M. Shen, C.N. Ong, B.H. Bay, Hypericin photoactivation triggers down-regulation of matrix metalloproteinase-9 expression in well-differentiated human nasopharyngeal cancer cells, *Cell. Mol. Life Sci.* 64 (7) (2007) 979–988, <https://doi.org/10.1007/s00018-007-7030-1>.
- [124] V. Stupáková, L. Varinská, A. Miroššay, M. Šarišský, J. Mojiš, R. Dankovčík, P. Urdzik, A. Ostrá, L. Miroššay, Photodynamic effect of hypericin in primary cultures of human umbilical endothelial cells and glioma cell lines, *Phytother. Res.* 23 (6) (2009) 827–832, <https://doi.org/10.1002/ptr.2681>.
- [125] O. López-Ocejo, A. Viloria-Petit, M. Bequet-Romero, D. Mukhopadhyay, J. Rak, R.S. Kerbel, Oncogenes and tumor angiogenesis: the HPV-16 E6 oncoprotein activates the vascular endothelial growth factor (VEGF) gene promoter in a p53 independent manner, *Oncogene* 19 (40) (2000) 4611–4620, <https://doi.org/10.1038/sj.onc.1203817>.
- [126] Q. Zhang, Z.-h. Li, Y.-y. Li, S.-j. Shi, S.-w. Zhou, Y.-y. Fu, Q. Zhang, X. Yang, R.-q. Fu, L.-c. Lu, Hypericin-photodynamic therapy induces human umbilical vein endothelial cell apoptosis, *Sci. Rep.* 5 (2015) 1–13, <https://doi.org/10.1038/srep18398>.
- [127] S.-J.M.Y. Yuan, D.-Q. Xu, Y. Shen, H.-Y. Yan, Y. Wang, W. Wang, Y.-J. Tan, Expressions of VEGF and miR-21 in tumor tissues of cervical cancer patients with HPV infection and their relationships with prognosis, *Eur. Rev. Med. Pharmacol. Sci.* 22 (19) (2018) 6274–6279, <https://doi.org/10.26355/eurrev.201810.16035>.

CAPÍTULO III

CONCLUSÕES

A avaliação da atividade antitumoral da TFD com HIP/P123 frente a um painel abrangente de linhagens celulares derivadas de câncer cervical humano, incluindo HeLa (HPV 18-positivo), SiHa (HPV 16-positivo), CaSki (HPV 16 e 18-positivo) e C33A (HPV-negativo), em comparação com uma linha de células epiteliais humanas não tumorigênicas (HaCaT), demonstrou que:

- As micelas de HIP/P123 apresentaram efeitos fototóxicos eficazes e seletivos, dependentes do tempo e da dose, nas células de câncer cervical, mas não em HaCaT;
- A HIP foi internalizada seletivamente em todas as linhagens de câncer cervical, mas não em HaCaT, indicando seu potencial de permear a membrana das células cancerosas cervicais;
- A HIP acumulou-se no retículo endoplasmático, mitocôndrias e lisossomos, resultando em morte celular fotodinâmica principalmente por necrose;
- A HIP/P123 induziu estresse oxidativo celular principalmente por meio do mecanismo da TFD do tipo II;
- A HIP/P123 foi capaz de inibir a formação de colônias, o que evidencia uma citotoxicidade a longo prazo nas linhagens de câncer cervical, sugerindo uma possível capacidade de prevenir a recorrência do câncer cervical;
- As micelas de HIP/P123 inibiram a migração e a invasão das células tumorais, principalmente por meio da inibição de MMP-2, evidenciando seu potencial em diminuir a formação de metástases;

Em conjunto, os resultados demonstraram que o tratamento com a TFD utilizando a HIP/P123 como FS teve efeito antitumoral seletivo em células de câncer cervical imortalizadas por HPV 16, HPV 18, HPV 16 e 18 juntos e sem HPV, indicando seu potencial como um candidato promissor para o tratamento do câncer cervical.

Ainda, indicaram um papel potencialmente útil das micelas HIP/P123 como uma plataforma para a entrega de HIP para tratar de forma mais específica e eficaz o câncer cervical por meio de TFD reforçando a necessidade da continuidade dos estudos especialmente dos testes pré-clínicos *in vivo*.

PERSPECTIVAS FUTURAS

Considerando os conhecimentos adquiridos com esta tese na busca de novos possíveis candidatos e modalidades terapêuticas para o câncer cervical, temos a intenção de realizar os seguintes estudos:

- Avaliar outras possíveis vias de mecanismos de ação da HIP/P123 em modelo de neoplasia cervical;
- Avaliar a atividade antitumoral da HIP/P123 em modelos *in vivo* (animais);
- Desenvolver e avaliar a atividade antitumoral de diferentes formulações farmacêuticas da HIP/P123 em modelo de neoplasia cervical e também em modelos animais.
- Elaborar uma revisão sistemática sobre o tratamento do câncer cervical utilizando a TFD.

O presente trabalho foi realizado com apoio da Coordenação de Aperfeiçoamento de Pessoal de Nível Superior - Brasil (CAPES) - Código de Financiamento 001.